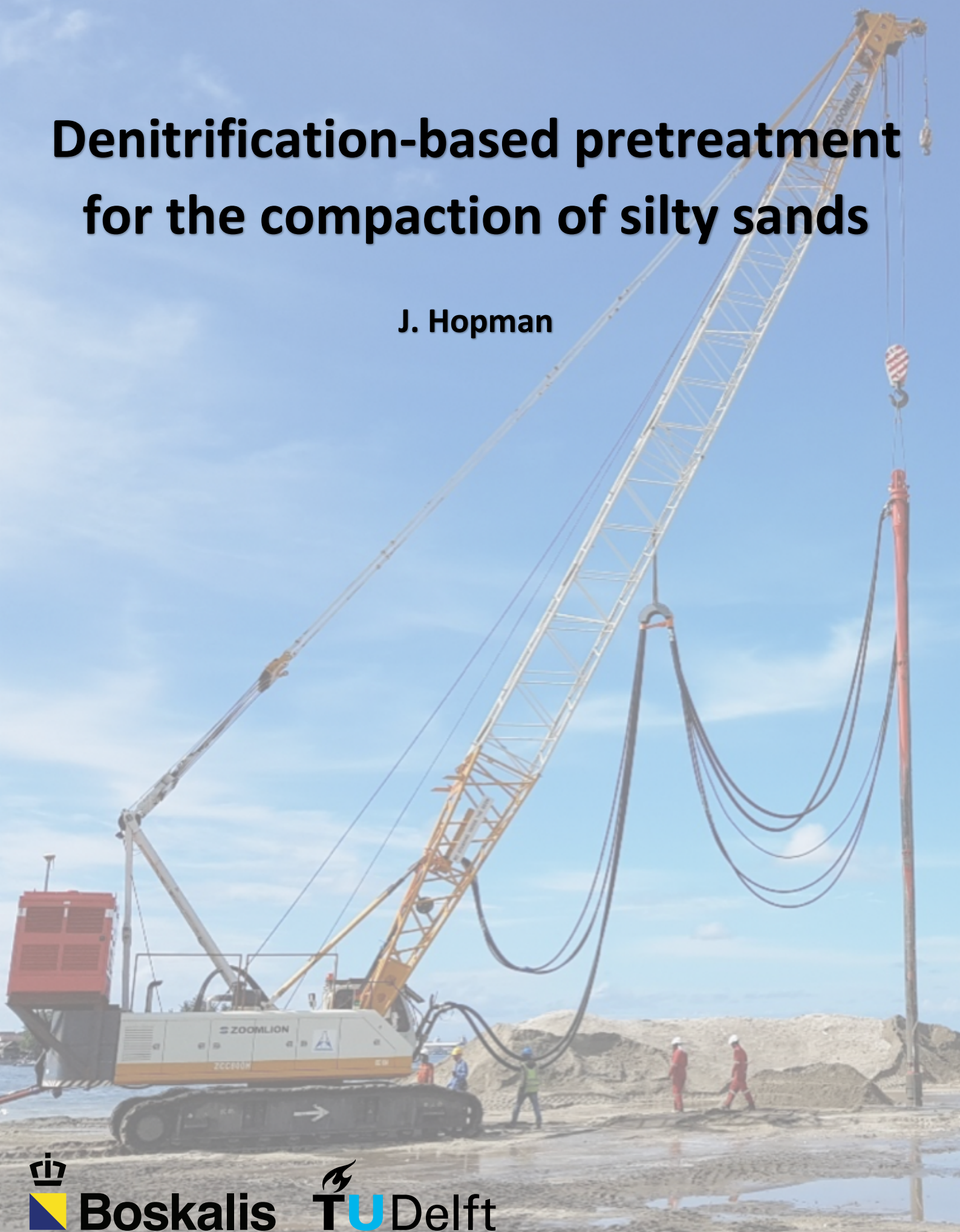


Denitrification-based pretreatment for the compaction of silty sands

J. Hopman



Cover picture: Vibro compaction performed by Cofra B.V.

Denitrification-based pretreatment for the compaction of silty sands

MSc Thesis

by

Jessy Hopman

in partial fulfilment of the requirements for the degree of

Master of Science in Applied Earth Sciences

December 2018

Graduation committee

Chair:

Prof. dr. C. Jommi

Geo-Engineering, TU Delft

Supervisor:

Dr. ir. A.A.M. Dieudonné

Geo-Engineering, TU Delft

External supervisor:

Prof. dr. ir. M.K. de Kreuk

Sanitary Engineering, TU Delft

External supervisor:

Dr. ir. L. A. van Paassen

Center for Bio-mediated and Bio-inspired Geotechnics (CBBG), Arizona State University

Company supervisor:

Ir. B. Vos

Hydronamic B.V., Boskalis

Company supervisor:

Dr. ir. W.R.L. van der Star

Subsurface and Groundwater Systems, Deltares

An electronic version of this thesis is available at <http://repository.tudelft.nl/>



ACKNOWLEDGEMENTS

This thesis presents the experimental and theoretical research that is performed as final part of the master Applied Earth Sciences at the Technical University of Delft. During my research I investigated the potential of a denitrification-based pretreatment for facilitation of compaction activities on silty sands.

I would like to thank my company supervisor, Bas Vos, for giving me the opportunity to work on this interesting topic and experience the enjoyable environment at the in-house engineering department of Boskalis (Hydronamic). This topic was investigated in an earlier stage by Gustav Andrag. His work and support were extremely helpful throughout the course of my research. I want to thank Cristina Jommi and Anne-Catherine Dieudonné for the numerous invaluable meetings and discussions and for keeping me on the right track when I lost direction.

I would not have been able to successfully conduct the biochemical part of this research without the help of my supervisors Merle de Kreuk, Wouter van der Star and Leon van Paassen. Thank you for helping me cross the bridges between the different scientific disciplines of this research. Also, I would like to thank Javier Pavez (TU Delft) and Jasper Visser (Boskalis Environmental) for their guidance and assistance during the experimental part of my research. Finally, the support of family and friends was naturally indispensable.

Jessy Hopman
Delft, December 2018

SUMMARY

Recent developments in bio-based soil improvement techniques include the use of the bacterially mediated process of denitrification to alter engineering properties of soils. Pham (2017) used the denitrification process to stimulate the production of gas and precipitation of calcium carbonate as a soil improvement method. The ability to desaturate a soil to its optimum saturation by means of gas production inspired the use of this method to improve the engineering properties of soils more efficiently by means of a two-stage process of desaturation and compaction. Andrag (2017) started a research to investigate the potential of this concept and developed a test setup for the assessment of its efficiency.

The prospects of this biogenic soil pretreatment method are further investigated in the current study. The objective of the research is to assess how the compactability of an initially saturated soil is influenced by the in-situ formation of gas bubbles and if this gas can be used to reduce the energy requirements for compaction of a soil to a given target density.

A review on existing literature is initially carried out to grasp the latest developments on this topic. Information from literature is used to determine the typical characteristics of soils on which compaction activities are often found to be ineffective. Based on this information, a representative silty sand with a high gas storage capacity is created for further experiments. It is found that gradation is one of the main properties controlling the water content-dry density relationship of soils. The water content-dry density relationship of soils composed from industrially produced material is found to be often significantly different from natural soils, which can be explained by differences in gradation.

A testing strategy is developed and a setup is established for assessment of the concept of biogenic soil pretreatment for reducing energy requirements for compaction. Denitrifying bacteria are cultivated with a chemostat setup which can supply bacterial inoculum for subsequent experiments. The effect of the biogenic pretreatment is evaluated by comparing the energy requirements for compression of treated and untreated soil samples from initial conditions to a given target density with a constant strain-rate.

Soil samples are successfully desaturated to targeted saturations by means of an engineered treatment regime. Concentrations of the substrates are determined based on the stoichiometry of the biochemical reaction, Henry's law, Boyle's law and the ideal gas law. Gas is produced at a steady rate inside the soil samples with a very limited amount of gas escaping, confirming the high storage capacity of the assembled sample material. The determined optimum saturation of the silty sand (80%), is therefore achieved without exceeding the gas percolation threshold of the soil. The gas that escapes the sample during the gas production stage and the loading stage, is captured with a gas trap that is included in the setup. The changes in water content and dry density of the soil during the experiment can be accurately predicted by means of a volume balance. The major part of the initially available nitrate in the pore fluid is consumed at the end of the experiments, with a limited amount of accumulated nitrite. Moreover, the denitrification process is successfully buffered by including calcium within the engineered substrate solution.

It is initially presumed that energy requirements for static compaction of a silty sand in the Rowe cell can be reduced by bringing the soil closer to optimum conditions in terms of saturation, before starting the loading stage. Based on an analysis of the work input per volume, it is found that the energy requirements for compaction increase slightly as a result of the biogenic pretreatment. In terms of compactability, no clear benefit is obtained from the biogenic pretreatment according to the energy-based assessment method that is used in this research. The slightly higher energy requirements for compaction of treated samples can possibly be explained by the formation of biofilm or entrapment of gas bubbles in the drainage lines of the setup. Cementation effects as a result of calcium carbonate precipitation are not expected to play a role, since calculations show that the relative amount of calcium carbonate in the soil is very limited at the end of the experiments.

It is recommended to further investigate the potential of the denitrification-based pretreatment for the compaction of soils by exploring new methods of assessment. It is suggested to focus on implementation of a dynamic loading component to the test method and to investigate the options for execution of a field experiment. Representation of conditions that apply in practice is thereby essential. The potential of biogenic pretreatment for improvement of the engineering properties of silts and clays can also be investigated as it might be a sustainable alternative for the relatively scarce and costly coarse-grained fill material that is normally used nowadays.

CONTENTS

Acknowledgements	v
Summary	vii
List of Figures	xi
List of Tables	xii
Nomenclature	xiii
1 Introduction	1
1.1 Problem statement	1
1.2 Proposed solution.	1
1.3 Hypothesis	2
1.4 Research question	4
1.5 Scope of work.	4
1.6 Structure of report	4
2 Review of Literature	7
2.1 Bio-mediated soil improvement techniques	7
2.2 Principles and controlling factors of denitrification	7
2.2.1 Oxygen.	8
2.2.2 Organic carbon	8
2.2.3 pH	8
2.2.4 Temperature	9
2.2.5 Inhibitors	9
2.2.6 Nitrate respiration and intracellular competition	9
2.3 Microbial ground improvement through denitrification	9
2.3.1 Reaction stoichiometry	10
2.3.2 Ac/N and C/N ratio	10
2.3.3 Concentration of substrate.	10
2.3.4 Gas percolation threshold	11
2.3.5 Calcite precipitation	11
2.3.6 Expansion of soil skeleton	11
2.3.7 Accumulation of harmful intermediates	11
2.4 Distribution of the gas phase	12
2.5 Compaction activities on soils	13
2.5.1 Problematic soils.	13
2.5.2 Water content versus dry density.	14
3 Methodology	19
3.1 Selection of soil sample	19
3.1.1 Compaction curves	20
3.1.2 Particle size distribution	20
3.1.3 Dry density limits	21
3.2 Cultivation of denitrifying bacteria	21
3.3 Rowe cell experiments	23
3.3.1 Calibration of diaphragm	24
3.3.2 Setup preparations.	24
3.3.3 Substrate solution	25
3.3.4 Sample preparation	26
3.3.5 Closing the cell.	27
3.3.6 Saturation stage	28
3.3.7 Reaction stage	28

3.3.8	Drained loading and relaxation	29
3.3.9	Water content during loading and relaxation stage.	30
3.3.10	Disassembly	31
3.4	OxiTop experiments.	32
4	Results	33
4.1	Compaction curves	33
4.2	Processed results Rowe cell experiments	35
4.2.1	Gas production and desaturation	35
4.2.2	Water content-dry density paths	36
4.2.3	Compression forces during loading and relaxation stage.	39
4.2.4	Work input loading stage.	39
4.2.5	Chemical analysis Rowe cell experiments	41
4.3	OxiTop experiments.	44
5	Discussion	47
5.1	Measurement accuracy	47
5.2	Drainage conditions	47
5.3	Compression of the gas phase.	51
5.4	Distribution of gas in the sample	52
5.5	Denitrification in soils	52
5.6	Experimental setup and method	53
5.6.1	Differences between experimental conditions and field conditions	53
5.6.2	Rate of loading and soil permeability	53
5.7	Potential of the denitrification-based pretreatment	54
6	Conclusion	55
7	Recommendations	57
	Bibliography	59
A	Soil sample measurements Rowe cell experiments	63
B	Chemical analysis Rowe cell experiments	64
C	Chemical analysis OxiTop experiments	66
D	Nutrient stock solutions	67

LIST OF FIGURES

1.1	Different scenarios for the two-stage process of desaturation and compaction (Andrag, 2017).	2
1.2	Presumed paths of compression forces over time for different degrees of saturation.	3
1.3	The four phases of this research.	5
2.1	Dissimilatory reduction pathways of nitrate (Rebata-Landa and Santamarina, 2012).	8
2.2	Graph produced by Keller (n.d.) GmbH to show the limits of application for deep vibro techniques.	14
2.3	Processed CPT results from reclamation project in Asia.	15
2.4	General compaction curves for different soil types (Salem, 2010).	16
2.5	Standard proctor compaction curves for fine soils from literature (saturation contours for $G_s = 2.65 \text{ g/cm}^3$). *From Terzaghi et al. (1996) **From Head (2006) ***From Gallage et al. (2016)	17
3.1	Standard and modified proctor compaction curves for composition 6.	20
3.2	Particle size distribution of soil selected for Rowe cell experiments (composition 6).	21
3.3	Chemostat setup for cultivation of denitrifying bacteria.	22
3.4	Rowe cell setup (adapted from Andrag (2017)).	23
3.5	Visualization of diaphragm calibration with a load cell for measuring the actual force exerted by the diaphragm.	24
3.6	Soil sample preparation in the Rowe cell.	27
3.7	Assembled Rowe cell setup at the start of an experiment.	28
4.1	Standard proctor compaction curves for several mixtures (saturation contours for $G_s = 2.65 \text{ g/cm}^3$).	33
4.2	Standard proctor compaction curves for soils from literature (saturation contours for $G_s = 2.65 \text{ g/cm}^3$). *From Terzaghi et al. (1996) **From Head (2006) ***From Gallage et al. (2016)	34
4.3	Volume balance during reaction stage of treated Rowe cell tests.	37
4.4	Saturation development during reaction stage of treated Rowe cell tests.	37
4.5	Gas production measurements during reaction stage of treated Rowe cell tests.	37
4.6	Dry density - water content paths of soil samples during loading stage.	38
4.7	Compression force and dry density developments during drained loading stage and relaxation stage.	40
4.8	Work done per unit volume (normalized for total strain) during loading stage of Rowe cell experiments.	41
4.9	Measured and predicted nitrate concentrations in pore fluid at beginning and end of treated tests.	42
4.10	Theoretical production of nitrogen gas for maximum and zero growth conditions and measured gas production during treated Rowe cell experiments.	43
4.11	Nitrogen balance from chemical analysis of sample pore fluid at begin and end of treated Rowe cell tests.	44
4.12	Average production of gas per liter of solution in OxiTop bottles.	46
5.1	Excess pore pressure development during the loading stage of Rowe cell experiments.	48
5.2	Stresses, pore pressure and strain development during loading of untreated soil sample ($S_w = 100\%$) with drainage valve closed.	48
5.3	Measured pressures for the "consolidation" stage of the Rowe cell experiment with closed drainage valve.	50
5.4	Volume balance for "consolidation" stage of the Rowe cell experiment with closed drainage valve.	50
5.5	Visualization of the scenario that leads to removal of water from around the diaphragm and therefore a partially saturated system.	51

LIST OF TABLES

3.1	Materials used during series of standard proctor compaction tests. *Krapfenbauer (2016) **Stewart (1992)	19
3.2	List of sample compositions that are assessed with the standard proctor compaction test in chronological sequence.	20
3.3	Grain diameters in μm at x% passing (D_x) and coefficients of uniformity (C_u) and curvature (C_C).	21
3.4	Minimum and maximum density and corresponding maximum and minimum void ratio of selected soil.	21
3.5	Volumes and concentrations of substrate solutions and bacterial solutions for OxiTop experiments.	32
4.1	Treatment regimes for treated Rowe cell experiments.	35
4.2	Soil sample properties at the beginning and end of the loading stage.	36
4.3	Reaction time, concentration and pH measurements of treated Rowe cell experiments.	42
4.4	Measurements of dissolved calcium and theoretical precipitation of calcium carbonate of treated Rowe cell experiments.	43
4.5	Removed fractions of ($NO_3^- + NO_2^-$) - N and Ca^{2+} at the end of the OxiTop experiment and measured final pH of the solution.	44
4.6	Measured total productions (prod.) of carbon dioxide (CO_3^{2-} , HCO_3^- , H_2CO_3 , CO_2^{aq} and CO_2^g) and nitrogen gas per liter of solution versus theoretical production according to the measured (meas.) consumption and metabolic stoichiometry.	46
A.1	Measurements Rowe cell experiments.	63
B.1	Chemical analysis of Treated Rowe cell experiments.	64
B.2	Nitrogen balance Treated 1.	65
B.3	Nitrogen balance Treated 2.	65
B.4	Nitrogen balance Treated 3.	65
C.1	Chemical analysis of Control bottles OxiTop experiment.	66
C.2	Chemical analysis of Soil bottles OxiTop experiment.	66
D.1	Composition of macro-nutrient stock solution. During all experiments 1 mL of the macro-nutrient stock solution was added for each 1 L of prepared solution (i.e. 1 mL/L).	67
D.2	Composition of micro-nutrient stock solution (Salek et al., 2016). During all experiments 1 mL of the micro-nutrient stock solution was added for each L of prepared solution (i.e. 1 mL/L).	67

NOMENCLATURE

Abbreviations

Ac/N	Acetate/Nitrate ratio
ASTM	American Society for Testing and Materials
Avg.	Average
BPC	Back Pressure Controller
BS	British Standard
CPT	Cone Penetration Test
C/N	Carbon/Nitrogen ratio
DPC	Diaphragm Pressure Controller
DNRA	Dissimilatory Nitrate Reduction to Ammonium
eols	End of loading stage (used as subscript)
eors	End of reaction stage (used as subscript)
MICP	Microbial Induced Calcite Precipitation
MID	Microbial Induced Desaturation
MIDP	Microbial Induced Desaturation and Precipitation
PSD	Particle Size Distribution
USCS	Unified Soil Classification System

Roman symbols

Symbol	Description	Units
A	Air content	-
A_{ϕ}	Inner area of Rowe cell	m^2
$c_{\text{subscript}}$	Concentration	mol/L
$c_{\text{subscript}}^g$	Concentration present in the gas phase	mol/L
$c_{\text{subscript}}^l$	Concentration present in the liquid phase	mol/L
C_c	Coefficient of curvature	-
C_u	Coefficient of uniformity	-
D_x	Grain diameters at x% passing	m
e	Void ratio	-
$F_{\text{compression}}$	Compression forces in Rowe cell	N
G_s	Specific gravity	-
H	Height	m
m	Mass	kg
$n_{\text{subscript}}$	Molar quantity	mol
P	Pressure	Pa
$P_{\text{diaphragm}}$	Pressure in loading diaphragm of Rowe cell	Pa
$p_{\text{subscript}}$	Partial pressure	Pa
pH	Measure of acidity or alkalinity on a log scale	-
ppm	Parts Per Million	-
r_{critical}	Critical radius for stable gas bubbles	m
R	Ideal gas constant (8.314)	J/mol/K

RD	Relative Density	-
s	Displacement	m
S _{DPC}	Displacement calculated from output DPC	m
S	Saturation	-
S _g	Gas saturation	-
S _w	Water saturation	-
t	Time	seconds
T	Temperature	K
T _s	Surface tension	N/m
u	Pore water pressure	Pa
u _n	Pressure at which gas bubbles nucleate	Pa
V	Volume	m ³
V _{BPC}	Volume Back Pressure Controller	m ³
V _{DPC}	Volume Diaphragm Pressure Controller	m ³
V _{excess}	Volume of excess liquid displaced from around diaphragm	m
V _g	Volume of gas	m ³
V _{gastrap}	Volume of gas in gas trap	m ³
V _{pf}	Volume of pore fluid	m ³
V _{sample}	Volume of soil sample	m ³
V _{tot}	Total volume	m ³
V _v	Volume of voids	m ³
w	Water content	-
Y _{subscript}	Stoichiometric coefficient	-

Greek symbols

Symbol	Description	Units
ϵ	Strain	-
$\dot{\epsilon}_{DPC}$	Strain rate calculated from output diaphragm pressure controller	-
$\dot{\epsilon}_{Trans}$	Strain rate calculated from output displacement transducer	-
$K_{H_{subscript}}$	Henry's coefficient	Pa·m/mol
μ	Calibration factor for correction of displacements in Rowe cell	-
ρ	Density	kg/m ³
ρ_d	Dry density	kg/m ³
ρ_s	Particle density	kg/m ³
ρ_{tot}	Total density	kg/m ³
ρ_w	Density of water	kg/m ³
σ	Total stress	Pa
σ'	Effective stress	Pa
ϕ	Porosity	-
ψ	Supersaturation	-

1. INTRODUCTION

Microbial ground improvement techniques are a trending topic in geotechnical engineering and are particularly interesting because of their non-disruptive nature and potential for a reduced environmental impact. An extensive research was done by Pham (2017) on microbial induced calcite precipitation (MICP) based on denitrification to investigate the potential of this process as ground improvement technique. By application of MICP, the soil is not only improved as a result of the calcite bonds formed between grains, but also due the formation of nitrogen bubbles, which increases the soil resistance to dynamic loading.

Andrag (2017) used the nitrogen gas produced during the first stage of this process to lower the water content of fully saturated soils closer to optimum conditions in terms of water content, thereby preparing them for subsequent compaction activities. In theory, the energy requirements for reaching a particular target density by compaction can be reduced if the soil is brought closer to optimum conditions in terms of water content. The precipitation of calcite should be limited during the first stage (the microbial induced desaturation stage) of this two-stage process as it counteracts the second stage (the compaction stage). Andrag (2017) performed multiple laboratory experiments using a hydraulic consolidation cell (Rowe cell) and showed that the water content of silty sands and sandy silts can be lowered close to any target value by means of a controlled process of microbial induced desaturation (MID) based on denitrification. Since the results were inconclusive in terms of reduced energy requirements after MID pretreatment, further research is required.

1.1. PROBLEM STATEMENT

The general objective of ground improvement activities is to increase the strength characteristics of a soil to prepare it for future loading conditions. Future loading conditions could refer to the construction of buildings, traffic or seismic activities. In seismically active areas ground improvement is specifically important in order to increase the resistance of soil against soil liquefaction.

Liquefaction is a well-known phenomenon in the field of geotechnical engineering that involves the substantial loss of strength and stiffness of saturated loose soils as a result of applied stresses. These stresses might be induced by earthquake events, but also static liquefaction can occur as a result of a sudden change in stress conditions by a monotonic triggering load. The rapid application of these stresses causes the soil to behave virtually undrained. This means water has no time to dissipate and no volume changes will occur. In loose and fully saturated soils, solid particles will tend to move into a denser state, but since no volume changes can occur, excess pore water pressures will be generated and effective stresses will decrease. If the effective stresses reduce to zero, the soil will start to behave like a liquid.

Land reclamations and landfills in seismically active areas are prone to liquefaction as a result of the often loose configuration of the soil caused by the deposition process. The development of land reclamations or landfills often includes compaction activities which is necessary to bring the soil to a higher relative density, increase the strength parameters for future constructions and improve liquefaction resistance. Compaction activities are inefficient in fully saturated fine soils with high fines contents due to the generation of excess pore pressures and slow dissipation. A pretreatment of these areas is required to facilitate compaction activities. A successful pretreatment increases the efficiency of the compaction process in terms of energy requirements. The current practise is to pretreat these soils by means of the installation of drainage assisting elements such as sand piles or stone columns. These techniques are very costly and time consuming, therefore an alternative solution should be investigated.

1.2. PROPOSED SOLUTION

The microbial denitrification process can be used to generate nitrogen gas in a soil body. If a protocol is developed that takes into account the soil conditions, soil characteristics and numerous other factors, a controlled gas production can be achieved and used to desaturate a soil. As water is expelled and replaced by the nitrogen gas, the pore fluid compressibility is changed, and the water content is decreased. There are two proposals for the use of this desaturation technique to improve the engineering parameters of a soil:

- The first application exploits the increased compressibility of the pore fluid directly, as the generation of excess pore pressure is restrained during earthquake events due to a volume reduction of the gas

bubbles. Ground improvement is achieved as the liquefaction resistance of the soil is increased.

- The second application aims at utilizing the gas created by denitrification to bring the soil to optimum conditions in terms of water content and subsequently increasing the dry density by application of (dynamic) loads. Again, there is an improved liquefaction resistance, but now as a result of the increased density of the soil.

The persistence and stability of the gas bubbles have to be taken into account for the first application, because earthquakes events cannot be predicted. Long term stability of the bubbles is not important for the latter application as desaturation and compaction activities are performed within a short time frame.

In coarse-grained material, pretreatment is in most cases not necessary because compaction activities can be performed quite efficiently. In soils finer soils with high fines contents, however, densification through dynamic loading is significantly inhibited because of the generation of excess pore water pressures. Theoretically the water content of fully saturated soils can be lowered to an optimum value, which will ensure a more efficient compaction process. This optimum value depends on the type of soil and the amount of energy that is applied. The achievable dry density for a certain amount of input energy can thus be increased if optimum conditions in terms of water content are induced. By using the denitrification process to desaturate the soil body, compaction activities can therefore in theory be made more efficient in terms of time and energy requirements.

1.3. HYPOTHESIS

Compaction curves are often used in the modern-day geotechnical society and show the relationship between dry density and water content for a particular amount of energy. Furthermore they give predictions of the optimum water content and maximum dry density. A prediction of the optimum water content can be used to define a target degree of saturation that should be achieved by microbial induced desaturation.

Figure 1.1a shows four different scenarios on a dry density versus water content plot. Scenario AD will occur when compaction activities are performed on a relatively permeable fully saturated soil. In these soils the pore water can almost immediately drain, thereby allowing the dry density to be increased. Compaction activities are often ineffective for less permeable soils under fully saturated conditions due to the generation of excess pore pressure. Path AD requires a lot of compactive effort for these soils. Measures have to be taken to assist drainage of water from these soils, which are often expensive.

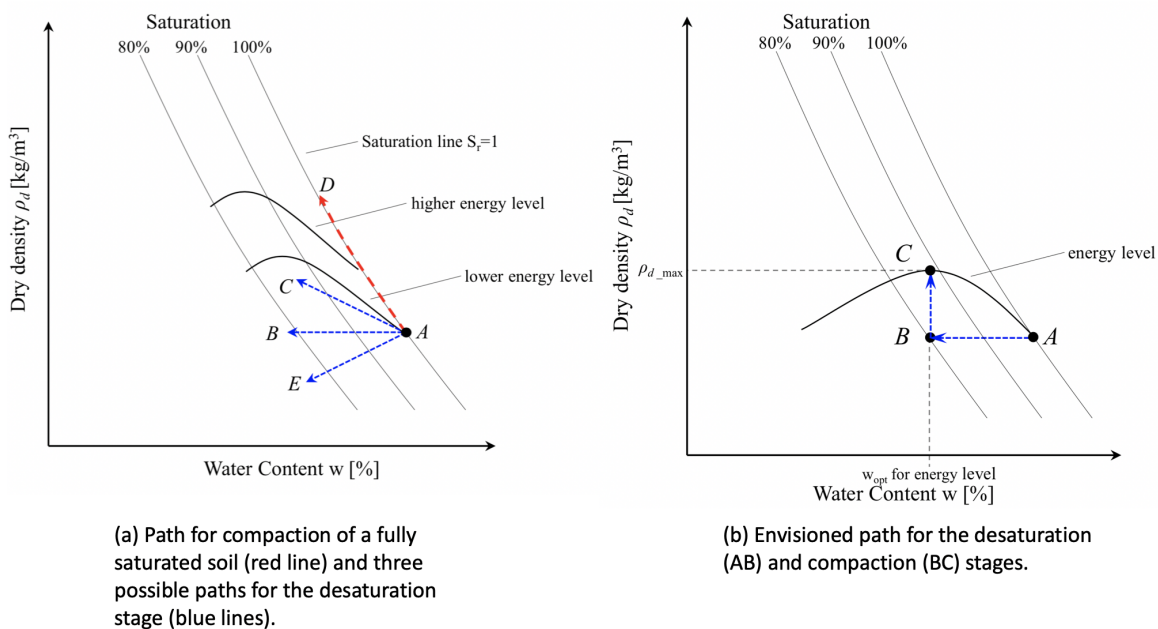


Figure 1.1: Different scenarios for the two-stage process of desaturation and compaction (Andrag, 2017).

Scenarios AC, AB, AE show the possible paths that can be followed during the microbial desaturation stage. Scenario AC would be the most efficient path that can be followed since desaturation is occurring simulta-

neously with an increase in dry density. Scenario AE on the other hand would make the subsequent compaction activities even less efficient since the dry density is decreased with respect to the initial situation. This basically means the soil body is expanding as a result of the gas production. Soil expansion as a result of desaturation is expected to be an issue, only under low confining conditions when the effective stresses are low and soil particles can be pushed apart by the pressure of the gas. Path AB is followed when no change in void ratio occurs during the desaturation stage.

The research performed by Andrag (2017) suggests that path AB is most likely path to be followed during microbial induced desaturation. It is expected that compaction activities after the desaturation stage will result in the expulsion and dissolution of gas bubbles. If the volume of water that is expelled from the soil during loading is limited, the water content is not changing significantly and the vertical path of BC is followed during the compaction stage (Figure 1.1b).

The goal of this research is to investigate if soils can be compacted efficiently by applying the biogenic pretreatment. The effectiveness of the method can be assessed by evaluating the results from multiple displacement-controlled loading experiments on samples with different degrees of saturation. A hydraulic Rowe cell setup can be used to perform displacement-controlled loading and allows for monitoring of the pressure development in the loading diaphragm as a result of the loading regime. This pressure development basically represents the resistance of the soil against compression (compactability). Compression forces can be back-calculated from the pressures by taking the loading area into account.

The presumed paths of the development of compression forces over time are shown in Figure 1.2. Both the displacement rate and initial relative density of these samples are equal during this fictional experiment and the optimum water content is assumed to correspond with a degree of saturation of 80%. Application of displacement-controlled loading on fully saturated fine soils will in general quickly result in generation of excess pore pressure. This can be recognized in Figure 1.2 as the forces quickly increase over time during displacement-controlled loading. The degree of saturation can be lowered to 90% by means of biogenic pretreatment, which brings the soil closer to its optimum water content. The pressure development during displacement-controlled loading is now less severe as can be seen by the 90% saturation path in Figure 1.2. This means less energy is required to reach the same target density. If the same displacement-controlled loading regime is used to compact a sample that has a degree of saturation of 80%, which corresponds to the optimum water content for this soil, the pressure development will be even less significant.

Energy requirements for reaching the target density are thus reduced as a result of the biogenic desaturation pretreatment. If the water content were to be lowered even more, to a value below the optimum water content, the energy requirements for reaching the target density are increased again. Suction pressures increase with decreasing water content and increase the strength and stiffness of a soil.

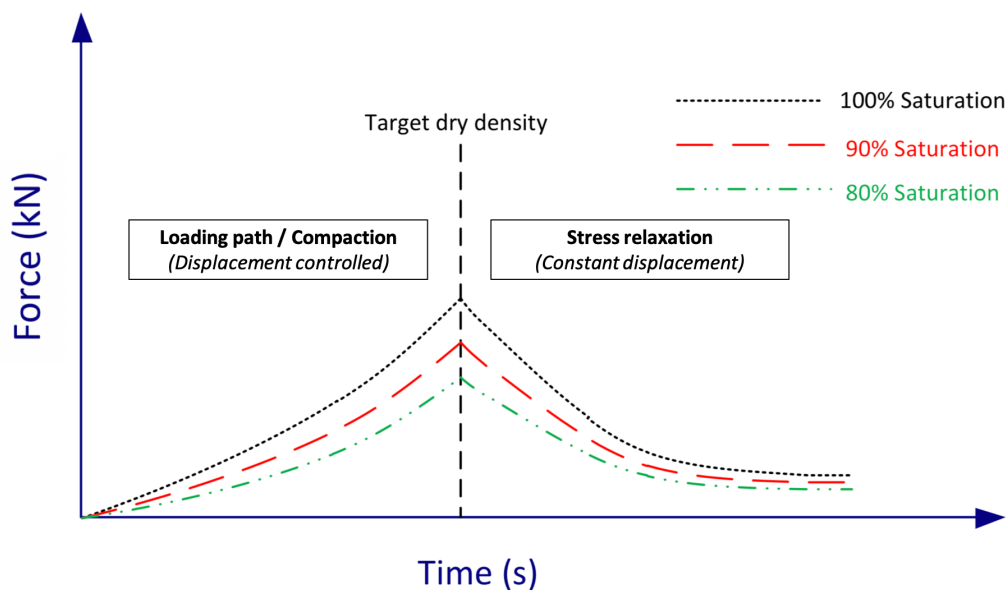


Figure 1.2: Presumed paths of compression forces over time for different degrees of saturation.

1.4. RESEARCH QUESTION

The main objective is to investigate the potential of the proposed solution for facilitating compaction activities on saturated soils that cannot be compacted efficiently with the conventional techniques.

As previous research (Andrag, 2017) was yet inconclusive, the following research question is formulated for the investigation:

- How is the compactability of an initially saturated silty sand influenced by the gas bubbles produced by denitrifying bacteria and can this gas be used to reduce the energy requirements for static compaction of the soil to a given target density?

1.5. SCOPE OF WORK

The following tasks are performed during this research:

- a literature study on the topic of microbial induced desaturation through denitrification, this includes an investigation on the principles and limiting factors of the microbial denitrification process.
- a literature study to identify the soil characteristics and boundary conditions that influence the effectiveness of compaction activities under (fully) saturated conditions.
- the search for a representative sample material that is suitable for the envisaged laboratory experiments, this includes the assessment of suitability by means of a series of index tests.
- development of a placement method that allows for preparation of fully saturated samples with relatively low initial density.
- the establishment of a chemostat setup for cultivation of denitrifying bacteria.
- a revision of the methods proposed by Pham (2017) and Andrag (2017) to predict and engineer a desaturation regime for a soil.
- a revision of the test setup proposed by Andrag (2017).
- the use of the same test setup to evaluate the energy requirements for static compaction of untreated (fully saturated) and treated (microbially desaturated) soil samples.
- measurements of gas production and gas composition in an additional incubation experiment.

1.6. STRUCTURE OF REPORT

Figure 1.3 shows the different phases of this research. The structure of this report is based on these four phases. In Chapter 2, a review of the relevant literature is given. First of all, bio-mediated soil improvement techniques are introduced. After that, the principles and controlling factors of denitrification are presented. Next, it is discussed how soils can be improved by means of the denitrification process. Finally, typical characteristics of soils that are difficult to compact are identified. In Chapter 3, the experimental procedures of laboratory tests are explained. In this chapter, the soil selection procedure, bacteria cultivation and experimental setups are discussed. In Chapter 4 the experimental results are shown and analyzed. Chapter 5 presents a discussion of the results. The measurement accuracy and drainage conditions are discussed. The differences between experimental conditions and field conditions are clarified and finally the MID pre-treatment is evaluated. The conclusions of this research can be found in Chapter 6. Finally, in Chapter 7, recommendations for future research are given.

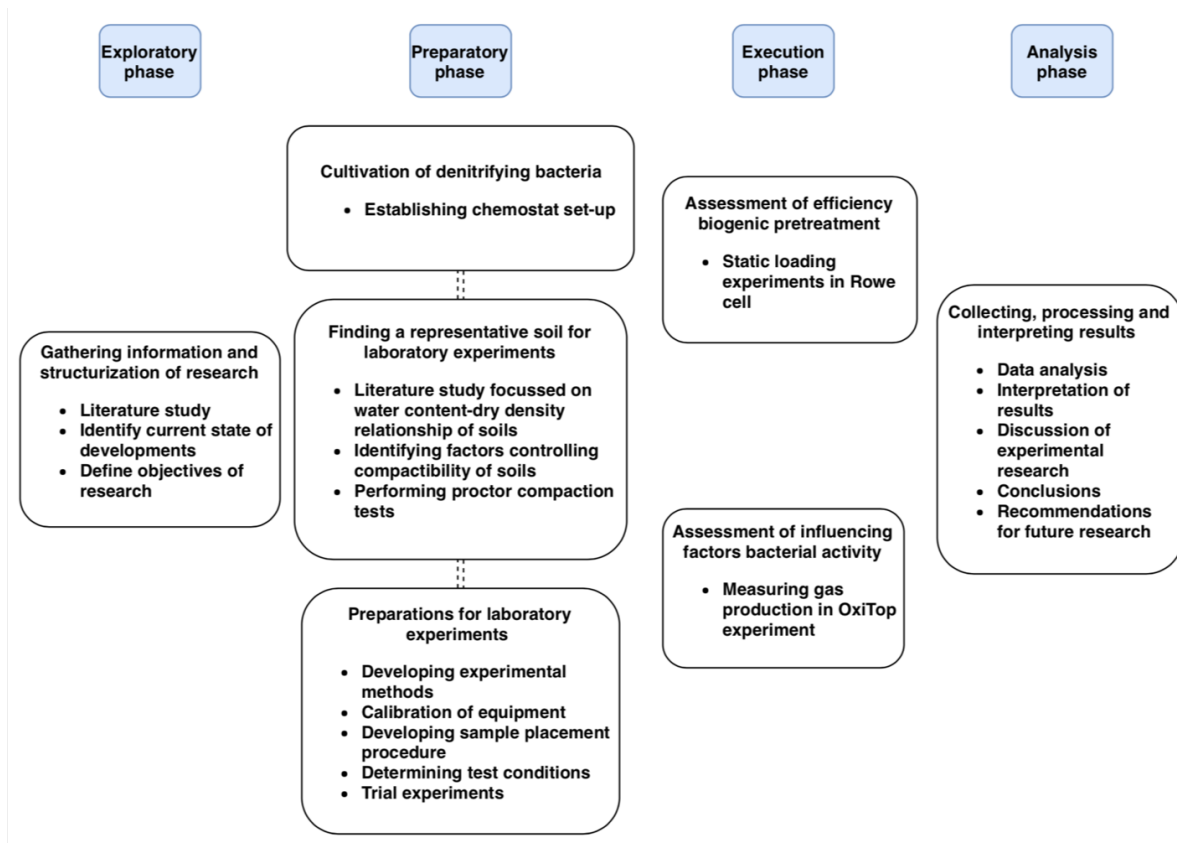


Figure 1.3: The four phases of this research.

2. REVIEW OF LITERATURE

Microbial geotechnology is an interdisciplinary science that has attracted the interest of scientific researchers and industrial professionals from different scientific disciplines (Wu, 2015). Denitrification-based soil improvement is one of the microbial geotechnologies that has shown promising results in earlier research (Andrag (2017), Pham (2017), Puzrin et al. (2011)). Knowledge from the different scientific disciplines involved has to be combined for the development of this new ground improvement technique.

2.1. BIO-MEDIATED SOIL IMPROVEMENT TECHNIQUES

Bio-mediated soil improvement comprises the use of biological processes for improving engineering properties of soils. There a number of different on-going investigations that involve specific biological processes within this relatively young discipline of geotechnical engineering. Some techniques aim at improving strength, stiffness, compressibility and permeability characteristics by means of soil cementation (DeJong et al., 2010). The cementation can be achieved by means of calcium carbonate precipitation from organic processes. Two biological processes that are used for this type of ground improvement, often called microbial induced calcite precipitation (MICP), are urea hydrolysis and denitrification (Andrag, 2017). Urea hydrolysis has been successfully implemented by van Paassen et al. (2010) during large-scale field experiments to improve the stiffness of a soil body.

Denitrification based MICP is a two-stage process that includes a desaturation stage and a precipitation stage. It might therefore also be called microbial induced desaturation and precipitation (MIDP). Denitrifying bacteria convert nitrogen oxides (NO_x) to molecular nitrogen (N_2) under anaerobic conditions. Nitrogen gas bubbles are produced which replace a part of the pore water and thereby desaturate a soil. The pH is rising during the process of denitrification as a result of the production of bicarbonate (HCO_3^-). The pH can be buffered by adding calcium (Ca^{2+}) to the process which results in the precipitation of calcium carbonate ($CaCO_3$) and production of acidity.

Denitrification-based MIDP has been extensively studied by Pham (2017). The potential of this method in altering hydro-mechanical behavior of sandy soils has been confirmed through laboratory experiments. The nitrogen gas produced during the first stage of MIDP can be used to bring fully saturated soils close(r) to optimum conditions in terms of water content. Energy requirements for subsequent compaction activities are expected to be reduced as a result of the microbial induced desaturation (MID).

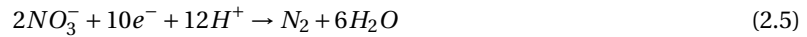
2.2. PRINCIPLES AND CONTROLLING FACTORS OF DENITRIFICATION

Denitrification is a microbial process that involves the dissimilatory reduction of one or both of the ionic nitrogen oxides (nitrate or nitrite) by facultative anaerobic bacteria, ultimately resulting in molecular nitrogen (N_2). This process takes place in the terrestrial biosphere and is part of the so-called nitrogen cycle (Ambus and Zechmeister-Boltenstern, 2007). The nitrogen oxides act as terminal electron acceptors in the absence of molecular oxygen (O_2), which is a more energetically favourable acceptor (Robertson and Groffman, 2015).

Nitrate (NO_3^-) and nitrite (NO_2^-) are the result of nitrification, which is an aerobic process that involves the oxidation of ammonia to nitrite and from nitrite to nitrate. Nitrification is performed by autotrophic bacteria (self-nourishing organisms), while denitrification is mainly performed by heterotrophic bacteria (organisms that depend on nutrition from other sources (Ashton Acton, 2013)). The pathway from nitrate to nitrogen is labeled as oxidative metabolism and involves the reduction of oxidized nitrogen compounds. Organic matter acts as electron donor during this process and is oxidized, which releases energy. The nitrogen compounds act as electron acceptor and are reduced. The relevant half reactions of reduction are given by Equation 2.1 to Equation 2.4.



The net balance redox reaction can be expressed as shown in Equation 2.5.



Specific enzymes are involved in each reduction step. There are therefore four different enzymes involved in the reduction of nitrate to nitrogen gas. The enzymes are also called reductases. There is another pathway possible for dissimilatory reduction of nitrate which results directly in the formation of ammonium (NH_4^+). This pathway is labelled as fermentative metabolism and is often abbreviated as DNRA, which stands for dissimilatory nitrate reduction to ammonium. The redox potential for reduction of nitrate to ammonium is lower than for oxidative metabolism, but fermentative metabolism can become the dominant pathway of reduction if nitrate ammonifiers out-compete denitrifiers. This may happen if the availability of nitrate is limited compared to organic carbon (van den Berg et al., 2016). In other words, this depends on the carbon to nitrate ratio. The two pathways for dissimilatory reduction of nitrate, denitrification and ammonification, are illustrated in Figure 2.1

Ammonia (NH_3), which is a primary pollutant in waste water, is oxidized to nitrate during the aeration stage of the water treatment process of a sewage plant. Denitrification is used subsequently to decrease the concentration of nitrate. Nitrification and denitrification are therefore important processes in the field of sanitary engineering. A lot of knowledge about the kinetics of denitrification has been acquired in the last few decades.

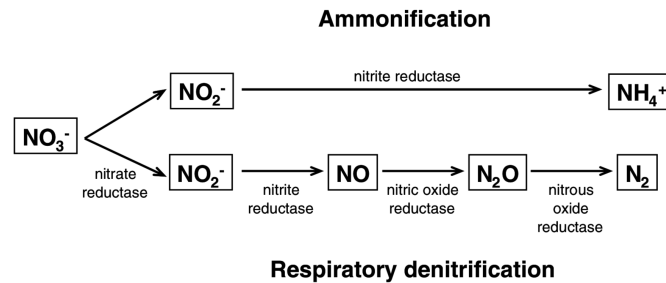


Figure 2.1: Dissimilatory reduction pathways of nitrate (Rebata-Landa and Santamarina, 2012).

2.2.1. OXYGEN

Several studies have shown that the presence of low concentrations of oxygen in soil decreases the overall rate of denitrification. The sensitivity to oxygen is somewhat stronger for the reductases involved with the last reduction steps of denitrification. This means that the nitric oxide (NO) and nitrous oxide (N_2O) reductases are significantly repressed in the presence of molecular oxygen. A larger mole fraction of nitrous oxide in the products of denitrification can be expected if conditions are not completely anaerobic (Knowles, 1982). Furthermore the presence of oxygen could trigger assimilatory nitrate reduction which results in the production of nitric oxide or ammonium as final products (van Spanning et al., 2007).

2.2.2. ORGANIC CARBON

An increase of the organic carbon concentration will result in a decrease of the $\text{N}_2\text{O}/\text{N}_2$ ratio according to Wu (2015). This means that more N_2 gas is produced relatively. Most of the denitrifying bacteria are heterotrophic, which means that the availability of organic carbon is essential for microbial activity (Braker and Conrad, 2011). It has been reported that depending on the source of organic carbon, different mole fractions of nitrous oxide can be found in the products of denitrification. Possibly different types of organic carbon influence the nitrogen reductases in a unique way, although overall rates of denitrification are similar (Knowles, 1982). Knowles (1982) also mentions that reduction shifts significantly towards ammonium in the presence of abundant carbon, provided that anaerobic conditions are maintained. The ratio between organic carbon and nitrogen (C/N ratio) also significantly influences the kinetics of denitrification. The influence of the C/N ratio on conversion efficiency will be discussed in subsection 2.3.2.

2.2.3. PH

The optimum pH for denitrification is reported to lie between pH 7.0 and pH 8.0 (Knowles, 1982). The overall rate of denitrification decreases outside of this range. Nitrogen oxide reductases are progressively inhibited

with decreasing pH. This leads to accumulation of nitrous oxide since the corresponding reductase is inhibited most significantly (Knowles, 1982). Prakasam and Loehr (1972) observed denitrification to occur up to pH 11 in wastes.

When a population of denitrifiers is supplied with the appropriate substrates (nitrate source + carbon source) under anaerobic conditions, it will often take a considerable amount of time before a significant amount of nitrogen gas is observed. The time before significant gas production is called the lag period. The lag period greatly depends on the initial pH of the environment in which the bacteria exist. The time before significant gas production will increase if the initial pH in a soil lies outside of the optimum range. In case of extreme pH conditions, no gas might be produced at all.

2.2.4. TEMPERATURE

Denitrification in soils decreases at low temperatures (<10 °C) but nevertheless continues up to the range of 0-5 °C, where larger mole fractions of N_2O and NO are found (Knowles, 1982). Dawson and Murphy (1972) report a denitrification rate at 5 °C which was 5 times smaller than the rate that was found at 20 °C from batch activated sludge denitrification tests. In addition, the initial lag period before significant microbial activity was found to increase with decreasing temperature.

Courstens et al. (2014) compared mesophilic denitrification with thermophilic denitrification by inoculating batch reactors at 34 °C and 55 °C with mesophilic activated sludge (26 °C). The mesophilic denitrifiers showed specific nitrogen removal rates that were twice as high as for the thermophilic denitrifiers. Nonetheless they found that the mesophilic denitrifiers were able to maintain their activity at 55 °C and showed significantly higher activities than reported before.

The temperature effects have to be taken into account when microbial induced desaturation through denitrification is implemented in the field, especially during the winter season in countries with relatively cold winters.

2.2.5. INHIBITORS

The term inhibitor relates here to denitrification inhibiting chemical compounds that are sometimes present in soil for specific reasons. Often these inhibitors 'entered' the soil as a result of human activity (e.g. pest control in the agricultural sector). Several inhibitors of denitrification have been identified. Although some of them inhibit only one specific reductase, it is more common to observe inhibitors exerting metabolic effects, thereby affecting multiple stages of (nitrate) reduction (Knowles, 1982).

There is also a dependency on the concentration of the inhibitor. Mitsui et al. (1964) found for example that the pesticide Vapam inhibits the reduction from nitrate to nitrogen in soils when present in a concentration of 20 parts per million (ppm) or higher. Inhibition of denitrification has to be taken into account if biogenic gas pretreatment is performed in areas where significant concentrations of inhibitors can be expected. For reclamation projects, this is most of the times not the case since the soil is often reclaimed from an offshore location. Conversely stimulation of the production of nitrate denitrifying reductases by nitrite, chlorate and azide has been reported by Calder et al. (1980) for certain bacteria species.

2.2.6. NITRATE RESPIRATION AND INTRACELLULAR COMPETITION

According to Glass and Silverstein (1998), many denitrifying bacteria, although capable of reducing nitrate to nitrite, cannot use nitrite or other reduced nitrogen as electron acceptors. Therefore a difference can be made between true denitrifying bacteria and nitrate respiring bacteria. While nitrogen gas is the end-product of true denitrifiers, nitrate respiration results in accumulation of nitrite as this is the most reduced product that these bacteria can produce. If both types of bacteria are present, nitrite will accumulate when the nitrate respiring population is growing more rapidly than the true denitrifying population.

Another explanation for the accumulation of nitrite during denitrification can be addressed to the observed intracellular competition between nitrate reductase and nitrite reductase (Wilderer et al., 1987) as the first one is preferred over the latter one as electron acceptor. Finally, Van Rijn et al. (1996) observed that for *Pseudomonas stutzeri*, a greater accumulation of extracellular nitrite occurred when supplying the bacteria with relatively oxidized substrates.

2.3. MICROBIAL GROUND IMPROVEMENT THROUGH DENITRIFICATION

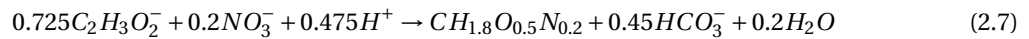
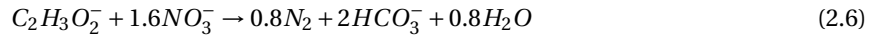
Denitrification is an important subject in various academic disciplines (e.g. biology, sanitary engineering, agriculture). As a result of this, a significant amount of knowledge has been gained through the years about

the kinetics of denitrification. In order to optimize the proposed biogenic gas pretreatment of saturated soils, this knowledge has to be used to develop an efficient strategy for field implementation. Field conditions such as the in-situ state of the soil, pH environment and temperature have to be taken into account and the engineered substrate solution has to be tuned based on these conditions. The overall strategy that is developed for biogenic pretreatment should allow for the controlled and predictable development of a specific volume of nitrogen gas, without accumulation of harmful compounds and contamination of the environment.

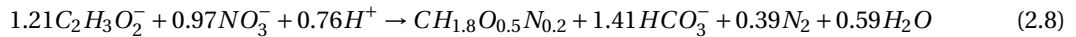
2.3.1. REACTION STOICHIOMETRY

Denitrification is the biological process that involves the breakdown of organic matter and dissimilatory reduction of nitrate by microbes and the production of biomass. This natural process can be stimulated in a laboratory environment by means of a bacteria enrichment. Essentially, denitrifying organisms need to be supplied with sufficient amounts of organic carbon source, nitrate source and nutrients. Anaerobic conditions have to be maintained because assimilatory reduction of nitrate may occur in the presence of oxygen.

The objective of a bacteria enrichment is to stimulate the production of biomass, it is therefore necessary to take a look at the stoichiometry of the relevant metabolic reaction. The stoichiometry of the metabolic reaction depends on the amount of energy that is generated by catabolism and the production of biomass by anabolism. The carbon energy source is converted by microbes to generate energy, this is expressed by the catabolic reaction. This energy can be used to create new biomass, and this is expressed by the anabolic reaction. If acetate ($C_2H_3O_2^-$) is used as electron and carbon donor, the catabolic and anabolic reaction will look like as in Equation 2.6 and Equation 2.7 respectively (Pham et al., 2016).



If maximum growth conditions are considered, the metabolic reaction can be provided by solving the energy balance (Equation 2.8, Pham et al. (2016)). The stoichiometric coefficients for maximum growth can be derived from this metabolic reaction. Equation 2.8 shows that the acetate-nitrate ratio (Ac/N ratio) for maximum growth conditions is equal to approximately 1.25.



The actual growth rate of biomass depends on the prevailing environmental conditions such as availability of nutrients and substrates. Also inhibiting compounds have to be considered. Macro-nutrients and micro-nutrients are normally added in laboratory experiments to avoid limitation of nutrients during bacterial growth. The pH rises as a result of denitrification, calcium is therefore added to the process. The bicarbonate produced by denitrification reacts with calcium to form calcium carbonate (Equation 2.9), which increases the acidity and therefore serves as buffer mechanism.



2.3.2. AC/N AND C/N RATIO

First thing that should be noted is that there is a significant difference between the supplied acetate/nitrate (Ac/N) ratio and the consumed Ac/N ratio. Pham (2017) observed that the most efficient supply ratio lies at 0.8. With this ratio all substrates were consumed most efficiently and the residual nitrate, acetate and calcium were limited. Lower Ac/N ratios resulted in accumulation of nitrite and other harmful intermediates, while higher Ac/N ratios resulted in significant amounts of residual acetate and calcium. According to Pham (2017), maximum growth stoichiometry lies at an Ac/N ratio of 1.25. Pham (2017) also observed that a high carbon/nitrogen (C/N) ratio positively affected the complete conversion of nitrate to nitrogen gas and limited the nitrite accumulation, while a low C/N ratio resulted in residual nitrate and accumulation of nitrite.

2.3.3. CONCENTRATION OF SUBSTRATE

Andrag (2017) assessed the efficiency of bio-mediated soil pretreatment with experiments in a Rowe cell and used a bacterial inoculum that originated from the Delft University of Technology's botanical garden. All the treatment regimes used during these experiments had a calcium-acetate-nitrate (Ca-Ac-N) composition of 36.5-39.9-33.2 mM, which is relatively low in terms of substrate concentrations. This corresponds with an

Ac/N ratio of 1.2 approximately, which is close to the stoichiometry of maximum growth (1.25). The accumulation of harmful intermediates in these experiments was limited.

Pham (2017) observed strong inhibition of denitrification as a result of nitrite accumulation when using a relatively high concentration of substrate solution in liquid batch experiments. The relatively high initial concentrations caused the Ac/N consumption ratio to approach the lower limit of 0.6, corresponding to stoichiometry conditions of pure maintenance. The Ac/N consumption ratio approached the high extreme (maximum growth) in the case of relatively low initial concentrations of substrate solution. No residual nitrite was observed at the end of the experiments. It should be noted that the initial Ac/N supply ratios were in fact similar.

2.3.4. GAS PERCOLATION THRESHOLD

The gas percolation threshold quantifies the amount of gas that can be maintained by a certain soil (i.e. the gas storage capacity). A continuous gas phase develops when the percolation threshold has been reached through the production of gas. Additional gas production will result in the escape of gas bubbles from the soil. The intended pretreatment might not be ultimately effective if the volume of gas that has to be produced to reach the optimum saturation lies above the percolation threshold. A reduction of compaction energy can, however, still be expected for most soils since the dry density increases with decreasing moisture content on the wet side of a compaction curve. The threshold depends on the confining pressure and the pore size distribution of the soil (Pham, 2017).

2.3.5. CALCITE PRECIPITATION

Calcium is added to the substrates to buffer the pH during denitrification. From Equation 2.9 it can be seen that protons are released when calcium and bicarbonate react to precipitate calcium carbonate. Calcium carbonate precipitation has to be taken into account for the proposed two-stage process of biogenic pretreatment and compaction. If the amount of calcium carbonate precipitation is limited, there is no significant buffering effect and the pH will increase excessively. This will result in nitrite accumulation and a reduced rate of denitrification. On the other side of the coin, soil strength can be increased by means of the calcium carbonate bonds formed between individual grains. A higher soil strength before compaction is obviously not desired for the two-stage process that is assessed in this research. However, Andrag (2017) showed that the amount of calcium carbonate precipitation is very limited when relatively low substrate concentrations (Ca-Ac-N = 36.5-39.9-33.2 mM) are used. Andrag (2017) found that less than 0.1% (by mass) of the treated specimens consisted of calcium carbonate at the end of the tests. The cementation effects are therefore negligible.

van Paassen et al. (2010), predicted that calcium overloading might result in inhibition of one of the reduction steps of denitrification, which leads to accumulation of intermediates. This was confirmed by Ivanov and Stabnikov (2016), who found that denitrification inhibited with dissolved calcium concentrations above 0.05 M.

2.3.6. EXPANSION OF SOIL SKELETON

If biogenic pretreatment were to be applied at relatively shallow depths, the production of nitrogen gas might result in expansion of the soil skeleton. This counter-acts the effectiveness of biogenic pretreatment for reducing the energy required for compaction activities. Expansion of the soil skeleton signifies a decreased density of the soil mass, which means that a certain amount of compaction energy is required to bring the soil mass back to its initial density.

Expansion of the soil skeleton is not expected to be an issue on most reclamations or landfill projects, because the soils that require a pretreatment are normally not very close to the surface. Sufficient counter-pressure is provided by the overlying soil. There was no expansion of the soil skeleton observed by Andrag (2017), who used a Rowe cell to assess the feasibility of biogenic pretreatment of silty sands and set the pressure conditions in the cell to represent conditions at 5 meters depth (total vertical pressure = 100 kPa and pore pressure = 50 kPa).

2.3.7. ACCUMULATION OF HARMFUL INTERMEDIATES

The intermediates of denitrification are nitrite, nitric oxide and nitrous oxide in order of most to least thermodynamically favorable. Accumulation of these intermediates is undesirable since all of them are harmful to organisms and the environment. Moreover, high concentrations of intermediate products are toxic to den-

itrifying bacteria according to van Spanning et al. (2007). Nitrous oxide might accumulate at low pH values, but this is not in the range of pH values expected to be normally encountered in the field. According to concentration measurements done by Betlach and Tiedje (1981), accumulation of nitrite is most of the times way more significant than accumulation of nitric oxide and nitrous oxide. Nitrite accumulation can be minimized by choosing a suitable Ac/N ratio and concentration for the substrate solution.

2.4. DISTRIBUTION OF THE GAS PHASE

The nitrogen gas that is produced by biogenic pretreatment, lowers the water content of soils as water is expelled from the pore space. The compressibility of the soil can be increased, because part of the nearly incompressible pore fluid (water) is replaced by a highly compressible medium (air). Rebata-Landa and Santamarina (2012) describes this as pore fluid softening. The compaction curve has to be taken into account since compressibility will decrease again with decreasing water content on the dry side of the compaction curve.

Another factor that has to be taken into account for biogenic pretreatment is the distribution of the gas phase. The compressibility and therefore the achievable final dry density of a pretreated soil depend on how gas bubbles are distributed throughout the medium. A homogeneous distribution of small bubbles is desired. Gas injection, which is an alternative desaturation method, will often result in percolation of air bubbles along preferential paths formed by large interconnected pore throats (Rebata-Landa and Santamarina, 2012). Gas generation by electrolysis is also proposed as desaturation method. Hydrogen and oxygen gases can be generated by sending a current through an electrode. The amount of gas generated, and thus the degree of saturation, can be controlled by regulating the electrical current. Arriving at a homogeneous distribution of gases with this method is, however, challenging because gases are generated close to the electrodes (Gokyer, 2009).

Predicting or controlling the distribution of the gas phase in the case of biogenic pretreatment is rather complex. The gases produced by denitrifying bacteria will initially dissolve in the pore fluid until the supersaturation threshold is reached after which bubble nucleation will occur. The supersaturation threshold depends on the gas concentration in the fluid and the gas concentration that is soluble in the liquid under the prevailing conditions (Rebata-Landa and Santamarina, 2012). A distinction can be made between homogeneous and heterogeneous bubble nucleation (Rebata-Landa and Santamarina, 2012). In porous media, bubble nucleation will generally occur at lower supersaturations due to the presence of mineral surfaces, this is termed heterogeneous bubble nucleation. In batch experiments homogeneous bubble nucleation is dominating since a limited amount of nucleation centers is available. At the supersaturation threshold, the pore water pressure approaches the pressure in the gas. The concentration of dissolved gas depends on the partial pressure of the gas and can be calculated using Henry's Law. The stability of the bubbles depends on their size. A critical radius ($r_{critical}$) can be defined at which bubbles are stable and will not redissolve into the pore fluid (Lubetkin, 2003). Equation 2.10 can be used to calculate the critical radius based on the surface tension (T_s), supersaturation (ψ) and pressure at which bubbles nucleate (u_n).

$$r_{critical} = \frac{2 \cdot T_s}{\psi \cdot u_n} \quad (2.10)$$

Stable bubbles can migrate through the porous medium as a result of pressure gradients and might coalesce with other bubbles to form larger bubbles. This way small bubbles can continuously 'feed' the larger bubble until it becomes trapped at pore throats. This is an important mechanism affecting the spatial distribution of the gas phase and might significantly affect the compressibility of the porous medium.

Denitrifying bacteria are responsible for the production of molecular nitrogen. The production of nitrogen gas essentially means the production (or nucleation) of bubbles. The growth rate and production rate of these bubbles will influence the spatial distribution of the gas phase. It is therefore important to take bacterial activity into account when considering the spatial distribution of the gas phase because the rate of gas production essentially depends on the activity of the denitrifying bacteria. The rate of gas production can be influenced by controlling the amount of substrates supplied to the bacteria but will also depend on the concentration of biomass. The spatial distributions of biomass and substrates are also of major influence on the distribution of the bubbles. If the distribution of biomass is non-homogeneous and large concentrations are present in certain areas, the gas production in these areas will be higher, thereby influencing the distribution of gas bubbles. A highly heterogeneous distribution of bacteria is not expected for existing in-situ bacteria. When micro-organisms are injected in a soil, the homogeneity of distribution has to be taken into

account. In conclusion, controlling the spatial distribution of the gas phase in the field brings about numerous challenges. Well developed injection strategies have to be used to ensure a homogeneous distribution of gas bubbles when soils are treated in-situ.

2.5. COMPACTION ACTIVITIES ON SOILS

Compaction activities are employed to improve soils and thereby preparing them for future conditions. Ground improvement might be required to prepare reclaimed areas or landfills for the construction of infrastructure or residential and industrial structures. According to Multiquip (2011), objectives of compaction can be summarized as:

- Increasing load-bearing capacity
- Preventing soil settlement
- Providing stability
- Reducing water seepage, swelling and contraction

Compaction forces can be applied in two ways: statically or dynamically. Static compaction methods are rarely used for ground improvement of granular reclamations or landfills as the influence depth is typically very limited. Dynamic compaction methods are significantly more effective for ground improvement of granular deposits. The higher energy levels produced with dynamic compaction are usually considered necessary to compact granular materials, although this is mostly based on experience. Static loading might be applied in areas with thick natural clay deposits as surcharges at ground level to induce settlement. This can be described as compaction by means of consolidation. Consolidation is the controlling process. Vertical drains are often used in combination with surcharges at ground level to accelerate the consolidation process. Dynamic or vibratory compaction methods are widely in use to perform ground improvement and a large variety of different dynamic techniques have been developed throughout the years, the most famous ones considerably being impact compaction and vibro compaction.

2.5.1. PROBLEMATIC SOILS

Keller Holding GmbH is a German ground engineering specialist that has decades of experience in the field of ground improvement by vibro compaction techniques. They produced the graph shown in Figure 2.2, which illustrate the limits of application for deep vibro techniques. The two vibro techniques that are shown, replacement and compaction, are used to improve the engineering properties of soils. Vibro compaction is effective in granular soils with a low fines content, vibro replacement is required in cohesive soils and granular soils with a high fines content. Andrag (2017) states that compaction is often debated in fully saturated fine-grained soils with fines content above 10-12%. A transition zone is shown in Figure 2.2, if this zone can be moved to the left by pretreating soils, the limit of application for vibro compaction could be extended. Since vibro replacement techniques are extremely costly, it would be interesting to investigate the feasibility of such a pretreatment.

Typically, sandy silt or silty sand mixtures are present in land reclamation projects as a result of the segregation caused by the weight differences of sand and silt. The particle size distribution of these mixtures are often found to lie within or close to the transition zone of Figure 2.2 and therefore affect the efficiency of compaction activities.

Layers or lenses of fine material are often encountered in reclamations and reduce the effectiveness of compaction effort on the material below these zones of fine material. The quality of a reclamation and effectiveness of compaction activities are often assessed by comparing the results from cone penetration tests (CPT) before and after ground improvement. By looking at these results the effect of these zones of fine material can be observed. Figure 2.3 shows the processed CPT results from a reclamation project in Asia.

The rightmost chart is a so-called I_c chart and provides a soil behaviour type classification based on the cone penetration test (Robertson and Wride, 1998). The soil behaviour type index (I_c) can be calculated from the parameters obtained during a cone penetration test. According to the soil type index legend provided by Robertson and Wride (1998), a soil is no longer classified as sand but as sand mixture (silty sand to sandy silt) when the soil behaviour type index is higher than 2.05 (and lower than 2.60). The efficiency of compaction activities might be significantly reduced for soils with a soil behaviour type index above this boundary. For this particular project, soils with a soil type behaviour index higher than 1.9 are classified as fines. Fines

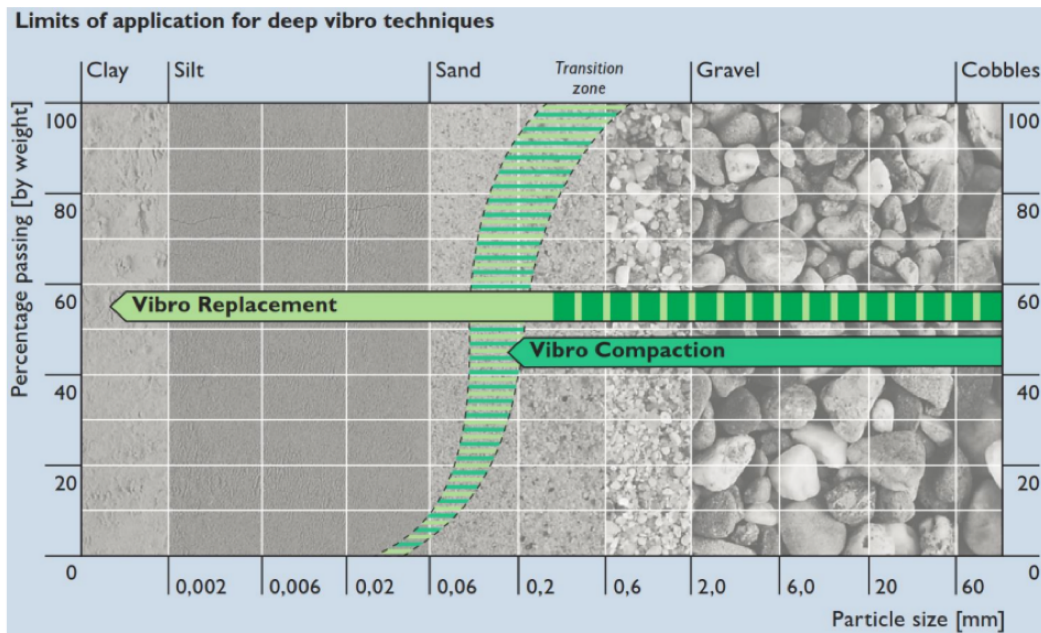


Figure 2.2: Graph produced by Keller (n.d.) GmbH to show the limits of application for deep vibro techniques.

are indicated with red rectangles in the I_c chart. The effect of these fines on the efficiency of compaction activities can be seen by analyzing the pre and post-compaction cone resistance values in the leftmost chart. The post-compaction CPT is performed after a first pass of a rapid impact compacter.

There is a clear increase in cone resistance after compaction for the first few meters. The high pre-compaction cone resistance peak at approximately 0 m MSL can be explained by the fact that only one CPT was performed before compaction and three CPT's were performed after compaction (a moving average of the three post-compaction CPT's is shown). However, according to the I_c chart there is a fines layer of approximately half a meter at -2.5 m MSL. At this depth the leftmost chart shows a sharp decrease in post-compaction cone resistance and a clearly reduced cone resistance can be observed in the sands below this depth. Below -4 m MSL even more layers with large amounts of fines are encountered. The post-compaction CPT's show only a minor increase in cone resistance for these layers. Apparently soils with a high fines content cannot be compacted efficiently and also limit the energy transfer to soils below.

Compaction activities would obviously not be required if the configuration of soils is relatively dense (high relative density) to start with. However, the deposition techniques that are commonly used to create artificial islands, for example spraying, often result in relatively loose deposits with relative densities around 30% or 40%. Excess pore water pressures are generated upon compaction of these soils due to the large fraction of fine material, which reduces the permeability. Permeability seems to play an important role with regards to the compactability of soils.

Lubking (1989) also mentions the influence of the shape of grains and surface roughness of sand particles. Well-rounded particles will rearrange themselves more easily into a denser configuration during load application because of the low degree of particle interlocking. More angular particles will experience more friction during loading (higher friction angle). So, in terms of compactibility, it is expected that well-rounded particles are easier to compact than more angular particles. At the same time, it could be argued that during an unloading phase, the more angular particles will experience smaller elastic strain (rebound) when compared to rounded particles due to this higher degree of particle interlocking.

2.5.2. WATER CONTENT VERSUS DRY DENSITY

The relationship between water content and dry density is a helpful tool for assessment of land reclamations in terms of relative density. Proctor tests are performed to construct compaction curves, which show the relationship between water content and dry density of a soil for a given input of compaction energy. By comparing the results from in-situ density tests (e.g. nuclear density method or sand replacement method) with the compaction curve from a proctor test, the relative density can be determined. The shape and position of

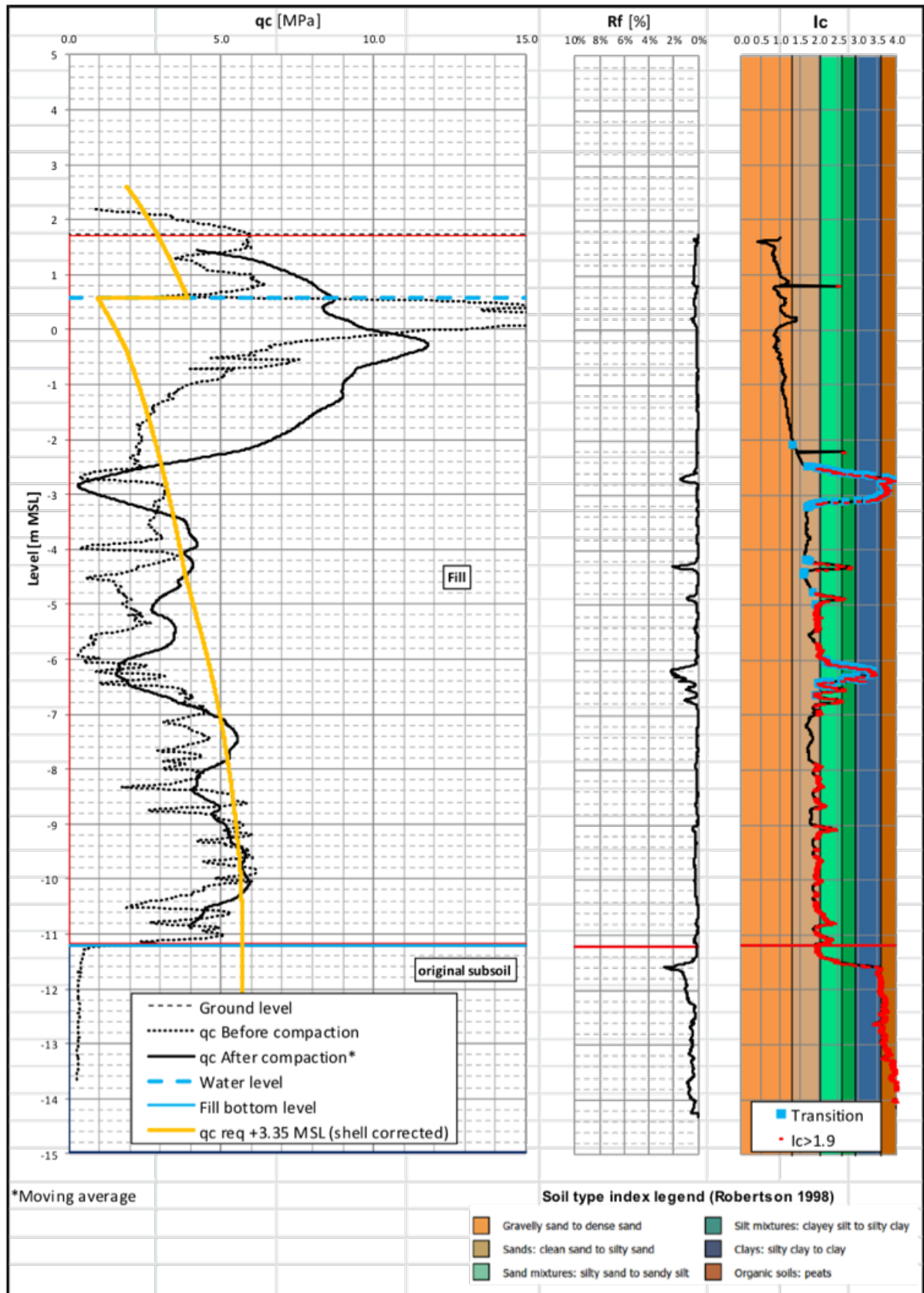


Figure 2.3: Processed CPT results from reclamation project in Asia.

a compaction curve depend on the type of soil and its particle size distribution.

The steepness of the compaction curve generally increases when going from a coarse-grained soil (gravel) to a fine-grained soil (clay), as can be seen in Figure 2.4. As the steepness of the curve increases, the effect of water content on dry density increases. In general it can be stated that an induced change in water content could result in a significant change in dry density for a given amount of compaction energy when dealing with a clay, but will only result in a minor change of dry density in the case of a gravel. From Figure 2.4 it can also be seen that the compaction curve moves up and to the left when going from a clay to a gravel. For a given amount of input compaction energy, the maximum dry density for a gravel is thus significantly higher than for a clay, the exact opposite can be said with regards to the optimum water content.

When looking at the effect of water content on compaction behaviour, a clear distinction can be made between granular and cohesive soils. According to Bergeson and Jahren (1999), many granular materials have a maximum dry unit weight at either the completely dry or nearly saturated condition. In between these two extremes, lower dry unit weights are obtained. These lower dry unit weights can be explained by a phenomenon called bulking (Hilf, 1991). Capillary tensional stresses develop under low water content at the water-air interface and hold the soil particles in place. This impedes the effectiveness of compaction activities. The high efficiency of compaction at the nearly saturated condition applies only to free-draining soils while the efficiency of compaction at the completely dry condition seems to be high for granular materials with up to 30 percent of fines (Forssblad, 1981). Uniform soils are the exception to this trend. Since particle sizes fall within a close range for uniform soils, the amount of rearrangement is too limited. This implies a small dependency of dry unit weight on water content (Parsons et al., 1992).

Obviously most natural soils will not consist solely of clay-sized particles or sand-sized particles. It is therefore necessary to look at the effect of the particle size distribution or soil gradation on the shape and position of the compaction curve.

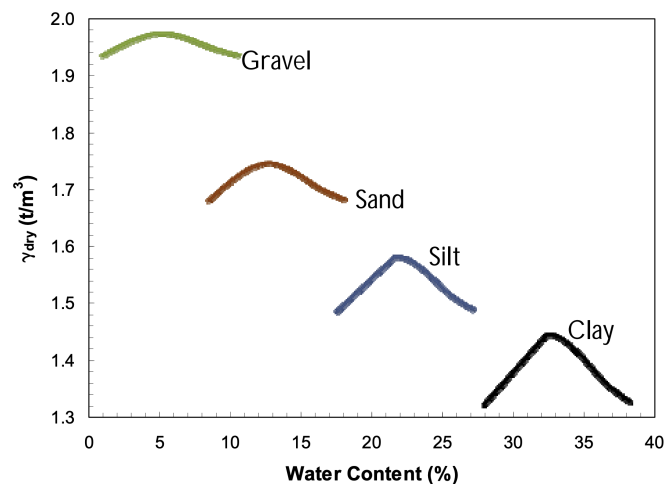


Figure 2.4: General compaction curves for different soil types (Salem, 2010).

Soil gradation is a geotechnical property that acts as indicator of other (geotechnical) engineering properties such as compressibility and conductivity. There are three main categories that can be defined with regards to soil gradation. Well graded soils, poorly or uniformly graded soils and gap graded soils. Well graded soils contain an entire range of different particle sizes, uniformly graded soils contain only one small range of particle sizes and gap graded soils contain two small ranges of particle sizes.

Well graded and gap graded soils can in principle be compacted to a higher dry density than poorly graded soils. In well graded or gap graded soils, finer particles (e.g. silt) will fill up the voids between the coarser particles (e.g. sand) upon compaction, thereby increasing the dry density. In a poorly graded sandy soil, particles can be rearranged into a denser configuration, but as no other grain sizes are present, the voids between the sand particles cannot be filled. Maximum dry densities that can be achieved after compaction are thus generally lower for poorly graded soils when compared to well graded soils.

The compaction curve of poorly graded soils are often more flat than for well graded soils. Changing the water content of the soil thus has no significant effect on the dry density that can be achieved. Still this insensitivity to water content cannot be explained by only considering soil gradation. The mean grain size and the

related permeability play an important role as Figure 2.4 indicates. A high fraction of fines in a coarse soil will also significantly affect permeability and the sensitivity of unit dry weight to water content. If water can drain easily from the soil during compaction activities, vibrations (i.e. energy) are more effectively transferred to the soil skeleton, thereby inducing rearrangement of soil particles. Excess pore pressures will develop in less pervious (e.g. cohesive) soils as the compaction energy is absorbed by the pore water. This counteracts the compaction activities.

Drnevich et al. (2007) mentions a clear difference in the effect of water content on compaction behavior between free-draining granular soils and cohesive and semi-pervious soils. The maximum dry unit weights and optimum water contents are well defined for cohesive and semi-pervious soils, while free-draining granular soils often show relatively flat compaction curves with multiple, gentle optima in terms of water content.

Figure 2.5 shows the standard compaction curves for typical fine soils from literature. The saturation contours are based on a specific gravity (G_s) of 2.65 g/cm^3 . A relatively flat compaction curve can be recognized for the fine uniform sand that was reported by Head (2006). This corresponds with the earlier mentioned information from literature. Based on this figure it can be argued that the saturation corresponding with the optimum water content, typically lies around 80% saturation for fine soils. The 80% saturation contour is indicated with a red color.

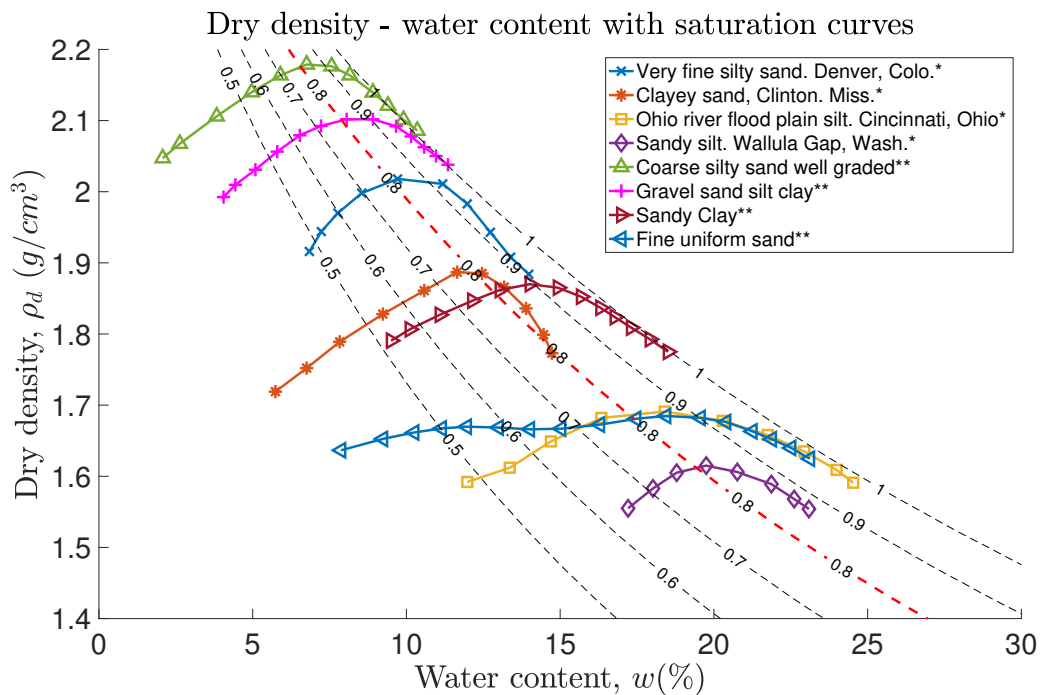


Figure 2.5: Standard proctor compaction curves for fine soils from literature (saturation contours for $G_s = 2.65 \text{ g/cm}^3$).

*From Terzaghi et al. (1996)

**From Head (2006)

***From Gallage et al. (2016)

3. METHODOLOGY

The potential of the denitrification-based pretreatment can be assessed by evaluating the energy requirements for compaction of a soil. If microbially treated and untreated soil samples are subjected to the same loading regime, the energy requirements for reaching a certain target density can be compared. This way, efficiency of the pretreatment can be assessed. A (hydraulic) Rowe cell is used to perform this assessment. Samples can be statically loaded with a constant strain rate in the Rowe cell by using a flow rate controller. The pressure development in the loading diaphragm of the Rowe cell can be monitored and represents the effort that is needed for compaction. Energy requirements can be derived from this.

3.1. SELECTION OF SOIL SAMPLE

Care should be taken when selecting a sample material for the envisioned experiments. Compaction activities are often found to be inefficient on soils with a relatively high fines content. Ideally, a representative ‘problematic’ soil from a project is obtained and used in the laboratory experiments to assess the efficiency of the biogenic pretreatment. It is unfortunately not possible to acquire such a soil. Therefore an alternative solution is sought.

A number of different aspects has to be taken into account for the selection of the soil. Since it is the intention to desaturate the soil to a saturation close to the optimum water content, it has to be assured that this goal is in fact achievable. It is therefore necessary to study the compaction curves of the sample material.

Andrag (2017) used denitrifying bacteria to desaturate fully saturated soils in a Rowe cell under in-situ stress conditions. The soil samples that were used during the experiments consisted of an industrially manufactured uniformly graded fine sand (Geba - Sibelco Benelux) mixed with different fractions of silica flour silt (M6 MILLISIL - Sibelco Benelux). Proctor compaction tests (BS 1377: 1990: Part 4) performed by Andrag (2017), showed an optimum water content at a relatively low degree of saturation (<80%). During the Rowe cell experiments it was found that the optimum water content of the sample material could not be reached with the microbial pretreatment. Gas started venting from the soil sample before reaching the optimum water content. The gas storage capacity of the sample material was therefore not sufficient to allow for reaching the target saturation corresponding with the optimum water content.

For the current research, it is decided to first perform standard proctor compaction tests with an automatic compaction machine on samples with the same composition as the ones used by Andrag (2017) to confirm the low optimum degree of saturation.

Next, an additional series of standard proctor compaction tests is performed, using different types of sample material and sample compositions. Table 3.1 shows the different sample materials that are assessed during the series of proctor tests. The aim is to find a suitable material for the envisioned experiments with a compaction curve that shows an optimum degree of saturation equal to or higher than 80%. A relatively flat compaction curve is not desirable because this indicates that the maximum dry density that can be achieved for the soil is not very dependent on moisture content. The specific gravity (G_s) is assumed to be equal to the particle density (density of water = 1 g/cm^3) for the materials reported in Table 3.1.

Table 3.1: Materials used during series of standard proctor compaction tests.

*Krapfenbauer (2016)

**Stewart (1992)

Name	Geba	GA39	Sluiseiland	M6	Kaolin
Type	Sand	Sand	Sand	Silt	Clay (Powder)
Origin	Industrial	Industrial	Natural	Industrial	Industrial
d50 (μm)	119*	91	200-300	30	< 2
Gs (g/cm^3)	2.65	2.65	± 2.65	2.65	2.60**

Table 3.2 presents the different compositions that are tested in a chronological sequence. The testing strategy is based on information from literature, results from previous tests and practical knowledge. The proctor compaction curves are presented in the next chapter together with an elaboration on the testing strategy and explanations for the obtained curves.

Table 3.2: List of sample compositions that are assessed with the standard proctor compaction test in chronological sequence.

	Geba	GA39	Sluiseiland	M6	Kaolin
Composition 1	92%	-	-	8%	-
Composition 2	84%	-	-	16%	-
Composition 3	-	92%	-	8%	-
Composition 4	-	92%	-	-	8%
Composition 5	30%	30%	-	40%	-
Composition 6	27%	20%	20%	30%	3%

3.1.1. COMPACTION CURVES

The final composition that is assessed during the series of proctor compaction tests, composition 6, is found to be suitable for the Rowe cell experiments. Figure 3.1 shows the standard and modified compaction curve (BS 1377: 1990: Part 4) of this sample material. The air voids content contours and degree of saturation contours are plotted in Figure 3.1a and Figure 3.1b respectively. The standard proctor curve shows an optimum water content (based on dry weight) between approximately 13.5% and 14%. This corresponds with a degree of saturation that is close to 80%. The saturation contours are based on a specific density (G_s) of 2.65 g/cm^3 . The shape of the modified compaction curve is similar to the standard compaction curve but it is shifted upwards and slightly to the left. According to literature, an increase of compactive effort will cause the optimum water content to decrease (shift to the left) and the maximum dry density to increase (shift upwards) while the corresponding degree of saturation remains almost the same. The net shift of the optimums (i.e. top of the curve) is indicated in Figure 3.1b with a red arrow. It is expected that the actual optimum water content for the modified proctor curve lies in between the two measurement points.

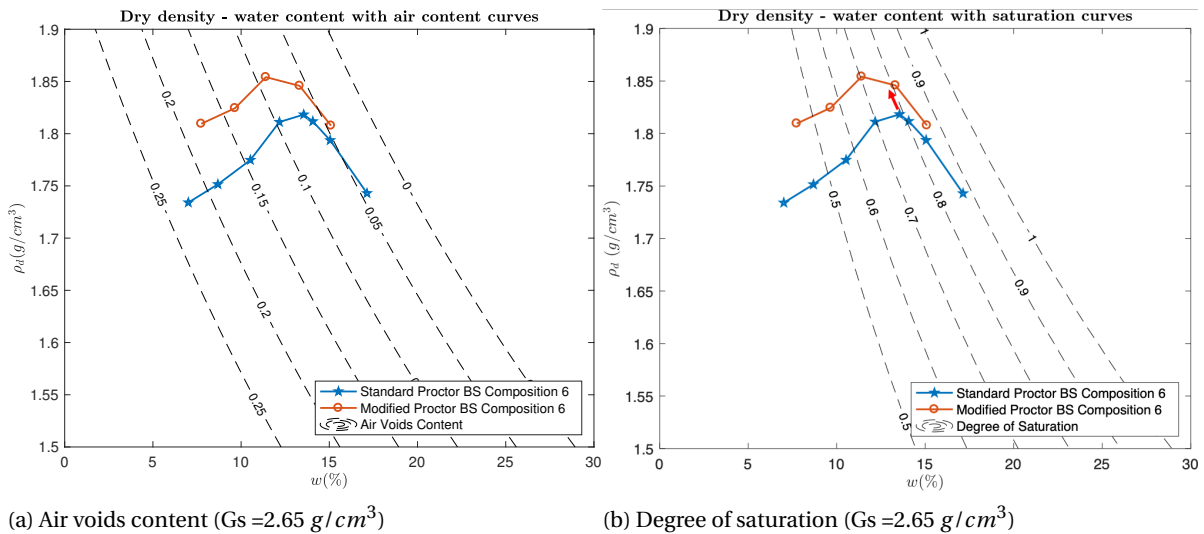


Figure 3.1: Standard and modified proctor compaction curves for composition 6.

3.1.2. PARTICLE SIZE DISTRIBUTION

The particle size distribution (PSD) of the selected soil (composition 6) is determined according to the RAW standard specified by CROW. The PSD determination includes a sieving experiment and a hydrometer analysis. The particle size distribution is shown in Figure 3.2. Further particle size characteristics can be found in Table 3.3. Fines are defined by the unified soil classification system (USCS) as particles passing the #200 sieve, which has a nominal sieve opening of 74 microns. According to the USCS, the fines percentage for this soil is therefore approximately 38%. Soils with a coefficient of uniformity higher than 6 and a coefficient of curvature between 1 and 3 are defined as well graded. If one out of two criteria is not met, the soil is defined as poorly graded. Based on the presented data the soil can be described as a silty sand.

Table 3.3: Grain diameters in μm at x% passing (D_x) and coefficients of uniformity (C_u) and curvature (C_c).

D_{10}	D_{20}	D_{30}	D_{40}	D_{50}	D_{60}	D_{70}	D_{80}	D_{90}	C_u	C_c
11	33	64	78	94	114	142	186	261	10.4	3.3

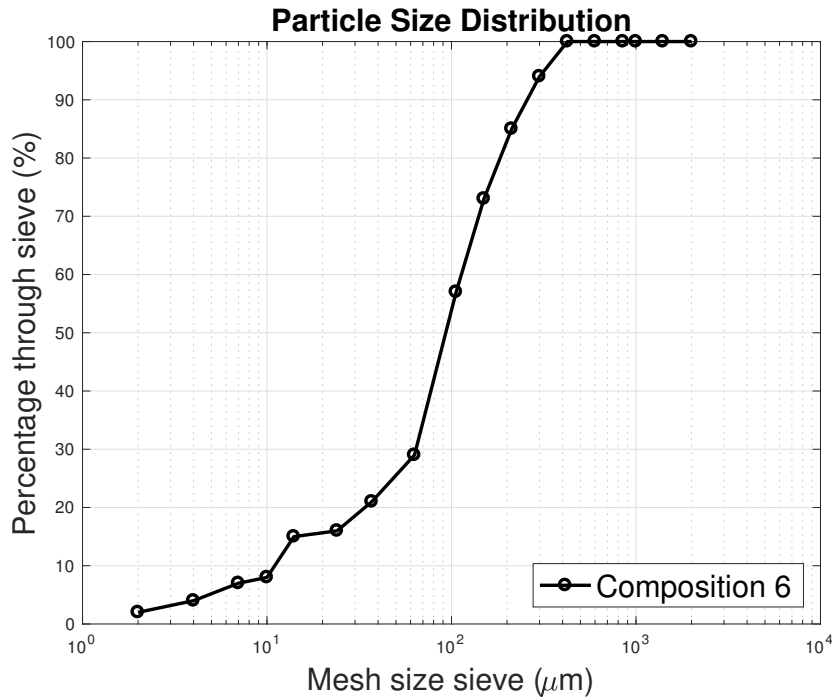


Figure 3.2: Particle size distribution of soil selected for Rowe cell experiments (composition 6).

3.1.3. DRY DENSITY LIMITS

The maximum and minimum dry density have to be determined in order to be able to evaluate compaction in terms of relative density. The void ratio and porosity corresponding to the maximum and minimum dry density can be calculated with Equation 3.1, if the particle density is known. Since the sample material consist mainly of quartz, a particle density of 2.65 g/cm^3 is used.

$$e = \frac{n}{1-n} = \frac{G_s}{\rho_d} \cdot \rho_w - 1 \quad (3.1)$$

The minimum dry density is determined according to BS 1377: Part 4: 1990 clause 4.4. The sample material is first dried in an oven for 24 hours at 105 degrees Celsius. A dry and empty cylinder is partly filled with the sample material. The minimum dry density is determined by shaking the cylinder and afterwards gently tilting the cylinder so that the material arrives in a loose state. This procedure is repeated ten times. The lowest density that is achieved is used as minimum density. The maximum dry density is taken from the modified Proctor test. Table 3.4 shows the dry density limits and corresponding void ratios.

Table 3.4: Minimum and maximum density and corresponding maximum and minimum void ratio of selected soil.

ρ_{dmin} (g/cm^3)	ρ_{dmax} (g/cm^3)	e_{max} (-)	e_{min} (-)
1.32	1.85	1.00	0.43

3.2. CULTIVATION OF DENITRIFYING BACTERIA

A bioreactor is employed for cultivation of denitrifying bacteria. Activated sludge from a wastewater treatment plant in Middelharnis, Netherlands, is used as inoculum for the cultivation experiment. The main goal

of the cultivation is to produce inoculum that can be used for the Rowe experiments to produce nitrogen gas bubbles in saturated soil samples, thereby expelling pore water and lowering the degree of saturation. The produced inoculum is also used in other supporting experiments.

Figure 3.3 shows the bioreactor that is used to realize the chemostat for cultivation of denitrifying bacteria. A chemostat describes an experimental setup that allows for the cultivation of a bacterial culture by a continuous supply of substrates and a continuous overflow of content exceeding the desired culture volume (Vazquez, 2017). This way the chemical environment in the reactor can be maintained static and the substrate availability can be controlled. The type of bacteria, dilution rate and composition of substrates determine the chemical environment. The specific growth rate of the bacteria culture can be controlled by changing the dilution rate while keeping the concentration of the supplied (limiting) substrate constant or vice versa. The specific growth rate will become equal to the dilution rate after some transient period. This also means that the biomass concentration in the reactor and effluent will become stable and equal to each other after reaching the static condition. This only applies when the maximum growth rate (or dilution rate) is not exceeded.

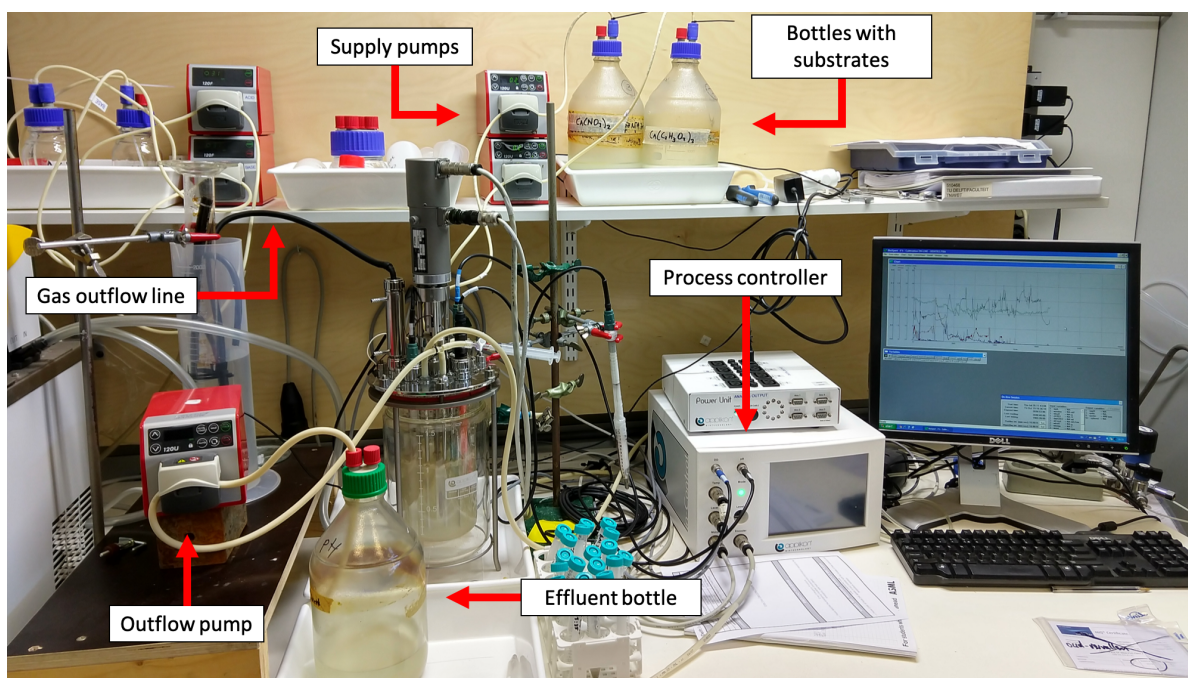


Figure 3.3: Chemostat setup for cultivation of denitrifying bacteria.

The substrates for bacterial growth of denitrifying bacteria are supplied from two air-tight 2 L bottles to the reactor. One bottle contains the nitrate source, calcium nitrate, the other bottle contains the organic carbon source, calcium acetate. Macro and micro-nutrients were initially added to the calcium nitrate substrate bottle to enable a continuous supply of nutrients. However, in a later stage it was decided to inject macro and micro-nutrients once a week directly into the reactor. It became clear that accumulations of nitrate and nitrite in the reactor could be assigned to a nutrient deficiency. The shortage of supply of nutrients from the substrate bottle can possibly be explained by a relatively low supply rate to the reactor. The list of macro and micro-nutrients and their concentrations can be found in Appendix D.

The acetate-nitrate ratio is always kept at 1.25, corresponding with maximum growth conditions (Equation 2.8). The substrates are separated to avoid premature chemical reactions. Two peristaltic pumps (Watson Marlow 120U) can be used to supply the substrates with a certain flow rate. The flow rates of the combination of pump and tubing have to be determined before starting the chemostat by setting the pumps to different speeds in terms of rotations per minute (RPM). Marprene tubing (Watson Marlow) is used for all connections on the chemostat. Marprene tubing is resistant to most chemicals and is impermeable to oxygen, nitrogen and nitrogen oxides. Nitrogen gas is continuously sparged through the culture volume to ensure anoxic conditions. An electric stirrer is attached to the cell top and can be set to different speeds to maintain thoroughly mixed conditions. Samples can be taken from the reactor with a syringe which is connected with tubing to

a connection into the culture volume. The sparged nitrogen gas and gasses produced by the bacteria move to the head space above the culture volume and can escape through a tube that leads to an upturned graded cylinder. The cylinder is partly immersed into water to maintain anoxic conditions.

Five different sensors are inserted into the culture volume to monitor the conditions in the reactor. These include a pH sensor, an electrical conductivity (EC) sensor, a dissolved oxygen (dO_2) sensor, a temperature sensor and a level sensor. The sensors are connected to a process controller (in-Control, Applikon Biotechnology), which allows for online monitoring of the conditions in the reactor. All unused connections on the bioreactor are carefully sealed to avoid oxygen infiltration.

The level sensor is used to control the culture volume. As soon as the liquid in the reactor reaches the sensor, an electrical current makes sure that the peristaltic outflow pump is switched on, which removes liquid from the reactor and transfers it to an air-tight 2 L effluent bottle. There is a risk of clogging in the outflow tube due to the transport of biomass. A slightly thicker tubing is used to avoid this. With the dO_2 sensor, anoxic conditions can be checked. If the dO_2 sensor indicates a rising oxygen level, it means that oxygen is entering the system somewhere. The pH and EC sensors are used to monitor bacterial activity. The concentration of substrates in the reactor can be followed through the EC sensor since the electrical conductivity is a function of the concentration of salts in solution. The effect of bacterial activity on the pH environment can be followed with the pH sensor. Nitrate and nitrite test strips are frequently used for a quick check of the nitrate and nitrite levels in the bioreactor. The supply pumps are momentarily stopped if the strips show a high concentration of one of the two components (or both).

The bacterial solution for the Rowe cell experiments and other supporting experiments is taken directly from the reactor (and not from the effluent) to acquire the most active inoculum. The effluent is not stirred and not sparged with nitrogen gas and for those reasons most likely less suitable for the experiments.

3.3. ROWE CELL EXPERIMENTS

A Rowe cell setup is used to determine the energy requirements for static compression of the selected soil with and without biogenic pretreatment. In-situ conditions are set before the start of the loading stage and represent the theoretical pressure conditions of a soil at approximately 5 meters depth with the ground water level very close to the soil surface. The total vertical pressure (σ_v) is therefore set to 100 kPa, assuming a volumetric weight of the soil of 20 kN/m^3 . The pore pressure (u), which can be regulated with a back pressure controller, is set to 50 kPa. This means the vertical effective stress (σ'_v) is also equal to 50 kPa. Figure 3.4 shows a schematic overview of the Rowe cell setup that is established for the experiments. The different valves are indicated with letters A to D. Connections are labeled with numbers 1 to 3. Two automatic controllers are included.

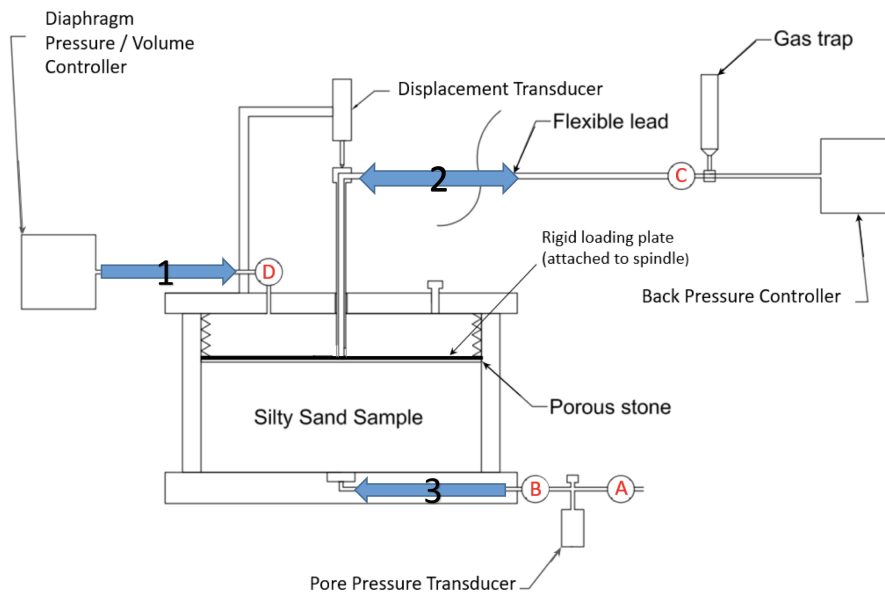


Figure 3.4: Rowe cell setup (adapted from Andrag (2017)).

The back pressure controller (VJ Technology 3000 kPa 250 cc APC) is used to apply back pressure to the soil sample. Pore pressure conditions can be regulated and drained loading conditions can be imposed during the loading stage with the back pressure controller. A gas trap is incorporated within connection 2 to capture gas escaping from the soil during the experiment. The diaphragm pressure/volume controller (Teledyne 1000D syringe pump) allows for setting not only target pressures but also target flow rates. This controller is used to saturate the soil sample after sample placement by flushing from the bottom of the cell and for application of a strain-rate controlled loading regime. Soil samples are hydraulically loaded by means of a loading diaphragm which is pressurized with the diaphragm pressure controller. Experiments are performed at 20 °C in a temperature controlled room.

3.3.1. CALIBRATION OF DIAPHRAGM

Side friction and diaphragm stiffness affect the force that is exerted by the diaphragm on the rigid loading plate on top of the soil sample. The difference between the actual force and the force calculated from hydraulic pressure and the cross-sectional area of the cell has to be determined before starting the experiments. This can be done by placing the cell body upside down on spacer blocks and removing the cell bottom as shown in Figure 3.5.



Figure 3.5: Visualization of diaphragm calibration with a load cell for measuring the actual force exerted by the diaphragm.

First the diaphragm has to be filled with de-aired water. A rigid plate has to be placed on top of the diaphragm to ensure a uniform surface. A spacer block on top of the rigid plate connects the diaphragm with the force measuring device and allows for measuring the force exerted by the pressurized diaphragm. Increments of diaphragm pressure are applied with a pressure controller that is connected to the diaphragm. The actual stress (σ) that is applied to the area of the cross section of the cell by the diaphragm (corrected for side friction and diaphragm stiffness) can be calculated with Equation 3.2, where F is the force measured by the force measuring device, m is the mass of rigid plate + spacer block and (A_ϕ) is the inner area of the Rowe cell.

$$\sigma = \frac{F + 9.81 \cdot m}{A_\phi} \quad (3.2)$$

Pressures that are stated in this report always refer to the actual forces that are exerted by the diaphragm on the rigid loading plate. This means the forces are corrected for side friction and diaphragm stiffness.

3.3.2. SETUP PREPARATIONS

The back pressure and diaphragm pressure controllers (abbreviated with BPC and DPC respectively) are first calibrated with Keller's medium-pressure-calibrator (MPX). The pore pressure transducer is calibrated by attaching one of the two calibrated automatic controllers to connection 3 and closing valve B. The controllers are prepared for the experiments by making sure no air is trapped within the controller or the attached pressure lines. The back pressure controller is partly filled with demi de-aired water and the diaphragm pressure

controller is filled with the pore fluid. Demi de-aired water is used as pore fluid for the control tests and substrate solution containing the nitrate and carbon source is used for the bio-mediated tests.

The next step is to flush inlet 3 (which leads to the porous insert at the bottom of the cell) with de-aired solution to ensure an air-free environment. The bleed screw on the pore pressure transducer is shortly opened to let the remaining air escape. A small amount of solution is left on the porous insert to avoid air infiltration. Valve A is momentarily closed to allow for determination of the mass of the empty Rowe cell. The rim drain and rigid porous disc are boiled in distilled water before use and are kept immersed in de-aired water before starting the experiment.

3.3.3. SUBSTRATE SOLUTION

The composition of the substrate solution that is engineered for the Rowe cell experiments depends on the amount of gas that has to be produced (V_g), which depends on the target saturation of the soil. Therefore, the first step is to determine the target saturation of the soil, based on which the volume of water that should be expelled can be determined. Until this point, the word saturation always related to the volume of water with respect to the total volume of pores in the soil sample expressed as a fraction, therefore it makes sense to call this the water saturation (S_w). Since the total volume of pores/voids (V_v) is eventually filled with a liquid phase (water) and a gas phase (nitrogen), it is possible to differentiate between water saturation and gas saturation (S_g). This can be expressed by Equation 3.3.

Two assumptions, suggested by Pham (2017), have to be implemented to be able to predict the gas production through denitrification in porous media:

- Nitrate (NO_3^-) is directly reduced to nitrogen gas (N_2) without accumulation of intermediates (nitrite (NO_2^-), nitric oxide (NO) or nitrous oxide (N_2O)).
- The amount of produced carbon dioxide (CO_2) is assumed to be negligible. The system mainly produces bicarbonate (HCO_3^-) due to the neutral pH.

The amount of water that should be expelled is equal to the volume of gas that should be produced. If the total volume (V_{tot}) and porosity (ϕ) of the soil sample are known, the volume of gas that should be produced to reach the target saturation can be calculated by Equation 3.4 and Equation 3.5.

$$S_g = 1 - S_w \quad (3.3)$$

$$V_v = \phi \cdot V_{tot} \quad (3.4)$$

$$V_g = S_g \cdot V_v \quad (3.5)$$

The porosity can be calculated if the dry density (ρ_d) and particle density (ρ_s) of the soil are known (Equation 3.6). It should be noted that in literature the terms bulk density and dry density are often used interchangeably. To avoid any confusion, only the term dry density will be used in this report. Dry density expresses the density of a soil as the mass of the (oven-dried) soil solids (m_d) per unit volume of the soil. When the mass of the pore fluids (i.e. water or substrate solution) is included in the density calculation of a soil, the term 'total density' will be used. Equation 3.7 and Equation 3.8 are provided for clarification and explain the terms dry density and total density respectively.

$$\phi = 1 - \frac{\rho_d}{\rho_s} \quad (3.6)$$

$$\rho_d = m_d / V_{tot} \quad (3.7)$$

$$\rho_{tot} = m_{tot} / V_{tot} \quad (3.8)$$

The molar quantity of nitrogen gas required to reach the target saturation ($n_{N_2^g}$) can be determined by implementation of the ideal gas law, provided that the pressure (P) and temperature (T) conditions are known (Equation 3.9). The ideal gas constant (R) is taken as $0.0821 \text{ L} \cdot \text{atm} \cdot \text{K}^{-1} \cdot \text{mol}^{-1}$.

$$n_{N_2^g} = \frac{P \cdot V_g}{R \cdot T} \quad (3.9)$$

The total concentration of nitrogen that is needed for the engineered solution ($c_{N_{2_{tot}}}$) can be calculated from the molar quantity of nitrogen gas required for desaturation of the soil sample ($n_{N_2^g}$). However, knowledge is required about the distribution of nitrogen in a solution. Part of the nitrogen gas will be present in a gaseous state ($c_{N_2^g}$), while the other part will be present in a dissolved state ($c_{N_2^l}$). This is expressed in Equation 3.10. The dissolved fraction of nitrogen can be calculated with Henry's law. Henry's law is shown in Equation 3.11, where $\kappa_{H_{N_2}}$ is Henry's coefficient for nitrogen gas ($1542.6 \text{ atm} \cdot \text{L} \cdot \text{mol}^{-1}$). An assumption has to be implemented to be able to use Henry's law. This assumption is as follows:

- The partial pressure of nitrogen (p_{N_2}) is equal to the pore pressure (u).

$$c_{N_{2_{tot}}} = c_{N_2^g} + c_{N_2^l} \quad (3.10)$$

$$c_{N_2^l} = \frac{p_{N_2}}{\kappa_{H_{N_2}}} \quad (3.11)$$

If the total volume of the sample is known, the gaseous fraction of nitrogen ($c_{N_2^g}$), can be calculated with Equation 3.12. Note that $n_{N_2^g}$ is calculated with Equation 3.9.

$$c_{N_2^g} = \frac{n_{N_2^g}}{\phi \cdot V_{tot}} \quad (3.12)$$

The next step is to calculate the concentration of nitrate that is required to reach the target saturation. Since the amount of nitrogen gas that is produced depends on the stoichiometry of the metabolic reaction, this has to be implemented in the next calculations. If maximum growth conditions are assumed, Equation 3.13 can be prepared with $[\frac{Y_{NO_3^-}}{Y_{N_2}}]$ equal to 2.49 ($= \frac{0.97}{0.39}$). The stoichiometric coefficients for maximum growth can be deduced from Equation 2.8.

$$c_{NO_3^- \text{ consumed}} = [\frac{Y_{NO_3^-}}{Y_{N_2}}]_{\text{maximum growth}} \cdot c_{N_{2_{tot}}} \quad (3.13)$$

Finally an acetate-nitrate ratio has to be selected in order to be able to determine the acetate concentration for the engineered substrate solution. An Ac/N ratio of 1.25 is chosen for the experiments which corresponds with maximum growth conditions (Equation 2.8).

Macro and micro-nutrients are added to the substrate solution to avoid nutrient limitation during bacterial growth. A chemical analysis is performed on the prepared substrate solution. The chemical analysis consists of concentration measurements of nitrogen-nitrate ($NO_3^- - N$), nitrogen-nitrite ($NO_2^- - N$) and dissolved calcium (Ca^{2+}) with the corresponding Hach Lange test kits (Hach Lange LCK 339, 341 & 327 respectively) and a spectrophotometer (Hach Lange DR600). Additionally, pH and EC measurements are performed with calibrated electrodes (Consort C3060). The same chemical analysis is performed on the pore fluid solution, consisting of substrate solution + inoculum, at the beginning and end of the Rowe cell experiments.

3.3.4. SAMPLE PREPARATION

There are three important criteria to be considered for the soil sample placement procedure.

- Initial density
- Homogeneity
- Reproducibility

First of all, the placement method should allow for the preparation of fully saturated samples with a relatively low initial density, representing the conditions commonly encountered in the field. Secondly, homogeneity of the samples is important. If one or multiple large cavities are present in a sample, this will influence the final results significantly. This makes the comparison of results of different experiments difficult. Finally,

the method should allow for preparing similar samples in terms of initial density and homogeneity. Reproducibility is therefore an important aspect of the placement method. It is opted to prepare samples in the Rowe cell in a partially saturated way and induce full saturation afterwards by flushing pore fluid through the porous insert at the bottom of the cell.

It is not possible to flush the denitrifying bacteria through the porous insert, therefore it is decided to mix bacterial solution from the bioreactor with the dry sample material to reach a target water content of approximately 10%. Demi de-aired water is used instead of bacterial solution for the untreated tests. Wetting of the dry sample material results in a more cohesive texture which helps in preparing relatively loose samples.

Since scooping results in lumpy and non-homogeneous samples, it is decided to use a relatively coarse sieve to prepare the samples in the Rowe cell. Sieving allows for preparation of homogeneous soil samples in the Rowe cell as can be seen in Figure 3.6. The Rowe cell is filled to the top with the sample material after which the mass of the filled cell is determined. The mass of dry sample material in the Rowe cell can be back-calculated from moisture content determinations. Samples are taken before and after filling the cell to obtain the average moisture content of the sample in the Rowe cell.



Figure 3.6: Soil sample preparation in the Rowe cell.

Next, the diaphragm pressure controller is attached to inlet 3 and the sample is saturated with the pore fluid. The prepared substrate solution is diluted during this flushing stage since the soil sample already contains a certain amount of moisture (i.e. bacterial solution). The concentrations of the substrate solution are therefore based on the previously observed water contents.

The flow rate on the volume controller is set to a low value (3 mL/minute) to avoid the development of a flow path (heterogeneity) at the lower part of the sample. The soil sample slowly collapses during the flushing stage. This collapse is caused by the loss of strength that is associated with a decreasing suction as a result of wetting. Other sample preparation methods are attempted but the preparation method that is described above is ultimately chosen because it allows for preparation of comparable samples in terms of homogeneity and initial density.

The controller is stopped when the flushed fluid almost reaches the top of the sample. The time required to completely flush the sample can be estimated by using the experience and information from earlier experiments. A small amount of solution is extracted from the sample with a syringe for a chemical analysis. The amount of extracted solution is accounted for in further calculations. After flushing, the porous disc is carefully lowered onto the sample by using fine threads, which can be removed without disturbing the sample. The initial height of the sample can be back-calculated by measuring the distance from the top of the cell to the porous disc (provided that the thickness of the porous disc is known). The space above the rigid porous disc is filled with demi de-aired water to the brim of the Rowe cell. Finally the rim drain is installed under water. The diaphragm pressure controller is subsequently detached from the pore pressure inlet after closing valve A for the remainder of the test.

3.3.5. CLOSING THE CELL

The cell top is first placed on spacers on top of the cell body, while assuring alignment of the bolt holes. The diaphragm is filled with demi de-aired water to approximately one-thirds full to be able to lower the diaphragm into the cell without creasing. Subsequently, the back pressure controller is connected to the Rowe cell with connection 2, which includes the gas trap. After that, connection 2 is flushed with demi de-aired water while lowering the rigid loading plate into the cell. The gas trap is tilted to ensure that all gas escapes.

After immersion of the rigid plate, the back pressure pump is stopped and valve C is closed. Connection 2 is now fully saturated with demi de-aired water. The diaphragm is fitted in the cell afterwards. After this, the spacers are removed and the cell top is lowered onto the cell body. Lowering of the cell top has to be done carefully since the rigid loading plate should not yet touch the sample. A torque wrench is used to tighten the bolts. This way the gaps between the metal flanges can be closed uniformly all round the perimeter. The height of the spindle can be used to determine the height of the sample in the cell. Use of the torque wrench makes this height determination with the spindle more reliable. Sample height determinations before and after closing the cell are compared afterwards.

After tightening the bolts, valve C is opened and the settlement stem is pushed downwards until the diaphragm is firmly bedded on the rigid porous disc after which valve C is closed again. Next step is to fill the diaphragm with demi de-aired water using the diaphragm pressure controller and with the bleed screw removed. The cell is slightly tilted to let all the air in the diaphragm escape. A seating pressure of 10 kPa is applied on the sample with the diaphragm pressure controller after re-installing the bleed screw. The initial height of the sample, based on the spindle height, is determined with a caliper. Finally, the displacement transducer is installed and set to zero. Figure 3.7 shows the assembled Rowe cell setup at the start of an experiment.

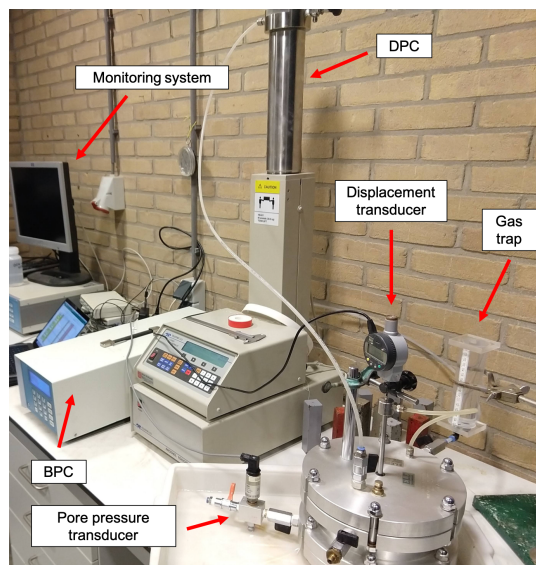


Figure 3.7: Assembled Rowe cell setup at the start of an experiment.

3.3.6. SATURATION STAGE

The saturation of the soil sample in the cell can be estimated by increasing the total vertical stress (i.e. diaphragm pressure) and following the pore pressure response under undrained conditions. The ratio between the increment in vertical stress and change in pore pressure, $\delta u / \delta \sigma$, is called the skempton B-factor and indicates how saturated the soil sample is. The British standard (BS 1377: Part 6: 1990) states that a ratio of 0.95 is usually accepted as an indication of sufficient saturation. If the B-factor is lower than 0.95, the back pressure controller can be used to saturate the soil sample by setting the back pressure equal to a value higher than the pore pressure but lower than the total vertical stress. During the first trials it is found that with the current preparation method, calculated B-factors are always above 0.95.

During the experiments the total vertical pressure is increased from the seating pressure (10 kPa) to the initial vertical pressure (100 kPa) with one intermediate step at 50 kPa. Back pressures are only applied if a significant difference between pore pressure and total vertical pressure is observed. The pore pressure has to be reduced after the saturation stage to arrive at the initial conditions ($\sigma_v = 100$ kPa and $u = 50$ kPa). This is done by decreasing the back pressure with a rate of 100 kPa per hour.

3.3.7. REACTION STAGE

The reaction stage describes the stage during which gas bubbles are generated by denitrifying bacteria. Water is expelled from the soil sample and forced through the spindle via the back pressure line into the back

pressure controller, which is kept at a pressure of 50 kPa. Gas bubbles that escape from the sample are caught in the gas trap which is connected to the back pressure line. The degree of saturation of the soil sample can be calculated from a volume balance. The following assumptions have to be applied (Andrag, 2017):

- Once initial conditions are reached ($\sigma_v = 100\text{kPa}$, $u = 50\text{kPa}$), the volume change in the back pressure controller is caused by gas production inside the soil sample.
- The sample is assumed to be fully saturated at the start of the reaction stage.
- All gas is assumed to be produced inside the soil sample.
- The gradual decrease in volume in the diaphragm pressure controller caused by leakage, allows for the equivalent volume of gas to be removed from the solution and formed in the soil sample.
- The density of the displaced pore fluid is assumed to be equal to the density of demi water.

The final assumption is assessed by Andrag (2017) with a hydrometer density test on a substrate solution with concentrations of calcium nitrate and calcium acetate of 16.6 mM and 19.9 mM respectively. The specific gravity of the substrate solution is found to be only 0.3% greater than that of demi water. The assumption can therefore be considered valid.

The degree of saturation can be calculated with Equation 3.14 where A is the air content. The air content of a soil is defined (Equation 3.15) by the ratio of volume of gas in the sample (V_{gas}) over the total volume of the sample (V_{sample}). The volume of gas in the sample can be derived from the volume changes in the pressure controllers (ΔV_{BPC} & ΔV_{DPC}) and the volume change of the soil sample (ΔV_{sample}), Equation 3.16 applies. The volume changes of the soil sample can be derived from the changes in sample height (ΔH_{sample}) measured by the displacement transducer (Equation 3.17).

During the reaction phase some gas escapes from the sample and ends up in the gas trap. The volume of gas in the sample from Equation 3.16 therefore needs to be normalized with the volume of gas in the gas trap at the end of the reaction stage ($V_{gastrap\text{eors}}$). Equation 3.18 can be used to take the volume of gas in the gas trap into account in the air content calculation. A normalized degree of saturation can be calculated by implementing Equation 3.18 into Equation 3.14.

$$S_w = 1 - \frac{A}{n} \quad (3.14)$$

$$A = \frac{V_{gas}}{V_{sample}} \quad (3.15)$$

$$\Delta V_{gas} = \Delta V_{BPC} + \Delta V_{DPC} + \Delta V_{sample} \quad (3.16)$$

$$\Delta V_{sample} = A_\phi \cdot \Delta H_{sample} \quad (3.17)$$

$$A_{normalized} = \frac{V_{gas} - V_{gastrap\text{eors}}}{V_{sample}} \cdot A \quad (3.18)$$

There is no actual reaction stage for the untreated tests with demi water as pore fluid. However during the untreated tests a certain amount of time is left between the end of the saturation stage (with sample at the initial conditions) and the start of the loading stage to let the system reach an equilibrium.

3.3.8. DRAINED LOADING AND RELAXATION

A constant flow rate can be set on the diaphragm pressure controller that is attached with connection 1 to the top of the cell. The rubber loading diaphragm can thus be filled with de-aired water while maintaining a constant flow rate. This allows for a strain controlled loading regime. The strain rate can be calculated since the flow rate ($\Delta V/\Delta t$) and loading area (A_ϕ) are known. Equation 3.19 applies where ΔS_{DPC} indicates the changes in displacements as calculated from the output of the diaphragm pressure controller.

A displacement transducer is installed at the top of spindle to check the actual strain rate. It is found that a nearly constant ratio existed between the strain rate calculated from the volume calculation of the loading diaphragm (Equation 3.19) and the strain rate calculated from the displacement transducer ($\dot{\epsilon}_{Trans}$). The

DPC strain rate ($\dot{\epsilon}_{DPC}$) needs to be corrected with a calibration factor (μ) to find the real time strain rate that corresponds with $\dot{\epsilon}_{Trans}$ as in Equation 3.20.

$$\frac{\Delta V / A_{\phi}}{\Delta t} = \frac{\Delta S_{DPC}}{\Delta t} \quad (3.19)$$

$$\frac{\dot{\epsilon}_{DPC}}{\mu} = \dot{\epsilon}_{Trans} \quad (3.20)$$

As the rubber diaphragm is filled with de-aired water and therefore expands, the pressure in the diaphragm ($P_{diaphragm}$) will increase as the soil is getting compressed and will continuously behave stiffer. The pressure in the diaphragm is monitored by the controller and gives an idea about the soil resistance against compression. The pressure in the rubber diaphragm can be expressed as compression force ($F_{compression}$) by using Equation 3.21.

$$F_{compression} = \frac{P_{diaphragm}}{A_{\phi}} \quad (3.21)$$

Valve C, which connects the soil sample with the back pressure controller, is left open during the drained loading experiments. Drained conditions can be assumed for the loading stage if the rigid porous disc and back pressure line exhibit no obstruction for water or gas leaving the soil sample.

Soil samples are loaded to a certain target density. The target density is selected after performing a series of trial experiments in the Rowe cell with untreated soil samples. After reaching the target density, the diaphragm pressure controller is set to a flow rate of 0 mL/min. The pressure development in the loading diaphragm can be followed during this soil relaxation stage. The soil relaxation stage is continued until no more significant changes in sample height or loading diaphragm pressure occur.

3.3.9. WATER CONTENT DURING LOADING AND RELAXATION STAGE

Fully saturated conditions are applied and checked during the saturation stage. The degree of saturation changes during the reaction stage of treated tests and can be calculated by means of the volume balance described in subsection 3.3.7. Once the drained loading stage initiates, this volume balance can no longer be applied as some of the liquid from around the diaphragm is displaced due to expansion of the diaphragm. Andrag (2017) suggested the following set of assumptions to be able to predict the water content during a loading stage in the Rowe cell:

- It is assumed that the soil sample remains fully saturated during the untreated tests. The assumption is verified with the volume balance and water content determinations.
- It is assumed that only liquid is displaced from between the diaphragm and the cell wall into the back pressure line.
- All the gas that is displaced from the soil sample is assumed to accumulate in the gas trap.
- It is not expected that soil particles are compressed or crushed in the Rowe cell. Sample volume changes are therefore attributed to pore volume changes.
- The displaced pore liquid is assumed to have the same density as that of water ($\rho_w = 1.0$).

The volume of the loading diaphragm will increase during the loading stage as (de-aired) water is supplied by the diaphragm pressure controller. The diaphragm can in principle only move in the downward vertical direction. This means that the displacement of the soil sample can be linked to the volume changes of the loading diaphragm. It was already noted that a calibration factor is required to be able to link these two parameters. Excess liquid is displaced from around the diaphragm during the loading stage. The volume of excess liquid (ΔV_{excess}) displaced can be calculated by comparing the volume changes of the loading diaphragm with volume changes of the soil sample as in Equation 3.22, where (ΔH_{sample}) is the change in sample height measured with the displacement transducer.

$$\Delta V_{excess} = \frac{\Delta V_{DPC}}{\mu} - \Delta H_{sample} \cdot A_{\phi} \quad (3.22)$$

The volume change in the back pressure controller (ΔV_{BPC}) is the sum of liquid displaced from around the diaphragm and the pore fluid volume (V_{pf}) displaced from the sample (Equation 3.23). Gas will also escape from the soil sample during the loading stage. For this reason the term pore **fluid** volume is used because it comprises both the gas phase and the liquid phase. A normalization that takes the amount of gas in the gas trap at the end of the loading stage ($V_{gastrap_{eols}}$) into account, is required in order to be able to calculate the saturation and water content during the loading stage, this is expressed in Equation 3.24. The changes in the normalized pore fluid volume $\Delta V_{pf_{norm}}$ represent the flow of **liquid** in or out of the soil sample.

$$\Delta V_{BPC} = \Delta V_{pf} + \Delta V_{excess} \quad (3.23)$$

$$\Delta V_{pf_{norm}} = \frac{\Delta V_{pf} - V_{gastrap_{eols}}}{\Delta V_{pf}} \cdot V_{pf} \quad (3.24)$$

The saturation development of the soil sample during the loading stage can be calculated by taking the saturation and volume of voids at the end of the reaction stage into account ($S_{w_{eors}}$ and $V_{v_{eors}}$ respectively). The saturation at the end of the reaction stage is determined with the volume balance of subsection 3.3.7. The volume of voids can be calculated from the porosity and sample volume as shown in Equation 3.25. The saturation at a certain moment during the loading stage can be calculated by adding the displaced pore fluid volume ($V_{pf_{norm}}$) at that moment to the pore fluid volume at the end of the reaction stage ($V_{pf_{eors}}$) and dividing it by the current volume of voids (V_v) (Equation 3.26). The pore fluid volume at the end of the reaction stage ($V_{pf_{eors}}$) is calculated with Equation 3.27

$$V_v = \phi \cdot V_{sample} \quad (3.25)$$

$$S_w = \frac{V_{pf_{norm}} + V_{eols}}{V_v} \quad (3.26)$$

$$V_{pf_{eors}} = S_{w_{eors}} \cdot V_{v_{eors}} \quad (3.27)$$

Finally the water content (w) during the loading stage can be calculated from the saturation with Equation 3.28, where ρ_w represents the density of water (1 g/cm^3). Subsequently the total density can be calculated with Equation 3.29, which allows for determination of the dry density (Equation 3.30).

$$w = \frac{S_w \cdot e}{G_S} \quad (3.28)$$

$$\rho_{tot} = \frac{G_S \cdot (1 + w)}{1 + e} \cdot \rho_w \quad (3.29)$$

$$\rho_d = \frac{\rho_{tot}}{1 + w} \quad (3.30)$$

There is no flow of de-aired water in or out of the loading diaphragm during the relaxation stage of the Rowe cell experiments as the diaphragm pressure controller is set to a flow rate of 0 mL/min. The volume of the loading diaphragm can in principle not change and therefore a constant strain is maintained. Since there are no sample displacements or changes in pore pressure occurring during the relaxation stage, pore fluid should not be able to enter or leave the soil sample. This means that the water content and dry density stay constant during the relaxation stage and are equal to the dry density and water content at the end of the loading stage.

3.3.10. DISASSEMBLY

After the relaxation stage, the soil sample is unloaded and the Rowe cell is dismantled. The spindle height is measured before opening the cell. The loading diaphragm has to be carefully removed in order to avoid water from the diaphragm falling into the Rowe cell. The final water content of the soil sample is determined by collecting soil from different depths of the sample. The final sample height is measured inside the cell with a caliper. Pore fluid is extracted from the treated soil sample for chemical analysis. The final nitrate, nitrite and calcium concentrations are measured and the pore fluid pH and EC-values are determined.

3.4. OxiTOP EXPERIMENTS

Bacterial activity is influenced by the environment in which the bacteria exist. There might therefore be significant differences in the rate of denitrification, lag phase and composition of produced gases in a liquid culture when compared with the situation inside the Rowe cell. In the Rowe cell bacteria are exposed to a soil environment. The influence of the soil on bacterial activity can be assessed with an OxiTop measurement system. This system consists of a number of sample bottles with measurement heads that monitor the pressure development in the headspace above a solution. The production of (nitrogen) gas can be directly linked to bacterial activity. The OxiTop measurement system can therefore be used to assess the influence of the soil material on the denitrification process. The system also allows for extraction of small gas samples to determine the composition of the produced gas.

Quadruplicate measurements are performed with the OxiTop system. Four sample bottles (the control tests) are filled with a predetermined amount of bacterial inoculum and substrate solution. The remaining four sample bottles (the soil tests) are filled with the same quantities of inoculum and substrate but also contained a small amount of the soil that is used in the Rowe cell experiments (composition 6, Table 3.2). Preliminary experiments are performed to determine the volume that is occupied by a certain mass of the soil. The soil is first mixed with the bacterial inoculum to ensure a homogeneous distribution of biomass in the soil. Next, the mixtures of bacterial solution and soil are placed in the sample bottles after which the substrate solution is added.

All sample bottles are flushed with argon gas to expel any nitrogen gas and other gases before closing the bottles and starting the experiment. Stirring magnets are used for continuous mixing of the solutions in the sample bottles. Only small amounts of soil can be added to the bottles because otherwise the stirring magnets will not be able to keep the soil particles in suspension. Without continuous mixing of the soil, gas bubbles will get trapped and pressure developments in the head space will not be measured, provided that the soil does not heave.

A large batch of substrate solution is prepared for the OxiTop experiment. A sufficient amount of bacterial solution is extracted from the chemostat bioreactor shortly before preparation of the sample bottles. All bottles are filled with equal amounts of substrate and inoculum. The targeted concentrations and volumes are listed in Table 3.5. The maximum pressure in the head space of the bottles that can be measured with the OxiTop system is 35 kPa. The nitrate concentration that is listed in Table 3.5 is based on a conservative estimation of gas production (and pressure generation) in order to stay below the maximum pressure limit. Gas samples are taken approximately 2 days and 7 days after starting the experiment to evaluate the composition of the produced gas. The concentration of the two most important products of denitrification, carbon dioxide (CO_2) and nitrogen gas (N_2), can be measured with the available gas chromatograph (Agilent Technologies 7890A). The OxiTop bottles are placed in a temperature controlled room during the experiment, which is set to a temperature of 20 °C. The Rowe cell experiments are performed at the same temperature. The concentrations of nitrate, nitrite and dissolved calcium are measured at the beginning and end of the experiment with Hach Lange test kits (Hach Lange LCK 339, 341 & 327 respectively), using a spectrophotometer (Hach Lange DR 6000). Additionally, pH measurements are performed with a calibrated pH electrode (Consort C3060). The substrate solution consists of the nitrate source ($Ca(NO_3)_2$), the carbon source ($Ca(C_2H_3O_2)_2$), macronutrients (1 mL/L, see Appendix D) and micronutrients (1 mL/L, see Appendix D). The denitrification process is buffered by means of calcium carbonate precipitation.

Table 3.5: Volumes and concentrations of substrate solutions and bacterial solutions for OxiTop experiments.

Volume inoculum (mL)	40
Volume substrate (mL)	110
Volume soil (soil tests only) (mL)	10
Target concentration NO_3 in substrate (mM)	18.00
Target concentration $C_2H_3O_2$ in substrate (mM)	22.45
Ac/N ratio (-)	1.25

4. RESULTS

The information from literature is used to select a sample material for the Rowe cell and OxiTop experiments. The findings and observation that are done during the selection procedure are reported in section 4.1. After that, the potential of a denitrification-based pretreatment for compaction of the selected soil is assessed in the established Rowe cell setup. The results are presented in section 4.2. Additional measurements are performed with an OxiTop setup to determine the composition of the gas produced during denitrification in a soil environment. The findings are reported in section 4.3.

4.1. COMPACTION CURVES

Standard proctor compaction tests are performed with an automatic compaction machine on mixtures of the uniform Geba sand and the M6 silt (Table 3.1 and Table 3.2). Both materials are also used during the research of Andrag (2017). The tests are performed according to RAW guidelines. The compaction tests are stopped when an increment of water content results in inaccurate measurements of the dry density due to the soil becoming too wet. The final data points of the curves therefore represent the last accurate measurement of dry density.

Figure 4.1 shows the compaction curves for the Geba-M6 mixtures (Composition 1 & 2). It can be seen that an increase of the silt content (8% to 16%) results in the entire compaction curve moving upwards. The voids between the uniform sand grains are filled up with the silt particles. Increasing the silt content therefore results in higher dry densities as voids are filled up to a higher degree. Lubking (1989) argues that the dry density of the soil keeps on increasing until all voids are completely filled. Adding more fine material will eventually lead to a dry density decrease.

Both curves show an optimum saturation in the range of 60%-65% which is remarkably low for a relatively fine material. Andrag (2017) increased the silt content even further to 66% but observed an optimum saturation that is only slightly higher.

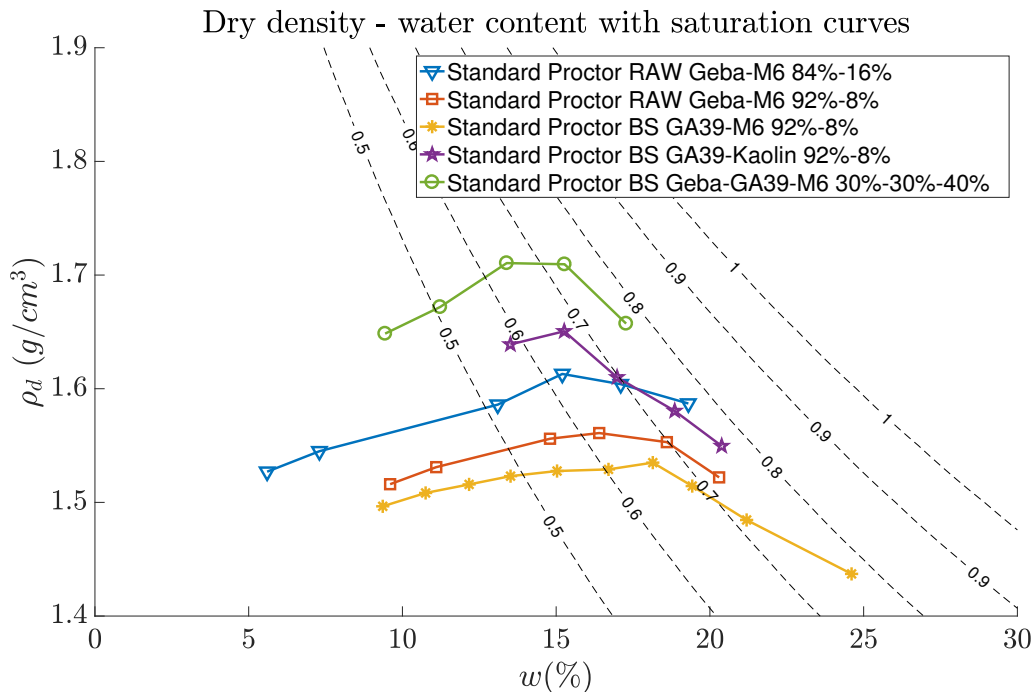


Figure 4.1: Standard proctor compaction curves for several mixtures (saturation contours for $G_s = 2.65 \text{ g/cm}^3$).

The behavior of the material can possibly be explained by the fact that the Geba sand is extremely uniform. The coefficient of uniformity and coefficient of curvature are found to be 1.47 and 1.17 on average respec-

tively (Krapfenbauer, 2016). Moreover, mixing this uniform sand with the M6 silt results in a gap-graded soil. Gap-graded soils are rarely encountered in nature, this makes the comparison with compaction curves from literature difficult. Gap-graded soils might show a compaction curve with a bi-modal distribution.

After the first series of compaction tests it is decided to assess the compaction characteristics of another industrially manufactured very uniform and fine sand, GA39 (Composition 3). A small fraction of M6 silt is added again. This time the proctor compaction test is performed manually according to British Standard guidelines. The compaction curve for this mixture shows an optimum water content in the same range as the Geba-M6 mixtures as can be seen in Figure 4.1. The shape of the curve is also comparable to the Geba-M6 mixtures.

The silt fraction is replaced for a Kaolin clay fraction to determine the influence of a less permeable and more active type of fine (Composition 4). Figure 4.1 shows a significant increase in dry densities but an optimum moisture content that is similar to the one that is found for the sand-silt mixture. The location of the curve with respect to the sand-silt mixture can possibly be explained by a more efficient spatial rearrangement of the clay particles resulting in higher densities for the same amount of compaction energy.

If the previously presented curves are compared with compaction curves of natural soils from literature (Figure 4.2), it can be seen that natural soils have an optimum water content at a degree of saturation that is significantly higher. It is expected that the uniformity of the artificial sand plays an important role in the shape and location of the compaction curves.

Two industrial sands (Geba and GA39) are mixed with a large fraction of silt (M6) in an attempt to increase the grading of the soil sample (Composition 5). The obtained compaction curve shows an optimum saturation that is slightly higher (65%-70%) than for the previous mixtures. This increase in optimum saturation cannot solely be attributed to soil gradation because the silt content of the mixture is also significantly higher than previous mixtures. The shape of this compaction curve is slightly different than for the previous mixtures. The increased grading of this mixture appears to increase the steepness of the compaction curve, representing a higher dependency of dry density on water content. This corresponds with observations from literature.

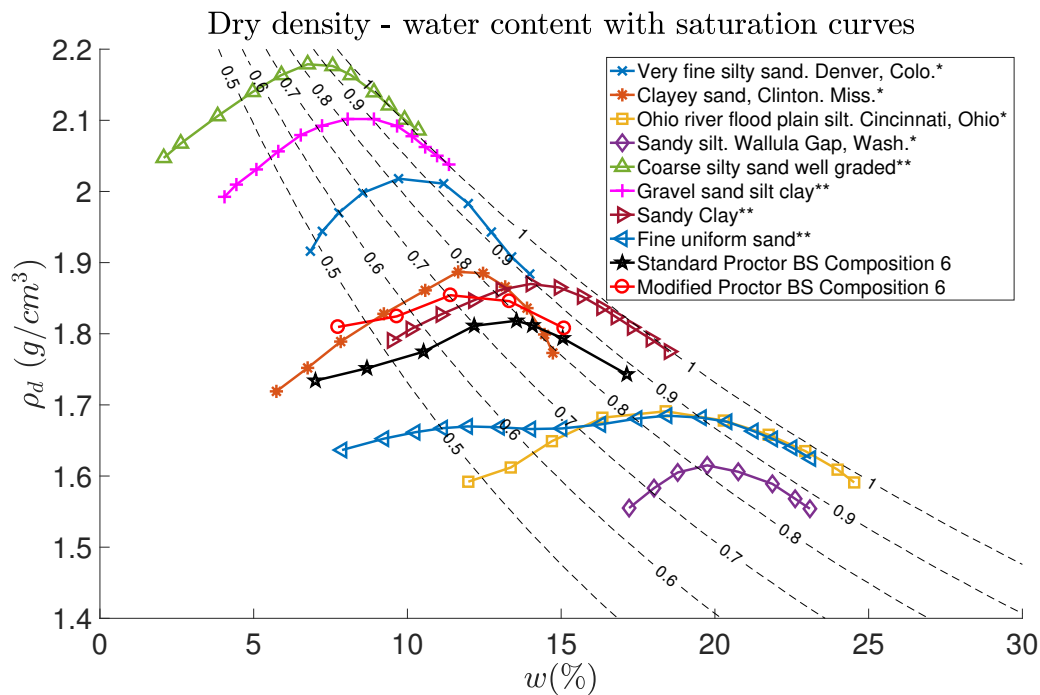


Figure 4.2: Standard proctor compaction curves for soils from literature (saturation contours for $G_s = 2.65 \text{ g/cm}^3$).

*From Terzaghi et al. (1996)

**From Head (2006)

***From Gallage et al. (2016)

Finally, two more components, a natural dredged sand from Amsterdam and a small fraction of Kaolin clay powder, are added to the soil mixture to increase the grading of the soil. The compaction curve of this final

mixture (composition 6) shows an optimum saturation close to 80%. The standard and modified compaction curve of composition 6 are presented together with compaction curves of various soils from literature in Figure 4.2. It can be seen that the standard compaction curve for composition 6 is comparable with the sandy silt from Wallula Gap, Washington (Terzaghi et al., 1996), in terms of shape and optimum saturation. Data points above 80% saturation are achieved for composition 6, with the curve running parallel to the 90% contour on the wet side of the optimum. The increased steepness and optimum water content of this mixture is thought to be mainly caused by the increased gradation. Industrially manufactured materials with a high degree of uniformity do not appear to exhibit the same dependency of dry density on water content as natural soils.

4.2. PROCESSED RESULTS ROWE CELL EXPERIMENTS

Trial experiments are initially performed to assess the reproducibility of the sample preparation method, to evaluate the placement density and to define a target density. Different strain rates are used during the loading stage of the trial experiments to evaluate the pressure development in the loading diaphragm. All trial experiments are performed with untreated soil samples, using de-aired demi water as pore fluid. Some trial experiments include an extended ‘reaction’ stage despite the absence of micro-organisms. This is done to assess the pressure developments and changes in sample height after setting the initial conditions.

The actual testing phase consists of six Rowe cell experiments: three tests on untreated fully saturated soil samples and three tests on treated desaturated soil samples. The three untreated tests can be compared to evaluate the precision and repeatability of the experiments. The tests are performed with appropriate conditions selected from evaluation of the results of trial experiments. The back-pressure valve (C) is left open during both the reaction stage and the loading stage, implying drained conditions during the experiments.

4.2.1. GAS PRODUCTION AND DESATURATION

The degree of saturation of all soil samples is initially brought to 100% during the saturation stage. Full saturation is affirmed through calculation of the Skempton B-factor. The back pressure has to be decreased at the end of the saturation stage to reach the initial conditions. It is assumed that no changes in saturation of the soil sample will occur as a result of the decrease in back-pressure. The degree of saturation is also assumed to remain unaltered during the loading stage of untreated samples. The volume balance that is discussed in subsection 3.3.9 is consulted to check if this assumption is valid.

The target saturation that has to be reached before loading the sample is set to 80% for the first two treated tests (Treated 1 and Treated 2) and to 90% for the third treated test (Treated 3). The developments in saturation and water content of these treated soil samples after the saturation stage are calculated from the volume balance presented in subsection 3.3.7. During the experiments it is observed that immediately after setting the initial conditions, a certain period of time is required before the system reaches an equilibrium. Small changes in sample height and volumes in the pressure controllers are recorded during this equilibration phase. The equilibration phase can be attributed to diaphragm expansion. It is assumed that the reaction stage starts once the equilibrium situation is reached. The required concentrations for the substrate solution are calculated based on the target degree of saturation, following the procedure described in subsection 3.3.3. The composition of the treatment regimes with Ca-Ac-N concentrations of the flushed substrate solution are listed in Table 4.1.

Table 4.1: Treatment regimes for treated Rowe cell experiments.

Sample (-)	Target saturation (%)	Ca-Ac-N (mM)	Ac/N - ratio (-)
Treated 1	80%	47.2-52.4-42.0	1.25
Treated 2	80%	47.2-52.4-42.0	1.25
Treated 3	90%	25.3-28.1-22.5	1.25

The volume balances and saturation developments for the reaction stage of the treated tests are presented in Figure 4.3 and Figure 4.4 respectively. The amount of gas in the gas trap at the end of the reaction stage has to be taken into account for the calculation of the saturation of the soil samples. This is done by a normalization. It can be observed that the differences between the normalized and the non-normalized saturations are

very small. This follows from the small volumes of gas in the gas trap at the end of the reaction stage during the different tests, which are also indicated in the figures. The gas percolation threshold of the soil apparently is sufficient and allows for reaching the target density.

Reductions in gas production rate can be observed for samples Treated 2 and Treated 3. Gas production virtually terminated at the end of the reaction stage of Treated 2. A sudden shift in saturation can be seen in Figure 4.4c. This shift is caused by a sudden volume change in the back pressure controller as can be verified from Figure 4.3c. An explanation for this observation can be a clogged connection between the sample and the back pressure controller. An accumulation of gas or fine material might have resulted in the drainage path getting momentarily clogged. There are no changes in pore pressure measured when the shift in saturation occurs.

The gas production measurements of the three treated Rowe cell tests are shown in Figure 4.5. The observed lag period is approximately 1.5 days for all experiments. A relatively steady rate of gas production can be noted after the initial lag period. This is particularly evident for Treated 1. Gas production continues after reaching the target saturation, indicating that not all nitrate in the pore fluid is yet removed and converted to nitrogen gas. The statistics of Treated 1 show a measured average daily gas production of 10.7 mL. The 25th and 75th percentile lie relatively close to the 50th percentile, in contrast to the other two treated tests. A higher production rate of gas can be noticed for the lower initial substrate concentration of Treated 3.

4.2.2. WATER CONTENT-DRY DENSITY PATHS

The soil sample properties from the treated and untreated Rowe cell tests are presented in Table 4.2. The values represent the soil sample properties immediately before the start of the loading stage (initial) and at the end of the loading stage when the target density is reached and the maximum load is applied on the sample (max-load). The accuracy of the calculated properties is dependent on the measurement errors of the height and mass determinations performed during the experiments. The accuracy of the reported values is estimated to be $\pm 0.01 \text{ g/cm}^3$ for the dry densities, $\pm 2\%$ for the relative densities and $\pm 0.02\%$ for the strains. A further elaboration on the accuracy of measurements is given in the discussion (section 5.1). From Table 4.2 it can be seen that the dry density is generally increased from around $1.63 \text{ (g/cm}^3\text{)}$ to $1.70 \text{ (g/cm}^3\text{)}$, this corresponds with a relative density increase of 10-13%. The dry density before loading of sample Treated 2 is found to be significantly higher than for the other experiments.

Table 4.2: Soil sample properties at the beginning and end of the loading stage.

	M_s (kg)	$\rho_{d_{initial}}$ (g/cm ³)	$\rho_{d_{max-load}}$ (g/cm ³)	$RD_{initial}$ (%)	$RD_{max-load}$ (%)	$\Delta \epsilon_{a_{loading}}$ (%)
Untreated 1 ($S_w = 100\%$)	1.24	1.63	1.70	65.0	77.5	4.37
Untreated 2 ($S_w = 100\%$)	1.25	1.63	1.70	66.4	77.0	3.77
Untreated 3 ($S_w = 100\%$)	1.25	1.62	1.70	63.6	77.0	4.73
Treated 1 ($S_w = 80\%$)	1.24	1.63	1.70	66.6	77.5	3.87
Treated 2 ($S_w = 81\%$)	1.26	1.67	1.70	72.1	77.7	2.02
Treated 3 ($S_w = 89\%$)	1.24	1.64	1.70	67.9	77.5	3.44

The changes of dry density, water content and degree of saturation can be plotted on a water content-dry density plane to determine the path that is followed during the different experiments. Possible scenarios for the two-stage process of desaturation and compaction are presented in Figure 1.2. Figure 4.6 shows the calculated paths for the series of Rowe cell experiments. The three figures on the left, 4.6a, 4.6c and 4.6d, present the paths that are followed during the untreated tests. Figures 4.6b, 4.6d and 4.6f on the right present the paths that are followed during the treated test.

As expected, there is virtually no change in dry density during the ‘reaction’ stage of the untreated samples. This confirms that the pressure controllers are properly working and contradicts the presence of a significant leak in the system. An extended reaction stage is executed (≈ 11 hours) for Untreated 1. The desaturation paths of the treated soil samples are nearly horizontal. Minor dry density increases can be observed during the reaction stage of these experiments. The settlements observed during the reaction stage of the treated samples are so small (< 0.05 mm) that they fall within the error margin of the measurements and can be disregarded. The hypothesized horizontal path of the desaturation stage (Figure 1.2) is thus confirmed for the applicable pressure conditions. This also means that there is no risk of soil expansion, providing that the soil is free to drain.

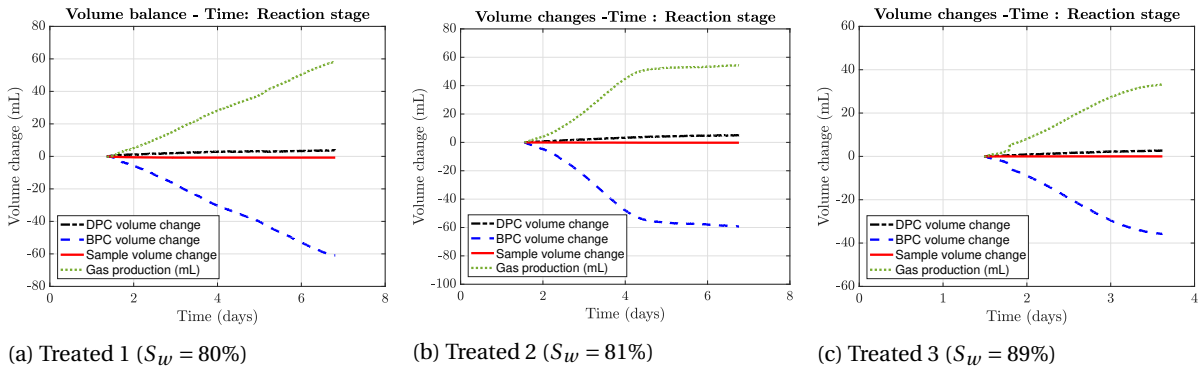


Figure 4.3: Volume balance during reaction stage of treated Rowe cell tests.

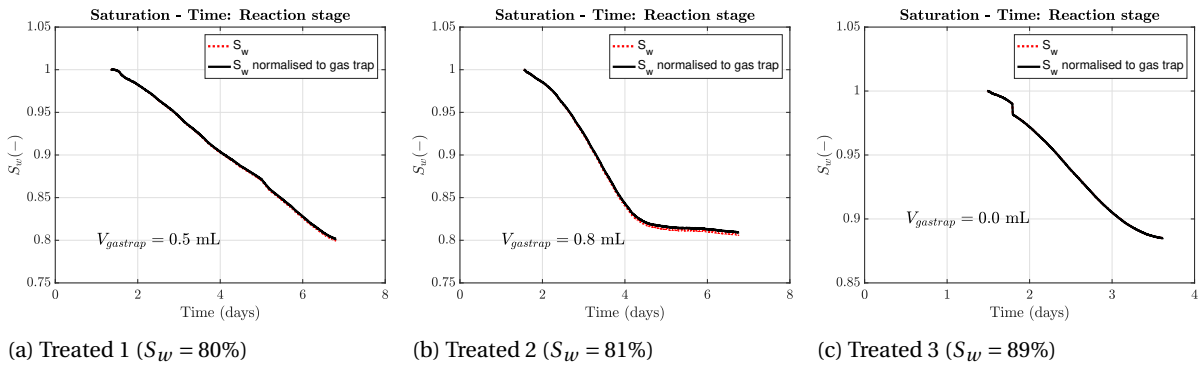


Figure 4.4: Saturation development during reaction stage of treated Rowe cell tests.

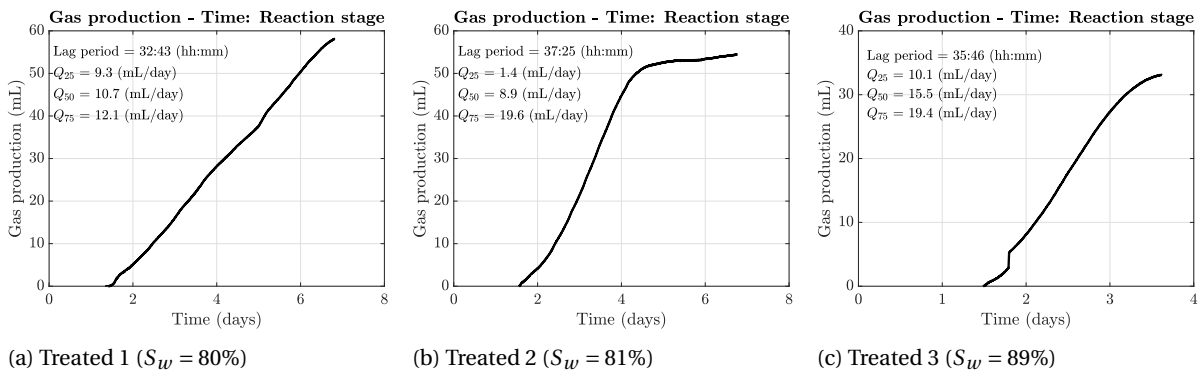


Figure 4.5: Gas production measurements during reaction stage of treated Rowe cell tests.

The volume balance of subsection 3.3.9 is applied to calculate the changes of water content and dry density during the loading stage. The solid black lines show the water content-dry density path that is calculated from the volume balance. The dashed red lines show the net path that is followed during the loading stage. From Figures 4.6a, 4.6c and 4.6e it can be observed that the calculated path during loading closely follows the 100% saturation contour for the untreated control tests, although small inconsistencies can be seen for the tests of samples Untreated 2 and Untreated 3. The treated tests show a loading path that is more vertical, meaning the degree of saturation is increasing during the loading stage. The net changes in saturation during the loading stage ($\Delta S_{w_{loading}}$) of the treated samples are displayed in the water content-dry density plots. The increase in saturation during loading is a result of the expulsion of gas bubbles from the soil sample, the decrease of sample volume and corresponding decrease in pore space and the compression of trapped gas bubbles in the soil.

The volume of gas expelled from the sample during loading is determined with the gas trap. The total

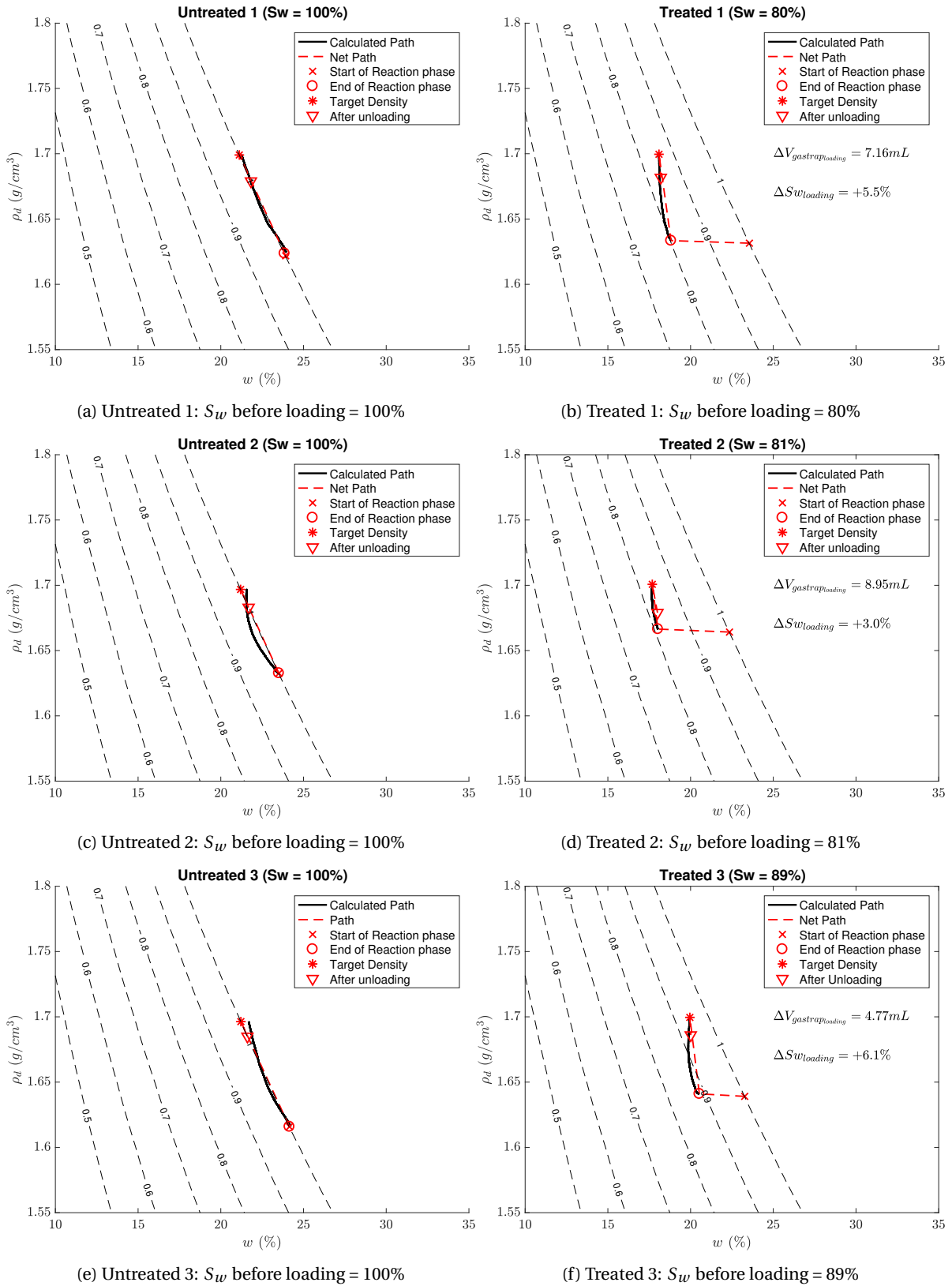


Figure 4.6: Dry density - water content paths of soil samples during loading stage.

changes in volume of gas in the gas trap during the loading stage are reported in Figure 4.6 and are used to determine the water content-dry density path during loading of the samples. It should be noted that the gas

trap is also incorporated into the setup during all the untreated tests. No gas is observed in the gas trap at the end of the loading stage for all the untreated tests.

4.2.3. COMPRESSION FORCES DURING LOADING AND RELAXATION STAGE

The pressure development in the diaphragm during the loading stage provides an impression of the stiffness of the soil sample. The treated and untreated soil samples are loaded by means of the diaphragm pressure controller, which is set to a flow rate of 1.0 mL/min. Compression forces are calculated from the observed pressure developments with Equation 3.21. The energy requirements for compaction from the initial density to the target density can be evaluated by comparing the development of compression forces during the loading stage for the different tests. It is presumed that the pressure developments in the loading diaphragm will be less significant for samples that are brought closer to optimal conditions in terms of water content.

The compression forces during the loading and relaxation stage are plotted against time in Figure 4.7a. The first observation from this figure might be that compression forces increase more rapidly and to a slightly higher level for Treated 1 and Treated 2, suggesting a (slightly) stiffer soil sample after microbial induced desaturation to 80% saturation. The compression forces at the target density are approximately at the same level for Untreated 1 and 2 and Treated 3 (90% saturation). Untreated 3 shows a slightly lower compression force at the target density.

The flow rate of the diaphragm pressure controller is set to 0.0 mL/min at the end of the loading stage, thereby initiating the relaxation stage. It can be seen in Figure 4.7a that compression forces reduce during the relaxation stage. Theoretically, no displacements should occur during a relaxation stage. Changes in displacements are, however, found in the data. The smallest displacements are found for the tests Untreated 1 and Treated 3. The other tests show slightly bigger displacements during the relaxation stage. The differences in total reduction of the compression force for the different tests can be linked to the observed displacements.

It is also obvious from Figure 4.7a that the time it takes to reach the target density (i.e. total loading time) is changing for the different tests. This can be explained by differences in strain rates during the loading stage and differences in initial dry densities. The diameter of the soil samples is relatively large compared to the height of the sample. Relatively small differences in the initial height of samples might therefore mean significant differences in the initial dry density. Samples that have an initial dry density that is closer to the target density, require less vertical displacement during the loading stage. Small differences in the required vertical displacement for reaching the target density result in significant differences in terms of loading time since the actual strain rate is relatively small ($< 0.05 \text{ mm/min}$). Small differences in strain rate are recorded with the displacement transducer during the different experiments, despite the fact that the diaphragm pressure controller is always set to 1.0 mL/min. The strain rate is expected to be affected by expansion of the rubber loading diaphragm and the presence of minor gas in the 'de-aired' diaphragm water.

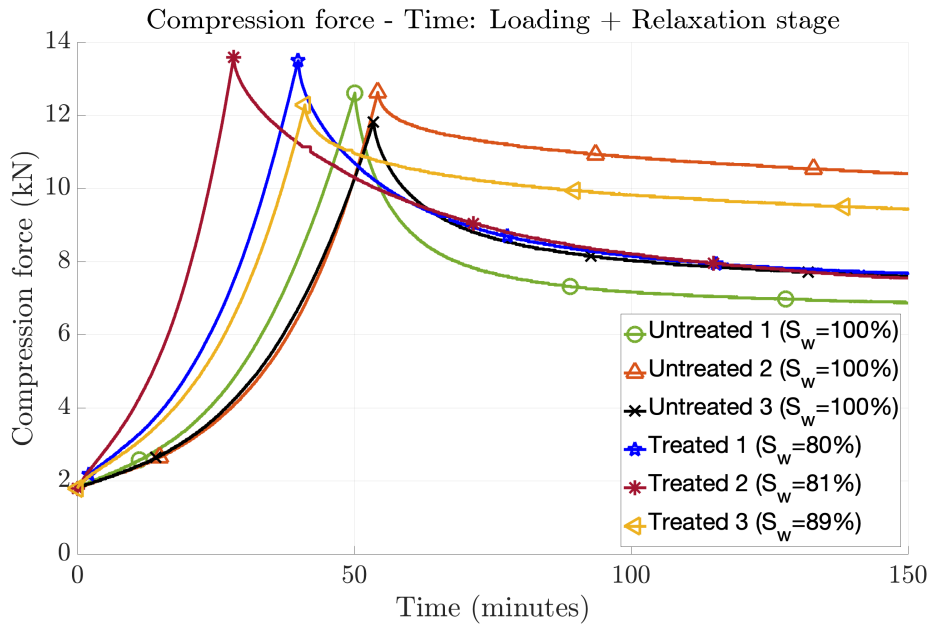
It makes sense to plot the compression forces against dry density to allow for a better comparison of the different experiments. Compression forces are plotted against dry density in Figure 4.7b. Although the curves of the different tests lie close to each other, some notable observations can be done.

First of all, it can be seen that the initial dry density of sample Treated 2 is significantly higher than for the other tests. This is caused by some complications during execution of the experiments. However, the observed compression force at the target density is similar to Treated 1 despite the higher initial density.

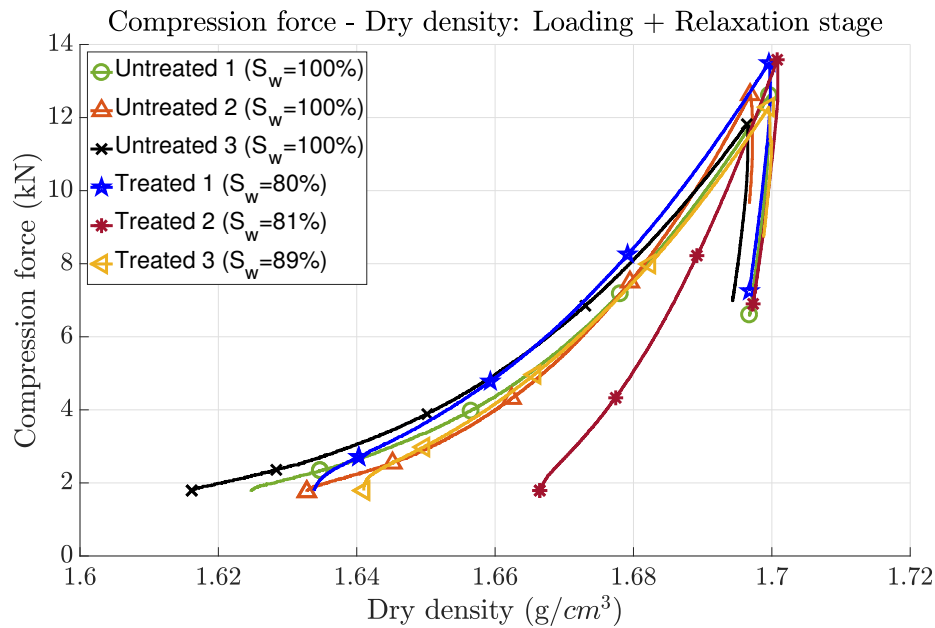
Secondly, it can be seen that the target density that is achieved for Untreated 2 and Untreated 3 is slightly lower than for the other tests. This makes Untreated 1 the best alternative for comparison of the treated and untreated tests. This figure also shows that the compression force at the target density is slightly higher for Treated 1 and Treated 2, which are both desaturated to 80% saturation. The compression force at target density for Treated 3 is approximately equal to Untreated 1.

4.2.4. WORK INPUT LOADING STAGE

The energy requirements for static compaction of a soil sample can be expressed as work done per unit volume. The work per unit volume can be calculated from the area under a (total) stress-strain plot. The total amount of strain during the loading stage is not equal for all experiments, because slightly different initial and final densities are obtained. Therefore, it seems fair to divide the work per volume by the total change in strain measured during the loading stage ($\Delta \epsilon_{a_{loading}}$). This normalization enables the comparison of results from different experiments. Equation 4.1 is applied to calculate the normalized work input per volume during the reaction stage.



(a) Compression force developments during loading and relaxation stage of Rowe cell experiments.



(b) Compression force versus dry density during loading and relaxation stage of Rowe cell experiments.

Figure 4.7: Compression force and dry density developments during drained loading stage and relaxation stage.

$$\frac{\int \sigma d\epsilon_a}{\Delta\epsilon_{a_{loading}}} \quad (4.1)$$

Figure 4.8 presents an evaluation of the normalized work input during the loading stage. The curves represent the work done per unit volume divided by total strain (of the loading stage) as a function of dry density.

From this figure it is evident that slightly more energy is required for compression of the treated soil samples. The work done per unit volume at the target density (1.7 g/cm^3) is comparable for the three untreated soil samples with only de-aired demi water in the pore space. The final points of the treated samples are all

found at a higher level in terms of work per volume. The energy requirements for compression of sample Treated 3, which is desaturated to approximately 90%, lie between the energy requirements for the untreated samples ($S_w = 100\%$) and the samples treated to 80% saturation. The curves of the different tests lie close to each other at the first part of loading stage, differences in work done per unit volume can only be observed at the higher range of dry densities. In accordance with earlier observations it can be noted that the final point of the curve of Treated 2 ($S_w = 81\%$) lies at a relatively high level in terms of work done per unit volume despite the higher initial dry density. This final point lies relatively close to the final point of sample Treated 1 which is also desaturated to 80% saturation. In conclusion, the curves show that with the current setup and method, no reductions in energy requirements for compaction are observed for pretreated (partially saturated) silty sand samples when compared to untreated (fully saturated) samples.

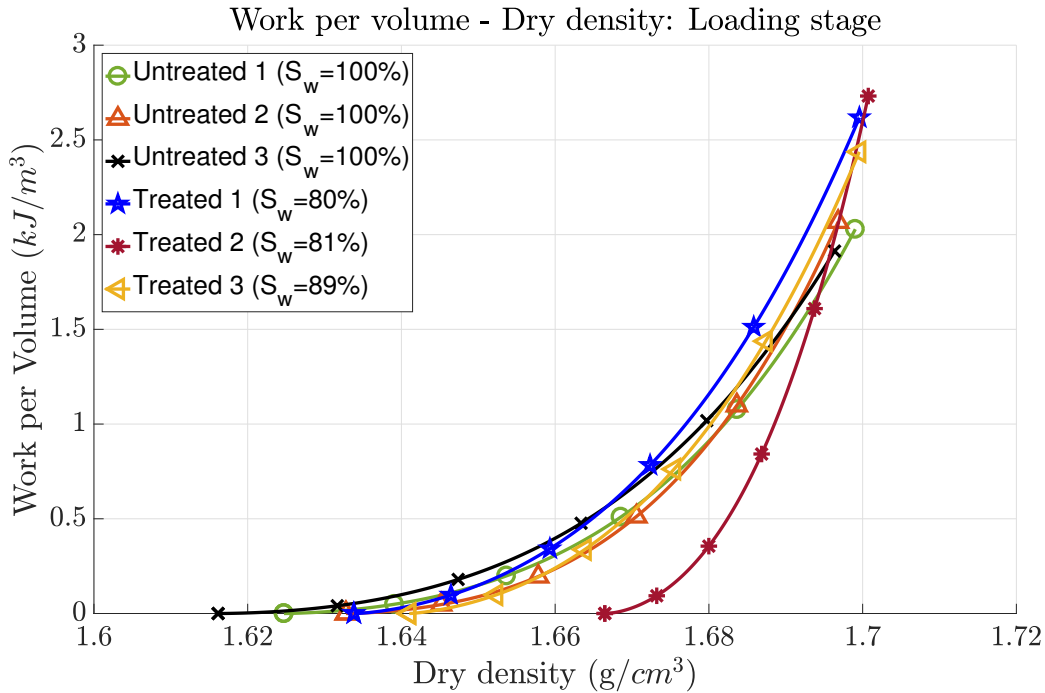


Figure 4.8: Work done per unit volume (normalized for total strain) during loading stage of Rowe cell experiments.

4.2.5. CHEMICAL ANALYSIS ROWE CELL EXPERIMENTS

A chemical analysis is performed on the pore fluid of the samples in the Rowe cell at the beginning and at the end of the experiments. The chemical analysis includes the determination of pH, EC and concentrations of nitrate, nitrite and calcium. Figure 4.9 presents the measured concentrations of nitrate for the different bacterially treated experiments together with a prediction of the initial nitrate concentration based on the volume of substrate solution added to the cell. The substrate solution, with predetermined NO_3^- concentration, is flushed from the bottom of the cell through the soil during sample preparation which allows for accurate monitoring of the volume of substrates added. The substrates are slightly diluted during flushing due to the initial water content of the soil in the cell.

The predicted initial concentrations closely match the measured concentrations for Treated 2 and Treated 3. A significant difference can be observed for Treated 1. The time between sample collection and the concentration measurement can result in minor depletion of nitrate in solution, thereby explaining a lower measured nitrate concentration. However, the initial concentration measured for Treated 2 and Treated 3 are higher than the predicted concentration. It is therefore more likely that the relatively low initial nitrate concentration is caused by an inaccurate measurement. The soil contains a small fraction of clay particles which is difficult to remove from the extracted pore liquid. Residual particles might have affected the chemical analysis by the Hach Lange spectrophotometer. Negligible concentrations of nitrite are found in the pore fluids at the beginning of the different tests.

Table 4.3 shows the reaction times of the treated tests together with the consumption/removal of substrates from the pore fluid solution during the experiment. The reaction time of Treated 1 and Treated 2 which are

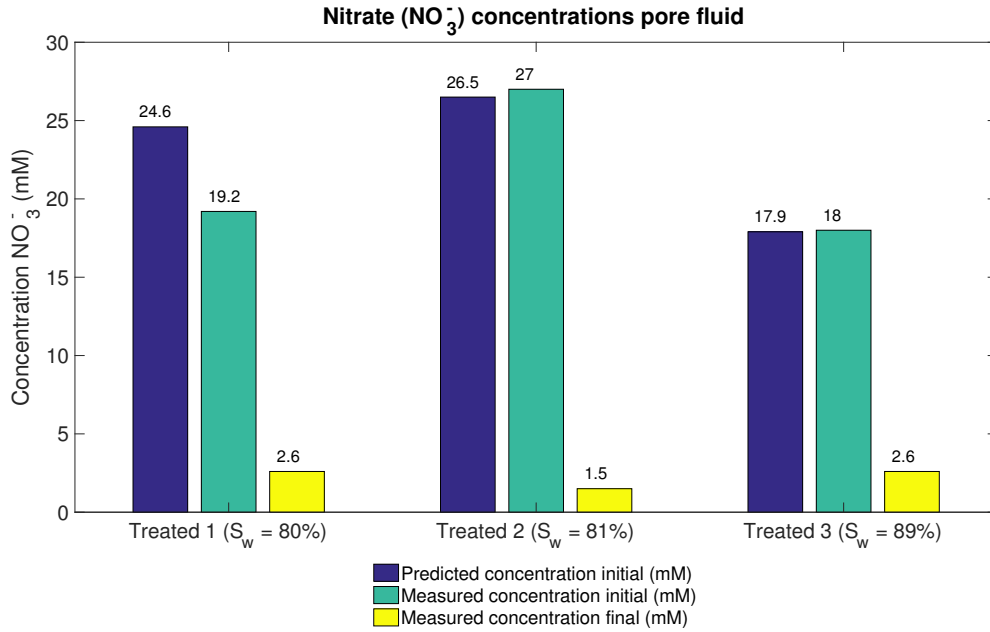


Figure 4.9: Measured and predicted nitrate concentrations in pore fluid at beginning and end of treated tests.

both desaturated to a saturation of 80% are comparable. This indicates that the average gas production rates are similar in both experiments. It can be seen that the major part of initially available nitrate is consumed for all tests. The consumed $(NO_3^- - NO_2^-) - N$ fractions of Treated 2 and Treated 3 indicate that more than 90% of the initially available nitrate is converted to nitrogen gas and biomass. The lower $(NO_3^- - NO_2^-) - N$ fraction of Treated 1 can be explained by the higher level of residual nitrite concentration which is shown in Table 4.3. The denitrification process in the pore fluid is effectively buffered by means of calcium carbonate precipitation as can be seen from the measured pH values at the beginning and end of the experiment in Table 4.3.

Table 4.3: Reaction time, concentration and pH measurements of treated Rowe cell experiments.

	Treated 1 ($S_w = 80\%$)	Treated 2 ($S_w = 81\%$)	Treated 3 ($S_w = 89\%$)
Reaction time (days)	7.1	7.0	4.6
$NO_3^- - N$ consumed (mmol)	5.0	7.3	4.8
$(NO_3^- - NO_2^-) - N$ consumed (mmol)	4.6	7.1	4.7
$NO_3^- - N$ consumed (%)	90%	96%	92%
$(NO_3^- - NO_2^-) - N$ consumed (%)	82%	93%	91%
NO_2^- concentration final (mmol/L)	1.8	0.9	0.3
pH pore fluid initial (-)	7.15	7.13	7.13
pH pore fluid final (-)	7.30	7.52	7.46

The actual stoichiometry of the metabolic reaction lies between zero growth conditions with $[\frac{Y_{N_2}}{Y_{NO_3^-}}] = [\frac{0.8}{1.6}]$ and maximum growth conditions with $[\frac{Y_{N_2}}{Y_{NO_3^-}}] = [\frac{0.39}{0.97}]$ (Equation 2.6 & Equation 2.8). A theoretical prediction of the volume of nitrogen gas produced for maximum and zero growth conditions can be done based on the amount of consumed $(NO_3^- + NO_2^-) - N$. The formulas presented in subsection 3.3.3 are used to perform these calculations. The dissolved fraction of nitrogen gas in the pore fluid at the end of the experiment is taken into account. The measured gas production is compared with the theoretical production in Figure 4.10. It can be noticed that the measured gas production falls just outside of the range predicted by maximum

and zero growth stoichiometry for Treated 1 and Treated 2. This is thought to be the result of carbon dioxide (CO_2) production. It is initially assumed that the fraction of carbon dioxide produced during the denitrification process is negligible due to the near neutral pH which results mainly in bicarbonate (HCO_3^-) production. Also the solubility of nitrogen gas (Henry's coefficient of $1542.6 \text{ atm} \cdot L \cdot \text{mol}^{-1}$) is significantly higher than for carbon dioxide (Henry's coefficient of $28.53 \text{ atm} \cdot L \cdot \text{mol}^{-1}$). Based on the measured gas production in the Rowe cell this assumption is not always valid.

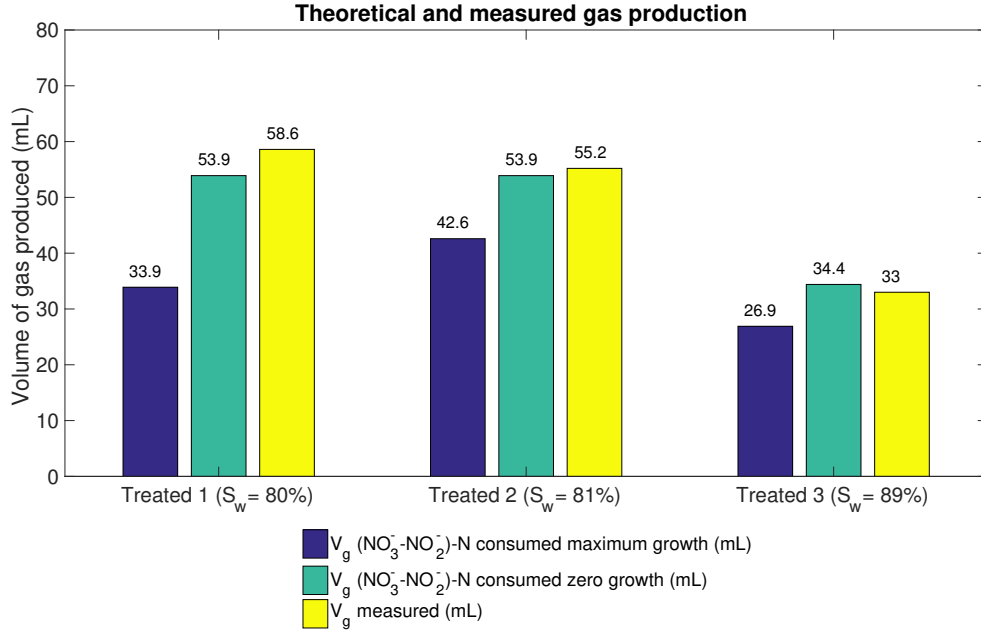


Figure 4.10: Theoretical production of nitrogen gas for maximum and zero growth conditions and measured gas production during treated Rowe cell experiments.

The theoretical calcium carbonate precipitation can be calculated from the measured dissolved calcium (Ca^{2+}) removed from the system. Table 4.4 shows that less than 1 gram of calcium carbonate per kg of soil is precipitated in all three tests. An increase of strength due to calcite precipitation is therefore not expected. Similar observations were done by Andrag (2017) for a treatment regime with relatively low substrate concentrations.

Table 4.4: Measurements of dissolved calcium and theoretical precipitation of calcium carbonate of treated Rowe cell experiments.

	Treated 1 ($S_w = 80\%$)	Treated 2 ($S_w = 81\%$)	Treated 3 ($S_w = 89\%$)
Ca^{2+} removed (mmol)	8.3	10.3	6.1
Ca^{2+} removed (%)	68%	75%	77%
$CaCO_3$ precipitated (g)	0.84	1.03	0.61
$CaCO_3$ precipitation per kg soil (g/kg)	0.68	0.82	0.50

A nitrogen balance can be established by comparing all measured quantities at the beginning and end of the experiments. Figure 4.11 shows the nitrogen balance for the three treated Rowe cell experiments. All fractions are calculated from measurements performed during the Rowe cell tests, except for the dissolved N_2 gas which is calculated with Equation 3.10 under the assumption that the partial pressure of nitrogen is equal to the pore pressure. The N-gap at the beginning of test Treated 1 can once again be explained by an erroneous measurement of initial nitrate concentration. A small N-gap can be observed for Treated 2 and Treated 3. Measurement inaccuracies, diffusion of substrates and production of other gases all have an influence on the nitrogen balance and might explain the N-gap.

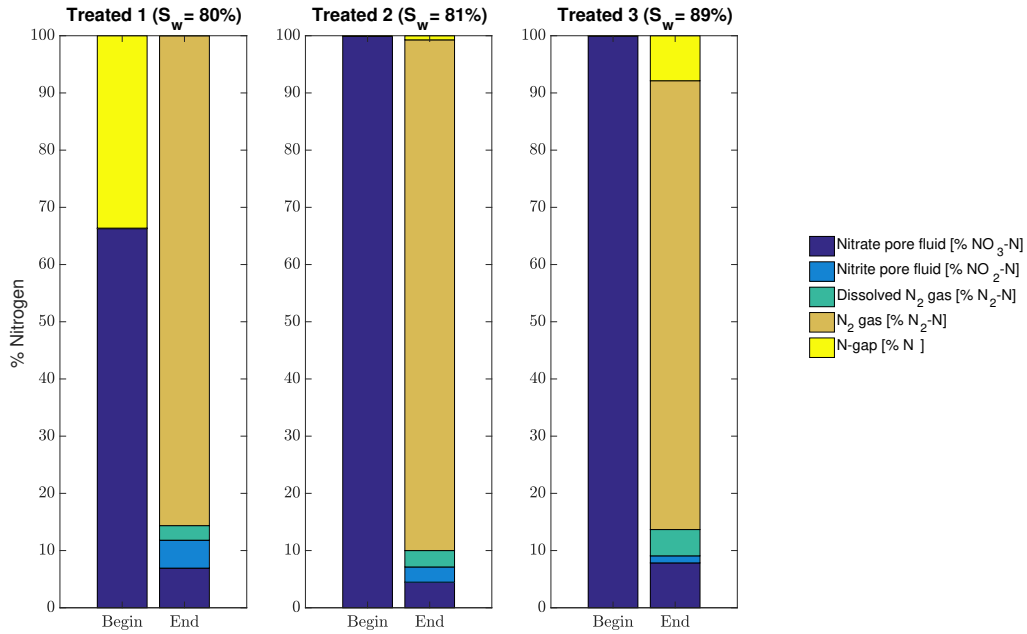


Figure 4.11: Nitrogen balance from chemical analysis of sample pore fluid at begin and end of treated Rowe cell tests.

4.3. OxiTOP EXPERIMENTS

The reaction time for the OxiTop experiment is set to seven days. All eight bottles initially contain the same amount of nitrate, acetate and calcium. A treatment regime with a Ca-Ac-N composition of 20.2-22.5-18 mM is applied (Ac/N ratio = 1.25). There is no nitrite measured at the beginning of the experiment. The bacterial activity in the different bottles can be evaluated by looking at the amounts of residual nitrate, nitrite and dissolved calcium at the end of the experiment, the pressure development as a result of gas production, the lag period and the composition of the produced gasses. The fractions of removed $(NO_3^- + NO_2^-) - N$ and Ca^{2+} are shown in Table 4.5 together with the final pH values of the solutions. Nearly all of the initially available nitrate is removed from the solution in all bottles according to the performed concentration measurements. The pH at the end of the experiment is in general slightly lower in the control solutions without soil.

Table 4.5: Removed fractions of $(NO_3^- + NO_2^-) - N$ and Ca^{2+} at the end of the OxiTop experiment and measured final pH of the solution.

	$(NO_3^- + NO_2^-) - N$ removed (%)	Ca^{2+} removed (%)	pH_{final}
Control-1	97.85	26.73	6.95
Control-2	99.78	33.44	6.93
Control-3	99.78	33.95	6.98
Control-4	91.88	22.08	6.77
Soil-5	99.03	32.92	7.04
Soil-6	99.00	34.99	7.03
Soil-7	98.96	32.05	7.01
Soil-8	98.42	27.24	7.05

5 mm Pressure developments in the head space above the solution are monitored during the experiment and can be used to calculate the gas production in terms of moles. Figure 4.12 shows the measured average gas production per liter of solution for the control tests and the soil tests with the standard deviation indicated by

the vertical bars. A part of the produced gasses will stay in solution and does therefore not contribute to the pressure increments in the head space of the bottles. The dissolved fraction of gas is not taken into account in Figure 4.12, but will be discussed in a later stage.

The temperature controlled room, in which the OxiTop bottles are placed, is initially set to 20 °C (the same temperature as for the Rowe cell experiment). However, changes in temperature are observed during the test. The temperature in the control room raises slightly as a result of the action of the stirring magnets. Unfortunately, the control room that is used can only regulate the temperature in terms of heating up, not cooling down. The day-night cycle can clearly be recognized from Figure 4.12. It should be noticed that the control room is normally operated at 35 °C.

It is immediately clear from Figure 4.12 that a larger amount of total moles of gas is produced in the bottles with soil. This is a surprising result because in theory similar total productions (of nitrogen gas) are expected since all bottles initially contain the same amount of substrates. The metabolic reaction (Equation 2.8) is used to predict the production of nitrogen gas. It is assumed that a negligible amount of carbon dioxide is produced due to the near neutral pH of the solution. This assumption, however, is contradicted by the gas composition measurements which are performed two and seven days after starting the experiment. A significant fraction of carbon dioxide is found in the gas samples despite the measured near neutral pH (Table 4.5).

The dissolved fractions of CO_2 and N_2 are calculated to get a complete overview of the bacterial activity. The partial pressures of nitrogen gas and carbon dioxide gas are determined from the measured final gas composition. The dissociation of CO_2 in water is taken into account by using a pH dependent Henry coefficient that includes CO_3^{2-} , HCO_3^- , H_2CO_3 and CO_2^{aq} . The total productions of N_2^* and CO_2^* per liter of solution are displayed in the second and third column of Table 4.6 and show that significant amounts of carbon dioxide are produced in all OxiTop bottles. The asterisks (*) are added to the chemical symbols to indicate that both the dissolved (aqueous) and gaseous phases are taken into account. Carbon dioxide has a high solubility, a large fraction of the produced carbon dioxide is therefore dissolved and dissociated in the solution. The theoretically produced N_2^* based on the measured $(NO_3^- - NO_2^-) - N$ consumption for maximum growth and zero growth are shown in the fourth and the fifth column respectively. The actual N_2^* production should in principle lie within these two extremes. It can be noticed that the measured N_2^* production falls far outside of the range predicted by maximum and zero growth stoichiometry for the control bottles. It is not completely clear why the measured production does not match with the theoretically predicted N_2^* . Leakages, measurement errors or inaccurate preparation of the OxiTop bottles can be named as potential causes.

Different concentrations of biomass in the bottles can also have resulted in distinct gas production patterns. The inoculum that is added to the bottles did not consist solely of denitrifiers. Competition between bacteria strains might have inhibited the activity of denitrifiers in solution. Although, final concentration measurements show that most of the nitrate is removed from the solution. Possibly, denitrifying bacteria are inhibited by ammonifying bacteria in the control bottles, thereby explaining why the measured N_2^* production is significantly lower than the theoretically predicted production. The unsterilized soil that is added to the solution might have positively affected the denitrification process, allowing denitrifying bacteria to convert the major part of initially available nitrate into nitrogen gas.

A link between carbon dioxide production and the removal of dissolved calcium cannot be made. It is clear, though, that a significant amount of the produced gas consists of carbon dioxide, which disproves the assumption that a negligible amount of carbon dioxide is produced during denitrification at near neutral pH. Excess production of carbon dioxide is not desired when biogenic pretreatment is implemented in the field to facilitate compaction activities due to the negative influence on the environment. It is therefore recommended to further investigate carbon dioxide production during denitrification. To exclude biological effects, it is recommended to sterilize soil sample material before starting an experiment.

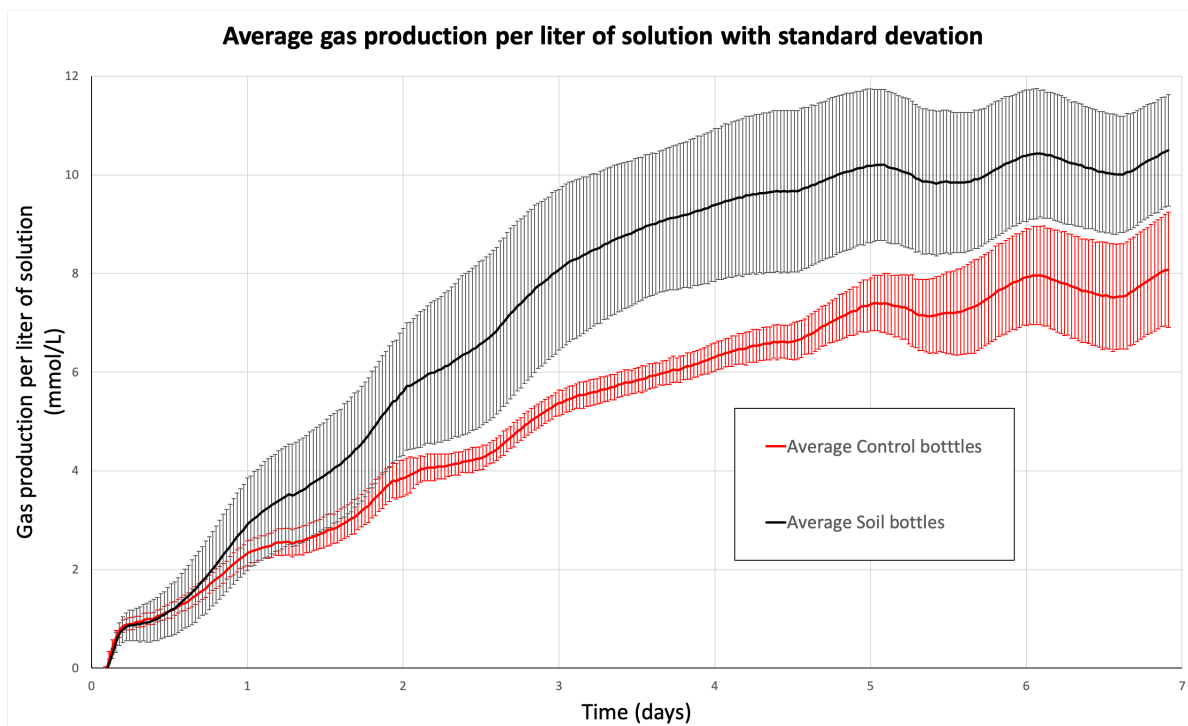


Figure 4.12: Average production of gas per liter of solution in OxiTop bottles.

Table 4.6: Measured total productions (prod.) of carbon dioxide (CO_3^{2-} , HCO_3^- , H_2CO_3 , CO_2^{aq} and CO_2^g) and nitrogen gas per liter of solution versus theoretical production according to the measured (meas.) consumption and metabolic stoichiometry.

Test - Bottle nr.	Prod. CO_2^* meas. (mmol/L)	Prod. N_2^* meas. (mmol/L)	Prod. N_2^* max growth (mmol/L)	Prod. N_2^* zero growth (mmol/L)
Control-1	17.35	2.78	7.16	8.91
Control-2	23.38	3.89	7.30	9.08
Control-3	24.44	4.07	7.30	9.08
Control-4	16.12	2.24	6.73	8.36
Soil-5	6.39	9.05	7.25	9.01
Soil-6	8.18	9.24	7.25	9.01
Soil-7	9.88	7.42	7.24	9.01
Soil-8	9.76	6.05	7.20	8.96

5. DISCUSSION

5.1. MEASUREMENT ACCURACY

The Rowe cell is a hydraulic consolidation cell that is traditionally used for the assessment of consolidation parameters of low permeability soils. Introduction of a more granular soil into the Rowe cell brings along a number of challenges and risks. During execution of the Rowe cell experiments it is noted that despite a well-developed protocol of actions it is difficult to guarantee a high level of precision and accuracy for some measurements. Risks for inaccurate or imprecise measurements are particularly associated with the sample height determination. An accurate and precise determination of the initial height of the soil sample in the Rowe cell is found to be difficult, especially with granular soils. This is because the surface of a granular soil is often relatively irregular. Furthermore, rearrangements in the soil skeleton occur significantly fast when a relatively loose soil sample is prepared. Small disturbances might already induce vertical displacement.

It is decided to carefully trim the sample surface before placing the porous disc to obtain a relatively smooth surface. The initial sample height is measured with a caliper from the top of the cell after the porous disc is placed. At least three measurements are performed to determine the initial height. It is sometimes found that the precision of these measurements is not very high. This is a result of the porous disc being pushed downwards by the caliper when performing the measurement.

After these measurements, the Rowe cell is filled to the top with de-aired water and the cell top is placed on the cell body. After bolting the cell, the rigid loading plate is carefully pushed downwards with the drainage valve open until it is in contact with the porous disc. Additional displacements are induced during these actions. These displacements are difficult to quantify because the Rowe cell is a closed and non-transparent system. A torque wrench is used to evenly tighten the bolts of the cell top during the different experiments and allow for verification of the sample height by means of spindle length measurements. The determined sample heights before and after closing the cell are compared but often show significant discrepancies. At the end of an experiment, the Rowe cell is opened and the sample height is determined once again with a caliper. These measurements are compared with the initial sample height and the monitored displacements during the experiment. It is found that the initial heights determined with the spindle (after closing the cell) give a more accurate prediction of the final sample heights than the initial heights determined with the caliper before closing the cell. However, it should be noted that small displacements are expected to occur when the cell top is removed. These displacements can unfortunately not be monitored but might explain why small differences are found between the measured final sample heights and the final sample height calculated from the spindle reference and transducer data.

An estimation of the accuracy of the measurements is made based on the different sample height determinations during the experiment. It is estimated that the actual sample height lies somewhere in the range between 0.99 and 1.01 times the measured sample height. Slightly dependent on the mass of dry solids in the Rowe cell, this translates into a dry density that is at most 0.01 g/cm^3 lower or higher than the value calculated from the measured sample height. The accuracy of the other properties presented in Table 4.2 can also be derived from the accuracy of the sample height measurements. It is found that an accuracy of $\pm 2\%$ and $\pm 0.02\%$ should be taken into account for the reported relative densities and strains respectively.

5.2. DRAINAGE CONDITIONS

The back pressure is kept at 50 kPa during the loading stage to maintain drained conditions. Nonetheless, small increments of pore pressure are recorded during the loading stage of all Rowe cell experiments. The developments of excess pore pressure are shown in Figure 5.1. From this figure it is evident that the greatest part of the excess pore pressure develops during the first 15-20 minutes of loading. Furthermore no significant differences can be observed between the treated and untreated soil samples.

The measured increments are nominal with respect to the vertical load that is applied, it can therefore be assumed that samples are indeed loaded under fully drained conditions. After performing the Rowe cell experiments with a drained loading stage, it is decided to perform an additional experiment with the drainage valve closed during the loading stage. Pore water can in principle not escape from the sample when the drainage valve is closed, an undrained loading stage can therefore be performed. No volume changes are expected when a fully saturated soil sample is loaded with the drainage valve closed since all the pores are

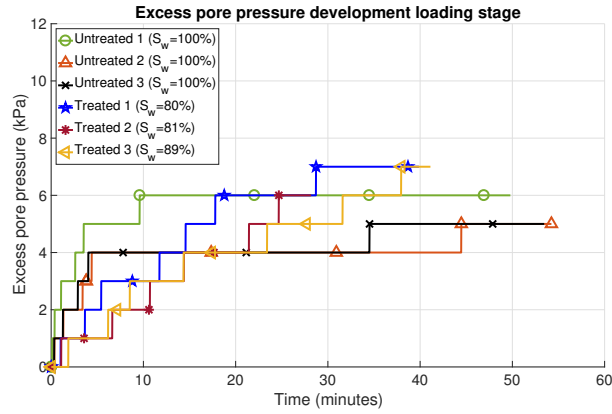


Figure 5.1: Excess pore pressure development during the loading stage of Rowe cell experiments.

filled with (nearly incompressible) water that cannot escape from the sample. The work that is applied will be transferred solely to the pore water, resulting in an increasing pore pressure that follows the changes in vertical stress. The expectation is that small volume changes will occur when microbially treated soil samples are subjected to a vertical loading regime with the drainage valve closed, since part of the voids is now filled with compressible gas.

A fully saturated sample is prepared in the Rowe cell for a first undrained and untreated experiment. After that a loading stage is performed with the drainage valve closed. Surprisingly, displacements are observed during the loading stage. Also it is observed that the pore pressure does not increase with the same rate as the total vertical stress. The stress and strains paths are presented in Figure 5.2 and show that the pore pressure starts deviating from the effective vertical stress after approximately 35 minutes.

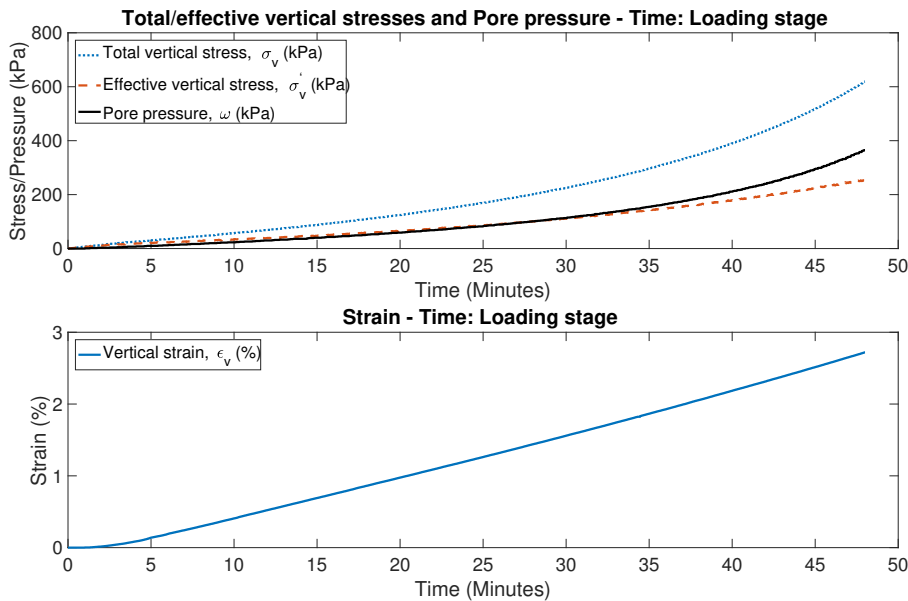


Figure 5.2: Stresses, pore pressure and strain development during loading of untreated soil sample ($S_w = 100\%$) with drainage valve closed.

These unexpected observations can be explained by three different causes:

- A leak in the system: undrained conditions are not guaranteed when there is a small leak in the system. When the cell top is not bolted properly to the cell body or the pore pressure connection is not completely closed, this enables pore water to escape from the sample.

- The soil sample is not fully saturated before starting the loading stage: saturation is checked through calculation of the Skempton B-factor during the saturation stage. It is assumed that the degree of saturation will not change when setting the initial conditions by reducing the pore pressure to 50 kPa (through application of a back pressure of 50 kPa).
- The soil sample is fully saturated but the overall system is not fully saturated: the space above the porous disc is filled with de-aired demi water before immersion of the diaphragm into the cell. The overall system is not fully saturated when there is air in the voids between the diaphragm and the cell wall.

The first explanation seems unlikely because a leak would most likely have been identified in a far earlier stage. Vertical pressure increments are applied with the drainage valve closed during the saturation stage. The displacement transducer, which can measure displacements up to 0.001 mm, shows a total displacement of 0.002 mm during the saturation stage. This means that there is basically no sample volume change. This observation confirms that there are no leakages during the saturation stage. It is unlikely that a leakage is created after the saturation stage.

The second explanation is contradicted by gravimetric water content determinations performed at the end of the experiment. The soil is found to be extremely wet and fluid when the cell is opened with no strength whatsoever. A duplicate water content determination is performed and shows an average water content of the soil of 23.34%. This value is compared with the theoretical water content for a fully saturated soil with a dry density equal to the one that is measured at the end of the experiment. A theoretical water content of 23.26% is calculated.

The third explanation can be evaluated by analyzing the volume balance and pressure changes in the system after setting the initial conditions. First a description of the scenario is given: "The back pressure is set to 50 kPa at the end of the saturation stage to arrive at the initial conditions. The pore pressure is approximately equal to 100 kPa at the end of the saturation stage, but reduces slowly after setting the back pressure. Water is being removed from the sample into the back pressure controller. The diaphragm pressure controller, which controls the vertical pressure, is kept at 100 kPa. This means the effective stress is increasing and settlements are occurring. This process can basically be described as consolidation. At the end of the consolidation process, the fully saturated soil sample is at the initial conditions and the reaction stage is initiated."

Two remarkable observations are done during the experiment:

(1) Despite the fact that the back pressure is reduced from 100 kPa to 50 kPa at a slow rate, it is observed that the vertical pressure reduces dramatically during the consolidation process as can be seen in Figure 5.3. A reduction in vertical pressure can definitely be expected as a result of sample settlement. It is also known that the pressure pump is not highly effective in reacting to pressure changes in the system. A significant amount of time is required to bring the pressure in the diaphragm back to a target pressure after a sudden pressure change. However, the large magnitude of vertical pressure reduction suggests that there is an additional factor causing the inability of the pressure pump to maintain the target pressure.

(2) The volume balance of Figure 5.4 shows that the volume of pore water that is being removed (Vol_{out}) during the consolidation process is much larger than the volume change of the soil sample. The removal of pore water from the cell is however balanced quite well by the volume of water entering the system (Vol_{in}) through the diaphragm pressure controller. The net volume of liquid leaving the Rowe cell during the consolidation process can be calculated by subtracting the volume going out from the volume going in. A relatively small amount of liquid is found to be leaving the system during the entire consolidation process. If this value is compared to the volume change of the sample it can in fact be argued that the soil sample is supersaturated ($S_w > 100\%$) after the consolidation process. This is not possible. The only logical explanation would therefore be that water is being removed by the back pressure controller from a different space.

Based on these two observations, it is suspected that water is being removed from the voids between the diaphragm and the cell wall during the consolidation stage. A visualization of the scenario is given in Figure 5.5. A negative pressure is applied by the back pressure pump during the consolidation stage to reduce the pore pressure in the system. A part of the water in the voids between the diaphragm and cell wall is therefore most likely being removed as a result of the suction at the end of the drainage channel. The water between the voids is located above the drainage channel, the potential energy might therefore stimulate the flow of water from the voids to the drainage channel. The overall system is no longer saturated as water is being displaced from the voids around the diaphragm. This makes completely undrained loading conditions

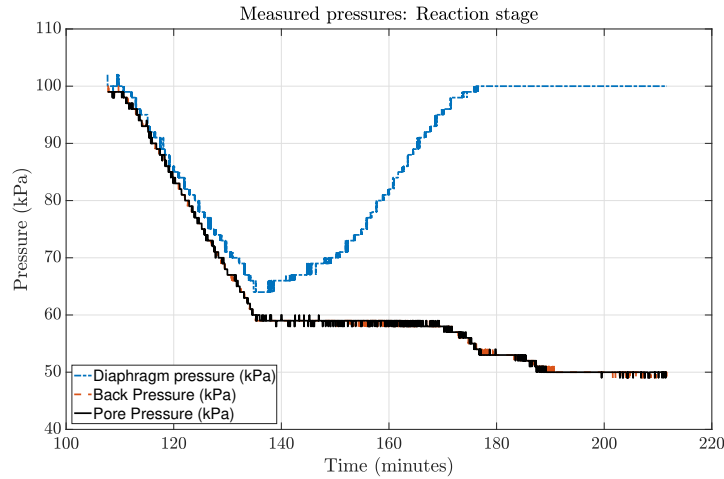


Figure 5.3: Measured pressures for the "consolidation" stage of the Rowe cell experiment with closed drainage valve.

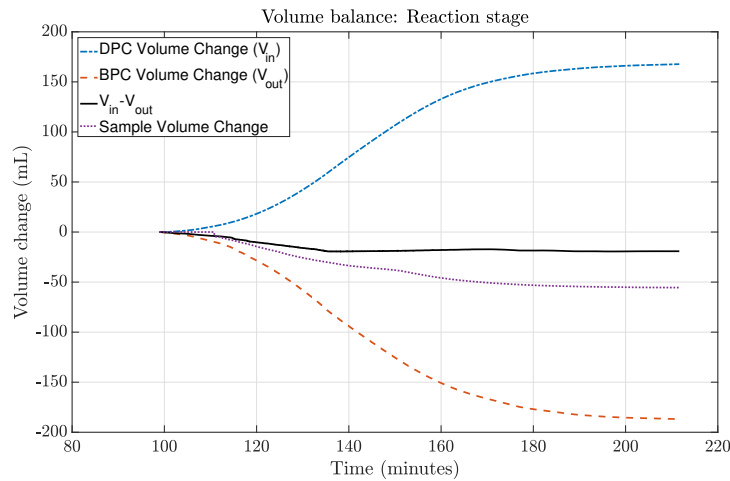


Figure 5.4: Volume balance for "consolidation" stage of the Rowe cell experiment with closed drainage valve.

impossible. The validity of the volume balances presented in subsection 3.3.7 and subsection 3.3.9 has to be re-evaluated.

VOLUME BALANCE REACTION STAGE

Static conditions apply during the reaction stage. Gas is produced inside the treated soil samples or directly below the porous disc. The production of gas results in the generation of excess pore pressures in the sample. The excess pore pressures are dissipated by removal of pore water from the sample by the back pressure controller. The amount of liquid or gas moving around the porous disc and rigid loading plate to the empty voids is expected to be limited because of the applied back pressure at the top of the sample. The volume balance for the reaction stage is therefore expected to remain valid.

VOLUME BALANCE LOADING STAGE

The pore water in the soil sample is rapidly pressurized when a loading stage is performed with the drainage valve closed. As a result of this, the pore water is pushed upwards into the empty voids. Settlements occur as water is removed from the soil sample and part of the applied work is transferred to the soil skeleton, resulting in an effective stress increase.

Pore water can escape through the drainage channel at the top of the sample when the drainage valve is open during the loading stage. Most of the pore water that is expelled from the sample is expected to be displaced to the back pressure controller, however small amounts of liquid and gas might be pushed into the empty voids between the diaphragm and cell wall. The volume balance of subsection 3.3.9 is applied to

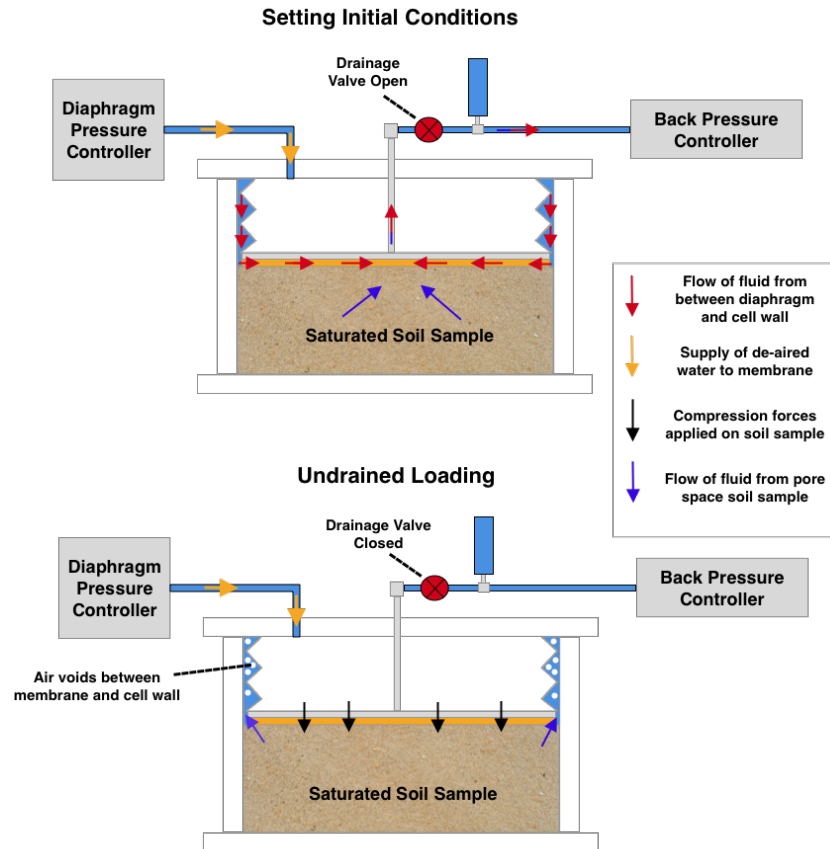


Figure 5.5: Visualization of the scenario that leads to removal of water from around the diaphragm and therefore a partially saturated system.

calculate the water content-dry density paths of fully saturated samples. A fully saturated sample should, in principle, follow the 100% saturation curve upon loading. It can be seen from Figures 4.6a, 4.6c and 4.6e that the calculated paths quite closely match the theoretical paths, especially for sample Untreated 1. The calculated saturation at target density is slightly higher than 100% for samples Untreated 2 and Untreated 3. This can be explained by pore water that is removed from the sample and pushed into the empty voids between the diaphragm and cell wall. The pore water that is pushed into these voids is not accounted for in the volume balance and therefore explains the calculated saturation of higher than 100%. Based on the accurate predictions of the water content-dry density paths of the fully saturated samples it can be concluded that the volume balance for the loading stage can be used to give reasonable predictions of the water content during loading.

5.3. COMPRESSION OF THE GAS PHASE

Previous research has shown that the compressibility of an initially saturated soil can be increased by the formation of gas bubbles in the pore fluid (Rebata-Landa and Santamarina, 2012). Even small size bubbles can change the pore fluid bulk stiffness significantly according to Sparks (1965). The density of the soil samples is increased during the drained loading stage of the Rowe cell experiments as a result of (1) rearrangement of soil particles, (2) the expulsion of gas and water and (3) the compression of gas bubbles. The volumes of the gas bubbles will decrease during the loading stage as a result of the increasing total vertical stress. According to the ideal gas law, the pressure in the gas bubbles will therefore increase. The increase in gas pressure is accompanied with an increase in the amount of gas dissolved in the pore solution (Henry's law). Boyle's law can be used to determine the change in volume as a result of a change in pressure. However, the relation between the air and water pressure needs to be known before Boyle's law can be used.

The compressibility of an air/water mixture and the relationship between air and water pressures (i.e. the pore fluid bulk stiffness) can be calculated with the methods proposed by Schuurman (1966). Boyle's and

Henry's law are implemented to take the compression and dissolution of the gas into account. However, the method cannot be applied to calculate the compressibility of the air/water mixture in the soil samples of the Rowe cell experiments because of a difference in drainage conditions. To simplify the calculations, undrained conditions are considered in the method proposed by Schuurman (1966). This means that the volume of water remains constant and free and dissolved gas cannot escape from the sample during loading.

In the Rowe cell experiments performed for this research, free and dissolved gas are allowed to leave the soil sample during loading. Despite the fact that the volumes of free gas and pore liquid escaping from the soil sample are monitored, it is difficult to predict the compressibility of the air/water mixture because the relationship between the air and water pressures is not completely clear in the Rowe cell experiments. In principle no water pressure increments are expected in a fully drained system, however small increments are recorded. Furthermore it is found during the OxiTop experiments that a significant amount of carbon dioxide gas is produced in addition to the nitrogen gas. A large part of the produced carbon dioxide is dissolved into the solution as bicarbonate or carbonic acid. The dissolved gas has to be taken into account for calculation of the air/water mixture compressibility. According to Schuurman (1966) compressibility and solubility of the air in the gas bubbles determine the compressibility of the air/water mixture.

5.4. DISTRIBUTION OF GAS IN THE SAMPLE

The concept of microbial induced desaturation for improved compactibility is based on the idea that soils have an optimum water content and corresponding maximum dry density. Soils can be brought to the optimum water content by means of microbial induced desaturation. However, the distribution of gas bubbles in the soil might be of major influence on the compactability improvements. It is expected that a homogeneous distribution of gas bubbles is most favourable for the reduction of energy requirements for compaction.

The Rowe cell is a non-transparent system, this makes an evaluation of the distribution of gas bubbles impossible. An important assumption for the reaction stage is that all gas is assumed to be produced inside the sample. However, it is possible that a significant part of the gas is produced in the top part of the soil sample directly below the porous disc. Gas pockets are identified on the surface of soil sample after opening the cell indicating the accumulation of gas below the porous disc. The distribution of gas in the soil sample might therefore not be homogeneous enough to result in a decrease of energy requirements for compaction.

5.5. DENITRIFICATION IN SOILS

More than 90% of the initially available nitrate is removed for Treated test 2 in the Rowe cell. Higher concentrations of residual nitrate and nitrite are measured at the end of Treated test 1 and 3. Residual nitrate in the system is caused by inhibition of the overall denitrification process. The denitrification process is influenced by multiple factors such as the pH, temperature, local inhibitors and the presence of oxygen. The applied treatment regime has to be attuned to these environmental factors for field applications. Zhang et al. (2009) measured the NO , N_2O , N_2 and NH_4^+ production in multiple natural forest soils from China and detected N in ammonium and soil organic matter after incubation. The amount of N gas produced is therefore a better measure of the rate of denitrification than the amount of NO_3^- that is removed. This might be an explanation for the relatively low production of nitrogen gas that is measured in the control tests of the Oxi-Top experiment. The composition of the gas that is produced in the Rowe cell experiments is not measured, so no conclusions can be drawn on the amount of N gas that is actually produced. Zhang et al. (2009) also measured NO and N_2O gas production and found no NO at the end the incubation, whereas N_2O was still detectable.

Based on the results of the OxiTop experiments it can be expected that a certain fraction of the gas produced in the Rowe cell consists of CO_2 . The oxidation state of carbon was found to control the ratio between carbon released as CO_2 and carbon assimilated into biomass, therefore playing a major role in the pH development during denitrification (Drtil et al., 1995).

The pH of the pore fluid is measured at the beginning and end of the Treated Rowe cell experiments and is presented in Appendix B. The initial pH value of the pore fluid is slightly higher than 7.1 for all Treated samples. Increased pH values are measured at the end of the experiments, with a maximum of approximately 7.5 for Treated test 2. The increased alkalinity of the pore fluid due to denitrification is buffered by means of calcite precipitation which normally keeps the pH below 8.0. According to Šimek et al. (2002) nitrogen gas is the major product of denitrification rather than N_2O at pH values higher than 7. The amount of produced N_2O gas during the Rowe cell experiments is therefore expected to be limited. If the results of the Rowe cell experiments of the current research are compared with the results of the Rowe cell experiments performed

by Andrag (2017), it can be noticed that a clear relation exists between the lag period and gas production rate on the one hand and the soil pH on the other hand. The reaction time for the desaturation stage took considerably longer for soil samples that had a relatively low initial pH.

When biogenic gas pretreatment is implemented in the field by means of injection, the negative effects of oxygen on the rate of denitrification are not expected to be significant, providing the injections are performed in a well-controlled manner. Biogenic pretreatment is performed on fully saturated soils below the water table where the oxygen concentration is generally limited. During the laboratory experiments, however, infiltration of oxygen can not be avoided. The soil sample is prepared in an unsaturated way and is saturated afterwards under atmospheric conditions. Some oxygen molecules will certainly have infiltrated the solution during this procedure. Oxygen is a more favorable terminal electron acceptor than nitrate, so during the reaction phase oxygen will first be depleted before the nitrates are converted to nitrogen gas. According to van Spanning et al. (2007), this can lead to assimilatory nitrate reduction which results in the production of nitric oxide or ammonium as final product. The Ac/N ratio will be affected by the presence of oxygen as a part of the carbon source (acetate) is no longer available for dissimilatory nitrate reduction. The observed nitrite accumulations in the Rowe cell experiments might be the result of a low Ac/N consumption ratio (Pham, 2017).

5.6. EXPERIMENTAL SETUP AND METHOD

A large fraction of the soil, selected for the Rowe cell experiments, consists of sand sized particles. Dynamic compaction is the most efficient method of compaction when it concerns granular material. Nonetheless, the Rowe cell, which has the ability to control pressure and drainage conditions, is chosen for assessment of the intended pretreatment despite the impossibility of dynamic loading.

This is because the initial assumption is that regardless of the method of compaction, static or dynamic, reductions in energy requirements for compaction of a 'problematic' soil should be observable after performing the intended pretreatment. However, clear differences can be identified when comparing the manner of compaction in the cell with compaction in the field.

5.6.1. DIFFERENCES BETWEEN EXPERIMENTAL CONDITIONS AND FIELD CONDITIONS

First of all, it is already noted that granular soils are conventionally compacted with dynamic techniques such as rapid impact compaction or vibro compaction. In contrast, soil samples are loaded statically in the Rowe cell.

Secondly, the soil is radially constrained by a solid steel wall in the Rowe cell, where in the field normally no such extreme constraints are found. More specifically it is the combination of the loading area and the total compaction area that is significantly different in the cell and in the field. The loaded area of soil samples in the Rowe cell is equal to the inner area of the cell (i.e. the loaded area is equal to the area that has to be compacted). This means that in principle no bulging of soil occurs upon loading and no shear stresses are developed. Shearing is an important mechanism when dynamic compaction is applied on granular soils in the field. Shearing assists the rearrangement of grains into a denser configuration. The Rowe cell is originally designed for the assessment of consolidation characteristics of clayey soils. Clayey soils consist mainly of flaky particles which will not necessarily be forced into a denser configuration by means of the application of shear forces. Dynamic compaction normally results in the expulsion of air from voids and a reduction in void ratio. It is believed that shearing assists in the expulsion of air as gas bubbles are destabilized (Andrag, 2017). The saturation of the soil increases as gas is expelled and the void ratio is reduced. There is no shearing effect in the Rowe cell, the expulsion of gas bubbles is therefore expected to be hampered.

A third difference between conditions in the field and conditions in the Rowe cell is related to drainage. Strict vertical drainage conditions apply in the Rowe cell. Gas bubbles can only drain through the small diameter spindle. Gas bubbles that are generated at the bottom of the soil sample are not very likely to be expelled during loading due to the absence of shearing forces and limited drainage conditions. Gas bubbles might escape more easily in the field where drainage conditions are in principle less strict.

5.6.2. RATE OF LOADING AND SOIL PERMEABILITY

The microbial induced pretreatment is proposed as solution for facilitation of compaction activities on soils that cannot be compacted sufficiently with conventional techniques. Excess pore water pressures are rapidly generated when dynamic compaction is applied to these soils because the rate of loading is high and the permeability is relatively low. It is possible that the rate of loading that is applied during the Rowe cell experiments is not high enough to obtain benefit from the biogenic pretreatment as a result of a relatively high soil

permeability.

Pore water drains easily from the soil sample if the permeability is high enough with respect to the rate of loading. Therefore, no significant differences in energy requirements are expected, especially if gas accumulates at the top of the sample below the porous disc. Trapped gas bubbles in the back pressure line or porous disc might in fact even obstruct the flow of pore liquid from the sample thereby affecting the drainage conditions and explaining the observed increased energy requirements for compaction after microbial pretreatment.

5.7. POTENTIAL OF THE DENITRICATION-BASED PRETREATMENT

On the contrary of what is presumed, it is found that energy requirements for static compaction are slightly higher for treated soil samples when compared to untreated (fully saturated) samples. It is not expected that soil cementation is the reason for the higher energy requirements after biogenic pretreatment, because the calculated amount of calcium carbonate precipitation at the end of the experiments is very limited. Possibly the formation of biofilm as a result of bacterial activity resulted in a slightly higher level of cohesion in the soil. Trapped gas bubbles in the drainage lines of the setup might also have influenced the energy requirements for compaction.

Nonetheless the denitrification process is successfully implemented to desaturate fully saturated silty sand samples to the optimum saturation. A rapid and steady production of gas is reached inside the soil samples with a very limited amount of gas escaping, displaying the high storage capacity of the sample material. The accumulation of nitrite is limited and the major part of initially available nitrate is converted to nitrogen gas. Furthermore, the pH measurements show that denitrification can be buffered effectively by addition of calcium to the process.

New methods of assessment will need to be developed based on the results of the current study and earlier work to further investigate the potential of denitrification-based pretreatment for the compaction of soils. There is no observed benefit from the biogenic gas in the soil according to the energy-based assessment method that is used in this research. Therefore, it is suggested to approach the biogenic pretreatment concept from a time-based perspective.

Puzrin et al. (2011) examined in-situ microbial gas production to engineer the consolidation properties of clayey sands (65% quartz sand, 20% illite and 15% bentonite) by changing the settlement-time profile. Negligible swelling of the samples was observed during gas production. Furthermore, it was found that biogenic pretreatment caused a shift of up to 50% of total displacement from primary consolidation settlement to immediate settlement with no change in total displacement or the coefficient of consolidation.

6. CONCLUSION

Compaction activities are often found to be ineffective on soils with high fines contents due the generation of excess pore pressure. Drainage assisting elements, such as sand piles, can be installed to facilitate the compaction activities on these soils, but are in general very costly. Therefore, the potential of a microbial induced desaturation (MID) pretreatment with denitrifying bacteria to improve the compactibility of these soils, is investigated during this research. The following research question is formulated:

- How is the compactability of an initially saturated silty sand influenced by the gas bubbles produced by denitrifying bacteria and can this gas be used to reduce the energy requirements for static compaction of the soil to a given target density?

A study is launched to identify the main parameters controlling the efficiency of compaction activities. It is found that the limits of application for conventional compaction techniques can be expressed by means of a particle size distribution (Keller, n.d.). The water content-dry density relationship can be used to predict the optimal conditions of a soil for compaction. Optimal conditions for compaction are commonly around 80% (Andrag, 2017). The amount of gas that can be maintained by a soil, the gas storage capacity, has to be taken into account for the pretreatment in order to make sure optimal conditions can be reached by means of gas production.

The particle size distribution and water content-dry density relationship are taken into account during a series of proctor compaction tests to select a representative sample material that can be used for an energy-based assessment of the MID pretreatment. The water content-dry density relationship of industrially produced soils with an extremely high level of uniformity is found to be remarkably different from natural soils as reported in literature. It is therefore confirmed that gradation is one of main factors influencing the water content-dry density relationship of soils. A silty sand with a relatively high gas storage capacity and optimum degree of saturation is created as sample material for further experiments. A novel sample preparation technique, that allows for the preparation of fully saturated soil samples with a relatively low initial density in a Rowe cell setup, is successfully developed. The reproducibility of the preparation technique is assured as it allows for production of comparable soil samples in terms of initial density and homogeneity. A chemostat setup is established for the incubation of a culture of denitrifiers and provides a continuous supply of active nitrogen producing bacteria. The bacteria have to be provided with macro and micronutrients to avoid inhibition of denitrification due to nutrient deficiency. It is found that weekly injections into the reactor are required to avoid limitation of nutrients.

The Rowe cell setup, which allows for measurement of gas production, is successfully used to reduce the saturation of soil samples to the targeted degrees of saturation. The saturation of soil samples is brought to the optimum saturation of 80% within approximately 7 days by means of an engineered treatment regime. The lag period before significant gas production is found to be approximately 1.5 days for all experiments. A faster rate of gas production is detected for a treatment regime with lower substrate concentrations. A gas trap is implemented in the Rowe cell setup and shows nominal amounts of gas escaping the soil sample during the reaction stage. This displays the relatively high gas storage capacity of the soil. Furthermore, the denitrification process, which results in the production of alkalinity, is successfully buffered by means of calcium carbonate precipitation.

The recorded settlements of treated soil samples during the reaction stage of the Rowe cell experiments are insignificant. This indicates that the risk of soil expansion or contraction is limited for the applicable pressure and drainage conditions. The treated and untreated soil samples are subjected to a strain controlled loading regime up to a selected target density under drained conditions. Two volume balances are used for the prediction of the developments of water content, dry density and degree of saturation of the soil sample during the reaction stage and loading stage. The validity of the volume balances is confirmed by the observed water content-dry density loading paths of fully saturated soil samples and gravimetric water content determinations.

Finally the energy requirements for compression of the soil samples to the target density are evaluated in terms of work input per unit volume. A normalization accounts for the differences in total applied strain during the loading stage, which are a result of small differences in initial and final density of the soil samples. A clear difference between treated and untreated samples is not found. Results show a slight increase of energy requirements for static compaction as a result of the biogenic pretreatment. In terms of compactability,

there is no observed benefit from the denitrification-based pretreatment. The increased energy requirements for treated soil samples can possibly be explained by the formation of biofilm as a result of bacterial activity or by entrapped gas bubbles in the drainage lines of the setup. Lastly, it is found in the additional OxiTop experiments that the assumption that a negligible amount of carbon dioxide (CO_2) is produced inside the soil samples due to the near neutral pH, should be scrutinized. Significant fractions of carbon dioxide gas are measured in addition to nitrogen gas at the end of the experiments.

In conclusion, during this study it is shown that a rapid and steady rate of gas production can be reached inside soil samples by means of an engineered substrate solution. Soils are successfully desaturated to a saturation of 80% with a single treatment, without expansion of the soil skeleton. The Rowe cell setup allows for an accurate analysis of the MID process with controlled pressure and drainage conditions. However, with the currently used setup and method of assessment no significant differences can be observed between treated and untreated samples, in terms of compactability. Based on results of the current study and previous research (e.g. Andrag (2017), Puzrin et al. (2011)), new methods of assessment can be developed to further investigate the potential of denitrification-based pretreatment for improving the compactability of soils.

7. RECOMMENDATIONS

The developed Rowe cell setup enables an effective method for desaturation of saturated soil samples by means of biogenic treatment. The setup allows for accurate monitoring of gas production. Moreover, the ability to control pressure and drainage conditions makes the developed setup effective in representing in-situ conditions.

The inability to perform a dynamic loading regime makes the suitability of the Rowe cell setup for an energy-based assessment of the improved compactability of granular soils disputable. It is recommended to explore different methods of assessment for further research into the potential of biogenic pretreatment of granular soils. The guiding principle for this is to make the test more representative to field conditions. Addition of a dynamic/cyclic loading regime is therefore considered to be crucial.

The current investigation showed that the water content-dry density behavior of industrially produced soils can be significantly different from what is experienced in practice. It is therefore advised to take care when selecting a soil for assessment of the intended pretreatment. Ultimately, a soil is collected from a site where conventional compaction techniques are found to be ineffective. A thorough preliminary examination of the behavior of the soil should be executed. The examination should include one or multiple proctor compaction tests for verification of the optimum water content, a grain size distribution analysis, maximum and minimum density tests and preferably a soil permeability test. The relationship between the permeability of the soil and the rate of loading is a crucial factor that has to be taken into account when a new testing method is developed. The efficiency of biogenic pretreatment is expected to be limited if the excess pore water pressure that is generated during loading can be dissipated rather quickly. It should also be investigated how much gas can be produced in the soil before a continuous gas phase develops. The optimum saturation of the soil should be achievable.

Confinement and pressure conditions are utterly important when it comes to the stiffness of soils and the behavior of the gas phase. Compaction activities are often ineffective on layers or lenses of fine soil, which are typically a few meters below ground level. It is most representative to incorporate these pressure conditions into the test setup.

The denitrification process can be employed as an effective method of gas production in soils. This way soils can be desaturated close to any selected target water content by implementation of the appropriate treatment regime. Soil desaturation through denitrification has already been implemented in field experiments (e.g. Burbank et al. (2011)), which were focused on improving the liquefaction resistance of soils and included no subsequent compaction stage.

A next step would be to perform a field experiment on a site/soil where conventional compaction techniques (without pretreatment) are found to be ineffective. Dynamic compactors should be used to perform the compaction activities to guarantee an ultimate representation of practice.

Finally, the applicability of microbial induced desaturation for the improvement of engineering properties of silts or clays could be investigated. Global sources of coarse-grained fill material, which can be used for reclamations, are depleted to such an extent, that often fill material has to be transported over long distances. This brings along significant costs and environmental pollution. A more sustainable alternative would therefore be to use an inferior fill material from a local source and to improve the engineering properties of the fill material by means of a biogenic pretreatment.

A collection of new challenges arises when biogenic pretreatment is applied to silty and clays. For laboratory experiments these challenges are mainly related to the sample preparation technique. The preparation technique should allow for the production of comparable samples with a homogeneous distribution of denitrifying bacteria and substrates. Substrates are flushed through the soil during the Rowe cell experiments of this research. Flushing of substrates might be problematic for soils of lower permeability so an alternative solution needs to be used. The efficiency of the pretreatment could also be tested in a larger-scale field experiment. Fill material can be pre-mixed with substrates and bacterial inoculum before deposition to bypass the necessity of injection.

Furthermore it is found in both the Rowe cell and OxiTop experiments that the assumption that a negligible amount of carbon dioxide is produced during denitrification due to the neutral pH is debatable. A further investigation into this matter is recommended.

BIBLIOGRAPHY

- Ambus, P. and Zechmeister-Boltenstern, S. (2007), Chapter 22 - denitrification and n-cycling in forest ecosystems, in H. Bothe, S. J. Ferguson and W. E. Newton, eds, 'Biology of the Nitrogen Cycle', Elsevier, Amsterdam, pp. 343 – 358.
- Andrag, G. (2017), 'Compaction of silty sands through biogenic gas desaturation pretreatment'. Msc thesis.
- Ashton Acton, Q. (2013), *Nitrogen compounds - Advances in Research and Application 2013 Edition.*, ScholarlyEditions.
- Bergeson, K. and Jahren, C. (1999), Embankment quality: Phase ii, Technical report.
- Betlach, M. R. and Tiedje, J. M. (1981), 'Kinetic explanation for accumulation of nitrite, nitric oxide, and nitrous oxide during bacterial denitrification', *Applied and Environmental Microbiology* **42**(6), 1074–1084.
- Braker, G. and Conrad, R. (2011), Chapter 2 - diversity, structure, and size of n₂o-producing microbial communities in soils—what matters for their functioning?, Vol. 75 of *Advances in Applied Microbiology*, Academic Press, pp. 33 – 70.
- Burbank, M. B., Weaver, T. J., Green, T. L., Williams, B. C. and Crawford, R. L. (2011), 'Precipitation of calcite by indigenous microorganisms to strengthen liquefiable soils', *Geomicrobiology Journal* **28**(4), 301–312.
- Calder, K., Burke, K. A. and Lascelles, J. (1980), 'Induction of nitrate reductase and membrane cytochromes in wild type and chlorate-resistant paracoccus denitrificans', *Archives of microbiology* **126**(2), 149–153.
- Courtens, E. N., Vlaeminck, S. E., Vilchez-Vargas, R., Verliefdde, A., Jauregui, R., Pieper, D. H. and Boon, N. (2014), 'Trade-off between mesophilic and thermophilic denitrification: rates vs. sludge production, settleability and stability', *water research* **63**, 234–244.
- Dawson, R. and Murphy, K. (1972), 'The temperature dependency of biological denitrification', *Water Research* **6**(1), 71–83.
- DeJong, J. T., Mortensen, B. M., Martinez, B. C. and Nelson, D. C. (2010), 'Bio-mediated soil improvement', *Ecological Engineering* **36**(2), 197 – 210. Special Issue: BioGeoCivil Engineering.
- Drnevich, V. P., Evans, A. C. and Prochaska, A. B. (2007), 'A study of effective soil compaction control of granular soils'. Technical report.
- Drtil, M., Németh, P., Kucman, K., Bodík, I. and Kasperek, V. (1995), 'Acidobasic balances in the course of heterotrophic denitrification', *Water research* **29**(5), 1353–1360.
- Forsblad, L. (1981), Vibratory soil and rock fill compaction, Technical report.
- Gallage, C., Dareeju, B., Dhanasekar, M. and Ishikawa, T. (2016), 'Effects of principal stress axis rotation on unsaturated rail track foundation deterioration', *Procedia engineering* **143**, 252–259.
- Glass, C. and Silverstein, J. (1998), 'Denitrification kinetics of high nitrate concentration water: ph effect on inhibition and nitrite accumulation', *Water Research* **32**(3), 831–839.
- Gokyer, S. (2009), Inducing and imaging partial degree of saturation in laboratory sand specimens, PhD thesis, Northeastern University.
- Head, K. (2006), 'Manual of soil laboratory testing volume 1: Soil classification and compaction tests, third edit', *Dunbeath: Whittles Publishing*.
- Hilf, J. W. (1991), Compacted fill, in 'Foundation engineering handbook', Springer, pp. 249–316.
- Ivanov, V. and Stabnikov, V. (2016), *Construction Biotechnology: Biogeochemistry, Microbiology and Biotechnology of Construction Materials and Processes*, Springer.

- Keller (n.d.), 'Deep vibro techniques 10_02e brochure'. (accessed April 7, 2018).
URL: <http://www.kellerholding.com/download-keller-publications.html>
- Knowles, R. (1982), 'Denitrification.', *Microbiological reviews* **46**(1), 43.
- Krapfenbauer, C. (2016), 'Experimental investigation of static liquefaction in submarine slopes'. Msc thesis.
- Lubetkin, S. (2003), 'Why is it much easier to nucleate gas bubbles than theory predicts?', *Langmuir* **19**(7), 2575–2587.
- Lubking, P. (1989), 'De dichtheid van grond', *Land + Water-nu NR. 7/8 (1989)*.
- Mitsui, S., Watanabe, I., Honma, M. and Honda, S. (1964), 'The effect of pesticides on the denitrification in paddy soil', *Soil Science and Plant Nutrition* **10**(3), 15–23.
- Multiquip (2011), 'Soil compaction handbook'. Brochure.
- Parsons, A. W. et al. (1992), *Compaction of soils and granular materials: a review of research performed at the Transport Research Laboratory.*, HMSO.
- Pham, P. (2017), Bio-based ground improvement through Microbial Induced Desaturation and Precipitation (MIDP), PhD thesis.
- Pham, V. P., Nakano, A., van der Star, W. R., Heimovaara, T. J. and van Paassen, L. A. (2016), 'Applying micp by denitrification in soils: a process analysis', *Environmental Geotechnics* **5**(2), 79–93.
- Prakasam, T. and Loehr, R. (1972), 'Microbial nitrification and denitrification in concentrated wastes', *Water Research* **6**(7), 859–869.
- Puzrin, A. M., Tront, J., Schmid, A. and Hughes, J. (2011), 'Engineered use of microbial gas production to decrease primary consolidation settlement in clayey soils', *Géotechnique* **61**(9), 785–794.
- Rebata-Landa, V. and Santamarina, J. C. (2012), 'Mechanical effects of biogenic nitrogen gas bubbles in soils', *Journal of Geotechnical and Geoenvironmental Engineering* **138**(2), 128–137.
- Robertson, G. and Groffman, P. (2015), Chapter 14 - nitrogen transformations, in E. A. Paul, ed., 'Soil Microbiology, Ecology and Biochemistry (Fourth Edition)', fourth edition edn, Academic Press, Boston, pp. 421 – 446.
- Robertson, P. and Wride, C. (1998), 'Evaluating cyclic liquefaction potential using the cone penetration test', *Canadian Geotechnical Journal* **35**(3), 442–459.
- Salek, S., Bozkurt, O., van Turnhout, A., Kleerebezem, R. and van Loosdrecht, M. (2016), 'Kinetics of CaCO_3 precipitation in an anaerobic digestion process integrated with silicate minerals', *Ecological Engineering* **86**, 105 – 112.
- Salem, M. (2010), 'Soil compaction, soil mechanics 2010-2011'.
- Schuurman, I. E. (1966), 'The compressibility of an air/water mixture and a theoretical relation between the air and water pressures', *Geotechnique* **16**(4), 269–281.
- Šimek, M., Jiřová, L. and Hopkins, D. W. (2002), 'What is the so-called optimum ph for denitrification in soil?', *Soil Biology and Biochemistry* **34**(9), 1227–1234.
- Sparks, A. (1965), 'Theoretical considerations of stress equations for partly saturated soils', *Civil Eng Bull, Capetown Univ/S Afr/*.
- Stewart, P. (1992), Lateral loading of piled bridge abutments due to embankment construction, PhD thesis, The University of Western Australia.
- Terzaghi, K., Peck, R. B. and Mesri, G. (1996), *Soil mechanics in engineering practice*, John Wiley & Sons.
- van den Berg, E. M., Boleij, M., Kuenen, J. G., Kleerebezem, R. and van Loosdrecht, M. (2016), 'Dnra and denitrification coexist over a broad range of acetate/n- NO_3^- ratios, in a chemostat enrichment culture', *Frontiers in microbiology* **7**, 1842.

- van Paassen, L. A., Ghose, R., van der Linden, T. J., van der Star, W. R. and van Loosdrecht, M. C. (2010), 'Quantifying biomediated ground improvement by ureolysis: large-scale biogROUT experiment', *Journal of geotechnical and geoenvironmental engineering* **136**(12), 1721–1728.
- Van Rijn, J., Tal, Y. and Barak, Y. (1996), 'Influence of volatile fatty acids on nitrite accumulation by a *Pseudomonas stutzeri* strain isolated from a denitrifying fluidized bed reactor.', *Applied and Environmental Microbiology* **62**(7), 2615–2620.
- van Spanning, R. J., Richardson, D. J. and Ferguson, S. J. (2007), Introduction to the biochemistry and molecular biology of denitrification, in 'Biology of the nitrogen cycle', Elsevier, pp. 3–20.
- Vazquez, A. (2017), *Overflow metabolism: from yeast to Marathon runners*, Academic Press.
- Wilderer, P. A., Jones, W. L. and Dau, U. (1987), 'Competition in denitrification systems affecting reduction rate and accumulation of nitrite', *Water Research* **21**(2), 239–245.
- Wu, S. (2015), 'Mitigation of liquefaction hazards using the combined biodesaturation and bioclogging method'. PhD thesis.
- Zhang, J., Cai, Z., Cheng, Y. and Zhu, T. (2009), 'Denitrification and total nitrogen gas production from forest soils of eastern china', *Soil Biology and Biochemistry* **41**(12), 2551–2557.

A. SOIL SAMPLE MEASUREMENTS ROWE CELL EXPERIMENTS

Table A.1: Measurements Rowe cell experiments.

	Untreated 1 S_w = 100%	Untreated 2 S_w = 100%	Untreated 3 S_w = 100%	Treated 1 S_w = 80%	Treated 2 S_w = 81%	Treated 3 S_w = 89%
M_s (kg)	1.24	1.25	1.25	1.24	1.26	1.24
$\Delta\epsilon$ loading stage (%)	4.37	3.77	4.73	3.87	2.02	3.44
Δp_d loading stage (g/cm ³)	0.075	0.064	0.081	0.066	0.034	0.059
Δw loading stage (%)	-2.73	-2.31	-2.94	-0.73	-0.34	-0.58
ΔH_{sample} loading stage (mm)	1.89	1.61	2.04	1.64	0.85	1.45
Loading time (s)	4385	3267	3243	3747	1698	5905
Avg. $\dot{\epsilon}$ loading stage (mm/min)	0.026	0.030	0.038	0.026	0.030	0.015
Avg. final w (gravimetric)	21.8	21.68	21.61	18.2	18.0	20.0

B. CHEMICAL ANALYSIS ROWE CELL EXPERIMENTS

Table B.1: Chemical analysis of Treated Rowe cell experiments.

	Treated 1 S_w = 80%	Treated 2 S_w = 81%	Treated 3 S_w = 89%
pH substrate initial (-)	6.92	6.95	6.98
pH pore fluid initial (-)	7.15	7.13	7.13
pH pore fluid final (-)	7.30	7.52	7.46
EC substrate initial (mS/cm)	6.1	6.2	4.5
EC pore fluid initial (mS/cm)	4.1	5.0	3.7
EC pore fluid final (mS/cm)	0.5	0.9	0.5
$NO_3^- - N$ substrate (mM)	37.87	40.42	27.49
$NO_3^- - N$ pore fluid initial (mM)	19.23	26.98	17.98
$NO_3^- - N$ pore fluid final (mM)	2.61	1.50	2.64
$NO_2^- - N$ substrate (mM)	0.00	0.00	0.00
$NO_2^- - N$ pore fluid initial (mM)	0.03	0.03	0.00
$NO_2^- - N$ pore fluid final (mM)	1.84	0.89	0.26
Ca^{2+} substrate (mM)	59.94	58.54	33.49
Ca^{2+} pore fluid initial (mM)	41.99	48.74	27.72
Ca^{2+} pore fluid final (mM)	17.31	15.18	7.52

Table B.2: Nitrogen balance Treated 1.

	Pore fluid initial	Pore fluid final	Gas
Volume (mL)	291	224	58.6
Nitrate (mmol $NO_3^- - N$)	5.59	0.58	
Nitrite (mmol $NO_2^- - N$)	0.01	0.41	
$N_2/NO/N_2O$ gas (mmol-N)		0.22	7.23
Total (mmol-N)	5.60	8.44	
N-gap (mmol-N)	-2.84		
N-gap percentage (of initial) (%)	-51%		

Table B.3: Nitrogen balance Treated 2.

	Pore fluid initial	Pore fluid final	Gas
Volume (mL)	282	227	55.2
Nitrate (mmol $NO_3^- - N$)	7.62	0.34	
Nitrite (mmol $NO_2^- - N$)	0.01	0.20	
$N_2/NO/N_2O$ gas (mmol-N)		0.22	6.81
Total	7.62	7.57	
N-gap (mmol-N)	0.05		
N-gap percentage (of initial) (%)	1%		

Table B.4: Nitrogen balance Treated 3.

	Pore fluid initial	Pore fluid final	Gas
Volume (mL)	289	248	33.0
Nitrate (mmol $NO_3^- - N$)	5.19	0.41	
Nitrite (mmol $NO_2^- - N$)	0.00	0.06	
$N_2/NO/N_2O$ gas (mmol-N)		0.24	4.07
Total	5.19	4.78	
N-gap (mmol-N)	0.41		
N-gap percentage (of initial) (%)	8%		

C. CHEMICAL ANALYSIS OxiTOP EXPERIMENTS

Table C.1: Chemical analysis of Control bottles OxiTop experiment.

	Control 1	Control 2	Control 3	Control 4
pH initial (-)	7.06	7.08	7.05	7.06
pH final (-)	6.95	6.93	6.98	6.77
$NO_3^- - N$ initial (mM)	18.21	18.21	18.21	18.21
$NO_3^- - N$ final (mM)	0.36	0.01	0.02	1.45
$NO_2^- - N$ initial (mM)	0.00	0.00	0.00	0.00
$NO_2^- - N$ final (mM)	0.03	0.03	0.02	0.03
Ca^{2+} initial (mM)	24.18	24.18	24.18	24.18
Ca^{2+} final (mM)	17.72	16.09	15.97	18.84

Table C.2: Chemical analysis of Soil bottles OxiTop experiment.

	Soil 5	Soil 6	Soil 7	Soil 8
pH initial (-)	7.08	7.07	7.07	7.06
pH final (-)	7.04	7.03	7.01	7.05
$NO_3^- - N$ initial (mM)	18.21	18.21	18.21	18.21
$NO_3^- - N$ final (mM)	0.14	0.15	0.16	0.25
$NO_2^- - N$ initial (mM)	0.00	0.00	0.00	0.00
$NO_2^- - N$ final (mM)	0.03	0.03	0.03	0.04
Ca^{2+} initial (mM)	24.18	24.18	24.18	24.18
Ca^{2+} final (mM)	16.22	15.72	16.34	17.59

D. NUTRIENT STOCK SOLUTIONS

Table D.1: Composition of macro-nutrient stock solution. During all experiments 1 mL of the macro-nutrient stock solution was added for each 1 L of prepared solution (i.e. 1 mL/L).

Name	Chemical formula	Stock solution conc. (mmol/L)
Ammonium sulfate	$(NH_4)_2SO_4$	3
Magnesium sulfate heptahydrate	$MgSO_4$	2.4
Monopotassium phosphate	KH_2PO_4	6
Dipotassium phosphate	K_2HPO_4	14

Table D.2: Composition of micro-nutrient stock solution (Salek et al., 2016). During all experiments 1 mL of the micro-nutrient stock solution was added for each L of prepared solution (i.e. 1 mL/L).

Name	Chemical formula	Stock solution conc. (mmol/L)
Boric acid	H_3BO_3	1.23
Zinc chloride	$ZnCl_2$	2.12
Copper(II) chloride	$CuCl_2$	0.54
Cobalt(II) chloride octahydrate	$CoCl_2$	0.43
Nickel(II) chloride octahydrate	$NiCl_2$	0.64
Manganese(II) chloride	$MnCl_2$	0.12
Sodium molybdate dihydrate	$NaMoO_4$	0.40
Iron(III) chloride	$FeCl_3$	10.60
Calcium chloride dihydrate	$CaCl_2$	0.31